

PhD Program in
Translational and Molecular Medicine
DIMET

XXVI Cycle, Academic year 2012-2013

University of Milano-Bicocca
School of Medicine and Faculty of Science

**RNA metabolism alteration in
Amyotrophic Lateral Sclerosis
models**

Alessia Loffreda- No.744988

Questa tesi è dedicata alla mia famiglia,
in particolare alla piccola Eleonora.

Chapter 1.....	6
General Introduction	6
1.RNA metabolism	6
1.1 Transcription of DNA and synthesis of RNA.....	6
1.2 Post-transcription modification of pre-mRNA resulting in mature mRNA.....	8
1.2.1 RNA processing and Editing	8
1.2.2 Splicing and mRNP formation	9
1.3 Regulation of gene expression by mRNA localization and translation	11
1.4 The role of tRNA in the translation of mRNA to protein	13
1.5 mRNA stability, degradation and quality control .	14
2. The evidence for altered RNA metabolism in amyotrophic lateral sclerosis (ALS)	16
2.1 Gene transcription.....	16
2.2.1 Editing	18
2.2.2 Splicing	19
2.3 mRNA localization and translation	24
2.4 The role of tRNA in the translation of mRNA to protein	25
2.5 mRNA stability	25
3. MicroRNA	29
3.1. Biogenesis and Role of microRNAs.....	29
3.2 MicroRNAs and Amyotrophic Lateral Sclerosis	33
3.3 Amyotrophic Lateral Sclerosis and Circulating miRNAs	35

4. DNA Damage Response	38
5. FIGURES AND TABLES	40
6. Scope of the thesis	46
7. References.....	48
Chapter 2.....	59
Unraveling the impact of microRNA on Amyotrophic Lateral Sclerosis pathogenesis	59
2.1 Abstract	60
2.2 Introduction	62
2.3 Results	67
2.4 Discussion.....	78
2.5 Figures and Tables	84
2.6 Materials and Methods	106
2.7 References	116
Chapter 3.....	124
FUS/TLS depletion leads an impairment of cell proliferation and DNA Damage Response ..	124
3.1 Abstract	125
3.2 Introduction	127
3.3 Results	133
3.4 Discussion.....	143
3.5 Figures and Tables	149
3.6 Materials and Methods	162
3.7 References	169
Chapter 4.....	174

Conclusions.....	174
4.1 Summary	174
4.2 Future perspective	180
4.3 References	186

Chapter 1

General Introduction

1.RNA metabolism

1.1 Transcription of DNA and synthesis of RNA

The first step in gene expression is transcription. RNA polymerase II (RNPII) is the enzyme that mediates mRNA transcription. However, in eukaryotic cells, this enzyme alone does not function efficiently; it needs to interact with other proteins, known as transcription factors, to produce transcripts. These factors either interact directly with the RNA polymerase or regulate its catalytic function by binding to *cis*-acting DNA sequences or another transcription factor. The RNA polymerase and the transcription factors that directly interact with it are the basal transcription machinery. The promoter contains a DNA sequence called the TATA box, which is located 25 nucleotides away from the site where transcription is initiated. Briefly, the TATA box is recognized and bound by transcription factor TFIID, which then enables the adjacent binding of TFIIB. The

rest of the general transcription factors, as well as the RNA polymerase itself, assemble at the promoter. TFIIF uses ATP to pry apart the double helix at the transcription start point, allowing transcription to begin. TFIIF also phosphorylates RNA polymerase II, releasing it from the general factors so it can begin the elongation phase of transcription. Here, RNAPII is associated with transcription elongation factors and helps in the recruitment of the splicing machinery (SR proteins, snRNPs) to splice sites in the pre-mRNA to facilitate efficient excision of introns. After transcribing the poly(A) signal (AATAAA), polyadenylation factors associated with the the cap-binding complex (CTD) form a functional complex on the pre-mRNA to catalyze endonucleolytic cleavage. Subsequently the transcription bubble disappears as the DNA re-hybridize.

Potential impediments to Pol II elongation are nucleosomes, which serve to both compact the DNA and exert regulatory control over transcription via modification of their component histones. Increased histone acetylation at the promoter region has been implicated in transcription, as this acetylation renders the nucleosomes more mobile. During elongation, Pol II requires additional histone acetylation transferases (HATs) to acetylate nucleosomes within the gene,

creating a highly dynamic balance between histones being expelled and deposited upon passage of Pol II through the DNA (Kristjuhan A et al. 2004).

1.2 Post-transcription modification of pre-mRNA resulting in mature mRNA

1.2.1 RNA processing and Editing

Immediately after the RNA is transcribed in the nucleus, capping, splicing, editing and 3' polyadenylation of the pre-mRNA occur. In mammals, RNA editing can be of two types, either the conversion of cytidine to uridine or the conversion of adenosine to inosine. Once the mRNA is transported into the cytoplasm, additional processing of the poly(A)⁺ tail can occur. The elements required for this and for subcellular localization, stability and translation are present in the 3' untranslated region (UTR). ACE, adenylation control element; CPE, cytoplasmic poly(A) element. The term editing describes the processes that change RNA sequences. In mammals, these mechanisms involve base modification/substitution: cytidine-to-uridine (thereby possibly creating new start or stop codons), uridine-to-cytidine and adenosine-to-inosine (potentially causing alterations in splice sites)

editing (Seeburg et al. 2002). A set of enzymes, called 'adenosine deaminases acting on RNA' (ADAR) converts an adenosine (A) into an inosine (I) (Seeburg et al. 2002).

1.2.2 Splicing and mRNP formation

After these initial editing events, the pre-mRNA is spliced into the mature form. Pre-mRNA splicing is a process in which intervening sequences (introns) are removed from an mRNA precursor. Splicing consists of two transesterification steps, each involving a nucleophilic attack on terminal phosphodiester bonds of the intron. In the first step this is carried out by the 2' hydroxyl of the branch point (usually adenosine) and in the second step by the 3' hydroxyl of the upstream (5') exon (Black et al. 2003; Wahl et al. 2009). This process is carried out in the spliceosome, a dynamic molecular machine the assembly of which involves sequential binding and release of small nuclear ribonucleoprotein particles (snRNPs) and numerous protein factors as well as the formation and disruption of RNA–RNA, protein–RNA and protein–protein interactions. The basic mechanics of spliceosome assembly are well known. Briefly, the process begins with the base pairing of U1 snRNA to the 5' splice site (ss) and the binding of

splicing factor 1 (SF1) to the branch point (Berglund et al. 1997) in an ATP-independent manner to form the E' complex. The E' complex can be converted into the E complex by the recruitment of U2 auxiliary factor (U2AF) heterodimer (comprising U2AF65 and U2AF35) to the polypyrimidine tract and 3' terminal AG (Kent et al. 2005). The ATP-independent E complex is converted into the ATP-dependent pre-spliceosome A complex by the replacement of SF1 by U2 snRNP at the branch point. Further recruitment of the U4/U6–U5 tri-snRNP leads to the formation of the B complex, which contains all spliceosomal subunits that carry out pre-mRNA splicing. This is followed by extensive conformational changes and remodelling, including the loss of U1 and U4 snRNPs, ultimately resulting in the formation of the C complex, which is the catalytically active spliceosome.

Alternative splicing (as opposed to constitutive splicing) refers to variations in splice site selection resulting in an mRNA species that contains or lacks a certain exon. It results in protein isoforms that differ in their peptide sequence and therefore can have different chemical and biological characteristics (Grabowsky et al. 2001). Alternative splicing in neurons can produce cell-specific levels of protein isoforms leading to cell-specific properties and function.

1.3 Regulation of gene expression by mRNA localization and translation

The ability to direct protein synthesis to specific somatotopic targets in response to cellular needs is further enhanced by the coordinated expression of multiple nascent mRNAs into functionally related “bundles” through macromolecules termed ribonucleoprotein (RNP) complexes (also termed RNA granules). This is the core of the *RNA operon theory* in which genes whose products are functionally related are expressed in the same temporal and spatial patterns (Bolognani et al. 2008; Keene et al. 2002; Keene et al 2007). RNP complexes contain ribosomal subunits, translation factors, decay enzymes, helicases, scaffold proteins, molecular motors and RNA binding proteins (RBPs) that control the localization, stability and translation of their RNA cargo (Anderson et al. 2006). Their composition is thus critical to the regulation of RNA metabolism. RBPs are themselves subject to considerable post-translational modification and provide a dynamic linkage between RNA processing and intracellular signaling pathways (Keene et al. 2007) and (Lukong et al. 2008). This ability is particularly important for neurons where is embodied in

the model of "asymmetrical protein translation" in which the site-specific synthesis of protein is dependent on the transport of translationally quiescent mRNA within transport RNA granules and then the unbundling of the granules to yield a translationally active polysome at the site at which protein is needed (Lin et al. 2005). While important to neuronal development, this process is increasingly seen as key to the mechanisms underlying neuronal plasticity, neuroregeneration, and when perturbed, neurodegeneration. Moreover, while the model allows for a localized rapid induction of protein synthesis with spatial precision, it also provides for a considerable level of post-transcriptional regulation of gene expression.

Three main types of RNA granules are present in the mature neuron, including transport granules (maintaining mRNA in a translationally silent state until transport to the site of nascent protein synthesis), stress granules (sequestering mRNA in a translationally silent state at times of neuronal injury) and cytosolic processing bodies (also known as P-bodies or degradative granules) (Wang et al. 2008; Hirokawa et al. 2006; Kanai et al. 2004). In general, it has been held that each of the three granules is discretely synthesized. However, both stress granules and P-bodies share a common origin. Both are simultaneously

assembled in response to cellular stress on untranslated mRNA derived from disassembled polysomes, and they share a number of proteins, including FAST, XRN-1, eIF4E, TTP and BRF2.

1.4 The role of tRNA in the translation of mRNA to protein

Translation of mRNA into protein occurs at the level of the ribosome. The translational machinery mainly consists of three components ensuring accurate decoding of the genetic message: the tRNA molecules, whose anticodons match the mRNA codons; the aminoacyl-tRNA synthetases, which esterify the cognate amino acid to the corresponding tRNA species; and the peptide chain termination factors that identify the termination codons. Following transcription, tRNA molecules undergo processing and modification to produce a mature tRNA. Modification of the nucleoside in position 34 is common. This nucleoside pairs with the third base in the mRNA codon, the base in the so-called “wobble” position. This pairing can be both canonical (as observed in the first two base pairs) or non-canonical (Agri set al. 2007; Crick et al. 1966). Absence of nucleoside modifications at position 34 influences

efficiency of decoding of mRNA; the precise molecular mechanisms are however incompletely understood.

1.5 mRNA stability, degradation and quality control

The nuclear exosome functions in the 3' processing of the precursors to stable RNAs, including the 5.8S rRNA component of mature ribosomes and many snoRNAs. The nuclear exosome is responsible for the surveillance and degradation of aberrant nuclear precursors of many types of RNA including pre-mRNAs, pre-tRNAs and pre-rRNAs. Regulated 3' degradation by the nuclear exosome is also implicated in the control of expression levels of some mRNAs. These exosome substrates therefore include both RNA species that should be matured by the removal of nucleotides to a precisely defined end point, and defective RNAs that will undergo rapid and complete degradation. The exosome participates in the 3' turnover of normal mRNAs, and therefore helps to determine mRNA abundance and, so, protein-synthesis rates. Also, the exosome rapidly degrades mRNAs with structural defects; the nonsense-mediated decay (NMD) pathway degrades mRNAs with premature translation-termination codons, whereas the

non-stop decay pathway degrades mRNAs that lack a termination codon altogether. In human cells, the exosome is also recruited to, and rapidly degrades, mRNAs that contain specific A+U-rich sequence elements (AREs). These are present in many mRNAs that encode proteins for which transient expression is important, including growth factors and proto-oncogenes. Furthermore, the exosome degrades the 5' fragments of mRNAs that are cleaved in the no-go decay pathway, which targets mRNAs on which translation has stalled (Houseley et al 2006).

2. The evidence for altered RNA metabolism in amyotrophic lateral sclerosis (ALS)

2.1 Gene transcription

One protein complex that associates with Pol II and has HAT activity is Elongator protein (ELP). Holo-Elongator is a six-subunit complex composed of two subcomplexes: core-Elongator (ELP1, ELP2 and ELP3) and a smaller component (composed of ELP4, ELP5 and ELP6). It is the ELP3 subunit which has HAT activity (Svejstrup et al. 2007). Recently, common genetic variants within the *ELP3* subunit were shown to affect the risk of developing sporadic ALS (Simpson et al. 2009). The genotype associated with an increased risk of motor neuron degeneration was associated with reduced expression of the ELP3 protein in the brain. Furthermore, gene knockdown of ELP3 in zebrafish embryos stunted motor axonal outgrowth suggesting a role of ELP3 in motor neuron development and biology (Simpson et al. 2009). This evidence suggests that reduced expression levels of ELP3 could contribute to motor neuron degeneration. Another gene thought to function in transcription and linked to motor neuron disease is the DNA/RNA helicase *senataxin* (*SETX*).

Missense mutations in *SETX* cause ALS4 (Chen et al. 2004). DNA helicases regulate chromatin remodeling, thereby modulating access to the DNA template (Tuteja et al. 2004). ALS4 is somewhat a misnomer, as the phenotype of these patients is more similar to dHMN with some upper motor neuron findings, than to ALS, and as its course is far more benign than that of ALS (Windpassinger et al. 2004). The yeast *SETX* ortholog, *Sen1*, is an essential gene that has been implicated in RNA processing, transcription and transcription-coupled DNA repair (Ursic et al 2004). A single point mutation in the helicase domain of Sen1 affects transcription termination by RNA Pol II on small nucleolar RNA (snoRNA) genes and a subset of protein coding genes (Steinmetz et al. 2006). Similar to Sen1, mammalian SETX localizes to the nucleus where it is thought to function in the repair of double-strand breaks induced by oxidative damage to DNA (Suraweera et al. 2007). More recently, mammalian SETX was found to interact with multiple proteins involved in transcription and pre-mRNA processing, and SETX depletion resulted in defects in Pol II transcription termination and pre-mRNA splicing (Suraweera et al. 2009).

2.2 Post transcriptional modifications

2.2.1 Editing

An mRNA edited by an ADAR is GluR2, the subunit 2 of the AMPA-type of glutamate receptor, an important player in excitotoxic motor neuron death. Excitotoxicity is the phenomenon of neuronal degeneration caused by stimulation of the glutamate receptors (Van Den Bosch et al. 2006). Excitotoxic motor neuron death is mediated through the influx of calcium through a Ca^{2+} -permeable AMPA receptor and is thought to play a role in the pathogenesis of ALS (Van Den Bosch et al. 2006). The GluR2 pre-mRNA codes for a glutamine (Q) at position 586 (nucleotides CAG) of the protein. ADAR2 (Kwak et al. 2005) changes adenosine into inosine, which codes for an arginine (R) (hence the name Q/R site) resulting in an arginine at position 586 in edited GluR2 protein. Its incorporation in the AMPA-type receptor reduces Ca^{2+} -permeability of the channel because of the presence of this positively charged arginine. The presence of an unedited GluR2 (containing glutamine in position 586) makes the channel more Ca^{2+} -permeable and renders the motor neuron vulnerable to glutamate-induced Ca^{2+} overload

and death. Mice that transgenically overexpress a GluR2 that cannot be edited develop a late-onset motor neuron degeneration (Feldemeyer et al. 1999; Kuner et al. 2005). Of major interest is the finding of failure of GluR2 editing in a majority of sporadic ALS (SALS) patients (Kawahara et al. 2004; Kwak et al. 2010), suggesting a role for editing failure in SALS

2.2.2 Splicing

Mutations in two proteins that have been implicated in mRNA splicing are known to cause ALS: the TAR DNA-binding protein TDP-43 and the protein FUS/TLS (FUsed in Sarcoma, Translocated in LipoSarcoma). Mutations in the TAR DNA-binding protein TDP-43 have been reported in both SALS and FALS (Sreedharan et al 2008; Gitcho et al. 2008; Yokoseki et al. 2008; Van Derlin et al. 2008; Kabashi et al. 2008). These mutations are rare, explaining less than 5% of the familial cases. TDP-43 is a nuclear protein that interacts with several RNPs and functions in transcription suppression and alternative splicing (Buratti et al. 2008) such as the skipping of exon 9 of CFTR in cystic fibrosis. All but one of the TDP-43 mutations identified in ALS are localized in exon 6, which encodes the hnRNP binding domain (Buratti et al 2005). A role for

this protein in neurodegeneration, and in particular in frontotemporal lobar degeneration (FTLD) and ALS, became clear through the finding that aberrantly cleaved, hyperphosphorylated and ubiquitinated TDP-43 is present in cytoplasmic inclusions in the spinal motor neurons of sporadic ALS patients and in the cortex of some patients with FTLD-U (Arai et al. 2006; Neumann et al. 2006). Thus, both wild type and mutant TDP-43 appear to play a pathogenic role, reminiscent of amyloid precursor protein in Alzheimer's disease and α -synuclein in Parkinson's disease. It remains to be clarified what this role is: the sequestering of TDP-43 in the cytoplasm resulting in depletion of the protein from the nucleus, resulting in mRNA splicing abnormalities (Neumann et al. 2006; Winton et al. 2008) or deficits in mRNA translocation (Strong et al 2007). Evidence for a loss-of-function mechanism has been presented in zebrafish, in which knockdown of TDP-43 results in motor axon abnormalities similar to those seen when overexpressing mutant TDP-43 (Kabashi et al. 2010). However, one finding might not be related to the other. Alternatively, it is possible that mutant TDP-43 is neurotoxic through a mechanism independent of its roles in the nucleus, such as the formation of aggregates, or binding of aberrant partners, again resulting in a gain-of-function (Nonaka et al. 2009;

Johnson et al. 2009). Recently, a mouse expressing mutant TDP-43 has been reported to develop a motor neuron phenotype (Wegorzewska et al. 2009). Unraveling the mechanism and significance of the proteolytic processing of TDP-43 in ALS and FTL, of its phosphorylation, ubiquitination and aggregation, as well as the effect of "mislocation" in the cytoplasm will be important to gain insight into its pathogenic mechanism.

Mutations in FUS/TLS (FUsed in Sarcoma, Translocated in LipoSarcoma) are found in probably less than 5% of familial ALS. Normally, the protein is predominantly located in the cell nucleus, but neurons from ALS patients with FUS mutations show cytoplasmic retention of the protein. FUS is a multifunctional protein (Kwiatkowski et al. 2009; Vance et al. 2009). In addition to 5'-transcriptional activating domains, it binds single-strand DNA, double-stranded DNA, RNA and transcriptional complex proteins (Yang et al. 1998; Wang et al. 2008). These attributes suggest a role in multiple aspects of RNA metabolism, presumably within the nucleus and the cytoplasm. Studies in neural tissues further suggest that FUS is implicated in mRNA transport, both along dendrites and into dendritic spines (Fujii et al. 2005; Belly et al. 2005). Numerous

mRNAs are thought to be translated locally in dendritic spines in response to synaptic activation (Sutton et al 2006). FUS could be involved in their transport and location and thus could be important in maintaining use-dependent synaptic function (Fujii et al 2005). Whether ALS-related mutations in FUS alter this function has not been elucidated, but it is likely that they perturb synaptogenesis and/or glutamate-induced excitotoxicity. By contrast, mutant FUS can be pathogenic through a toxic gain-of-function (e.g. cytoplasmic aggregates), independent of its normal cellular function, similar to what has been suggested for mutant SOD1 and mutant TDP-43. FUS/TLS staining is also seen in the brain of patients with atypical FTLD-U, suggesting that the wild type protein can also play a pathogenic role, another parallel with TDP-43 (Neumann et al. 2009). The identification of TDP-43 and FUS mutations in ALS indicates a significant leap forward for the field. Previously, only one rodent model was available for study. Mice and rats overexpressing a mutant SOD1 develop adult-onset motor neuron degeneration and are an excellent model to study ALS associated with SOD1 mutations, which explain approximately 20% of familial ALS. Generation of mutant TDP-43 and FUS rodent models will greatly help to elucidate common pathways of motor neuron

degeneration and to study therapeutic interventions that have relevance to more than mutant SOD1-mediated ALS.

That abnormalities of splicing can contribute to ALS is suggested by different evidences. First, one copy of SMN1 or genotypes resulting in low levels of SMN protein have been reported to represent a risk factor for ALS in humans (Corcia et al. 2006; Veldink et al. 2005) and deletion of one SMN allele in mice expressing mutant SOD1 aggravates motor neuron degeneration in these animals (Turner et al. 2009). Second, isoform expression of SMN interacting protein 1 (SIP1, now called Gemin2, is a binding partner of SMN and essential for snRNP biogenesis) has been reported to be different in human ALS muscle from controls (Aerbajinai et al. 2002). Finally, expression of a peculiar splice variant of the intermediate filament peripherin, Per 61, has been detected in motor neurons of SOD1G37R transgenic animals (but not in wild type animals) and in the lumbar spinal cord of ALS patients (Robertson et al. 2003) Per 61 is the result of retention of intron 4, resulting in a protein that is deficient in neurofilament assembly and is toxic to motor neurons in culture. Mutations in human peripherin have been identified in SALS (Gros-Louis et al. 2004) but their relationship with alternative splicing is unknown.

2.3 mRNA localization and translation

Alterations in RNA transport have been indirectly implicated in motor neuron degeneration. Experimentally, mutations in the dynein heavy chain, homopolymers of which contribute to the formation of the microtubule motor dynein complex and thus interact with dynactin (Levy et al. 2006), are associated with a progressive motor neuronopathy and severe impairments in retrograde axonal transport (Hafezparast et al 2003). Mutations in dynactin result in a variable motor neuron phenotype, including a single family in which both FTD and ALS co-segregated (Munch et al. 2005; Puls et al. 2003). The mechanism(s) by which dynein/dynactin mutations give rise to a motor neuron degeneration remain unknown, but likely include impairments in retrograde axonal transport of NF or RNPs (Levy et al. 2006). Although to date, no kinesin mutations leading to perturbations in anterograde RNP transport have been documented in ALS, reduced expression of the kinesin-associated protein 3 (KIFAP3) has recently been associated with enhanced survival in sALS (Landers et al 2005).

2.4 The role of tRNA in the translation of mRNA to protein

Low expression of Elongator protein 3 (ELP3) is a risk factor for ALS, as explained above. ELP3, in addition to its effect on RNA synthesis through histone acetylation and on axonal function through tubulin acetylation, is also involved in the formation of 5-methoxycarbonylmethyl (mcm5) and 5-carbamoylmethyl (ncm5) side chains of modified wobble uridines in tRNA (Huang et al.2005). Elongator-deficient yeast cells show growth retardation and defects in transcriptional elongation, exocytosis and tRNA modification. All but the tRNA modification defects are rescued by overexpression of hypomodified tRNA (Esberg et al.2006). Wobble-base modification thus appears to be a key regulatory step in cell proliferation and growth.

2.5 mRNA stability

Some aspects of the pathogenesis of motor neuron disease relate to mRNA stability. Neurofilament aggregates in motor neurons are a hallmark of sporadic as well as familial ALS (Troost et al. 2005). In the spinal cord of SOD1(G93A) transgenic animals,

neurofilament (NFL) aggregates contain *p190RhoGEF* (Lin et al. 2005). *P190RhoGEF* is a factor thought to stabilize NFL mRNA by binding to the NFL 3'-UTR. mRNA-bound *p190RhoGEF* is in dynamic competition with *p190RhoGEF* bound to unassembled NFL protein, a homeostatic mechanism that results in NFL mRNA breakdown when unassembled NFL protein accumulates (Lin et al. 2005). Aggregation of NFL and *p190RhoGEF* reduces the availability of *p190RhoGEF* to stabilize NFL mRNA in motor neurons. One study found that mutant SOD1 binds to the NFL mRNA 3'-UTR and destabilizes the NFL mRNA possibly through competition with binding factors such as *p190RhoGEF* (Ge et al. 2005). Loss of NFL in motor neurons has indeed been demonstrated in ALS patients. The role of *p190RhoGEF* is of particular interest, as loss-of-function mutations in *alsin*, which encodes a RhoGEF component, cause a motor neuron disease called ALS2, but which most frequently is an early-onset ascending upper motor neuron disorder (Hadano et al. 2001; Yang et al. 2001). Forced expression of *alsin* protects motor neuronal cells from toxicity induced by mutant SOD1 (Kanekura et al. 2004) which fits in this model.

A similar effect related to mRNA stability could contribute to motor neuron degeneration associated with reduced levels of *vascular endothelial growth*

factor (VEGF). Mice genetically modified to lack hypoxia-induced upregulation of VEGF develop a progressive, late-onset motor neuron degeneration (Ootuyse et al. 2001). Polymorphisms in the *VEGF* gene which are correlated with low VEGF expression levels can also be associated with ALS at least in a subpopulation of patients (Lambrechts et al. 2003; Lambrechts et al. 2009). Administration of VEGF prolonged survival significantly in rodent models for ALS (Ruiz de Imodovar et al. 2009). In both human tissue and presymptomatic mutant SOD1 mice, VEGF levels in the spinal cord are reduced, possibly because of a decreased stability of VEGF mRNA in the presence of mutant SOD1 (Lu et al. 2007). The exact mechanism has not been identified but is thought to involve the RNA stabilizing protein human antigen R (HuR) (Lu et al. 2007). Mutations in *angiogenin* (*ANG*) are a rare cause of familial and sporadic ALS (Greenway et al. 2006). Angiogenin is a member of the pancreatic ribonuclease A (RNaseA) superfamily is a known inducer of neovascularization. Angiogenin is present in the developing nervous system and strongly expressed in motor neurons (Greenway et al. 2006; Subramanian et al. 2007). It protects neurons from hypoxia. Mutations in *ANG* affect its nuclear localization, angiogenic activity and, of interest, ribonucleolytic

activity (Crabtree et al 2007; Wu et al. 2007); mutant angiogenin is toxic to motor neurons Subramanian et al. 2008). In neuronal cultures angiogenin increases neurite outgrowth, an effect that is affected by pharmacological inhibition of the ribonucleolytic activity of angiogenin Subramanian et al. 2007). The mechanism through which mutant angiogenin induces motor neuron degeneration is far from understood.

3. MicroRNA

3.1. Biogenesis and Role of microRNAs

MicroRNAs (miRNAs) are a class of ~22 nucleotides non-coding RNA molecules representing a superior mechanism by which to regulate gene expression.

MiRNAs biosynthesis is conserved during evolution and consists of two steps that take place in the nucleus and the cytoplasm, respectively (Bartel et al. 2004; Siomi et al. 2010). In the nucleus, miRNAs are largely transcribed by RNA polymerase II as primary-(pri-)miRNAs. At this stage, pri-miRNAs present several hairpin structures, each consisting of a stem and a terminal loop, and are subject to a 5'-capping, 3'-polyadenylation, editing, and splicing processing (Cartew et al. 2009; Kim et al. 2009). The processed pri-miRNAs are next "cropped" into smallest hairpin-structures precursor of ~70 nucleotides (called pre-miRNAs) by a nuclear microprocessor complex composed of Drosha, an RNase III enzyme (RNASEN), and DGCR8 (DiGeorge Critical Region 8) protein. The last is also called Pasha (Partner of Drosha) in *D. melanogaster* and *C. elegans* (Lee et al. 2003). These proteins form a complex with several cofactors (e.g., DEAD box RNA helicases p68 [DDX5]; p72 [DDX17];

heterogeneous nuclear ribonucleo-proteins [hnRNPs]) important for the specificity of Drosha activity (Gregory et al. 2004). Due to RNase activity, Drosha cleaves the 5' and 3' arms of the pri-miRNA hairpin (Han et al. 2004), while DGCR8 is necessary for the interaction with the pri-miRNA for the site-specific cleavage (Han et al. 2006). Thus, Drosha cleaves 11 base pairs away from the single-/double-stranded RNAs at the level of the hairpin stem base (Han et al. 2006). The cleavage occurs co-transcriptionally (Han et al. 2004; Han et al. 2006; Kim et al. 2007; Morlando et al. 2008) and generates a product with 2 nucleotides with 3' overhang that is specifically recognized by Exportin-5, which transports the pre-miRNAs into the cytoplasm via a Ran-GTP-dependent mechanism (Kim et al. 2009; Okamura et al. 2007). Alternatively, miRNAs may be generated by splicing and debranching of short hairpin introns (Okamura et al. 2007; Ruby et al. 2007) called "MiRtrons", or by processing of small nucleolar RNAs (snoRNAs), transfer RNAs (tRNAs), and endogenous short hairpin RNAs (shRNAs) using a microprocessor complex independent route (Babiarz et al. 2008; Ender et al. 2008; Saraiya et al. 2008; Cole et al. 2009; Czech et al. 2009; Miyoshi et al. 2010). In the cytoplasm, the pre-miRNA enters into the RISC Loading Complex consisting of Dicer (RNase), the double-

stranded RNA-binding domain proteins TRBP, PACT and the core component Ago2 (Gregory et al. 2004; Haase et al. 2005; Lee et al. 2006; MacRae et al. 2008). Dicer, TRBP, and PACT process pre-miRNAs to ~22 nucleotides long miRNAs duplex (Haase et al. 2005; Lee et al. 2006; MacRae et al. 2008; Chendrimada et al. 2005). The two miRNA strands are then separated and the guide strand is associated with an Argonaute protein within the RISC, where it is directly involved in the silencing of target messages. Thermodynamically the miRNAs duplex is asymmetric (Khvorova et al. 2003; Schwarz et al. 2003). As a consequence, miRNA strand whose 5'-end is less stably base-paired will usually be chosen as the strand guide. In contrast, the miRNA strand of which the 5'-end is more stably base-paired (the passenger strand) will be excluded from the RISC Loading Complex and generally degraded (Cartew et al. 2009; Kim et al. 2009; Siomi et al. 2009). The biogenesis of microRNA is represented in Figure 2.

Non-Canonical Function of microRNAs

Recent studies have shown that miRNAs are also re-imported, perhaps, via exportin-1 or importin-8, from the cytoplasm to the nucleus through a combination with Argonaute proteins. Here, miRNAs could regulate

gene expression at the transcriptional level (Kim et al. 2008; Chen et al. 2012; Xia et al. 2013; Salmena et al. 2011; Carninci et al. 2005). Additionally, evidence has highlighted a new regulatory circuit in which miRNAs can crosstalk each other through a new smart “biological alphabet” represented by the “MRE” sequences that “act as the letters whose different combinations may form an entire universe of words” (from Salmela et al. 2011). In detail, Pandolfi’s hypothesis has proposed that mRNAs, miRNAs, transcribed pseudogenes, and long noncoding RNAs (lncRNA, a class of non-protein coding transcripts, usually 200 to 1,000 of nucleotides in length) using MRE sequences “talk” to each other and suggested that this “competing endogenous RNA” (ceRNA) activity forms a large-scale regulatory network across the transcriptome (Salmela et al. 2011), and acts as player in the human genome for regulating the distribution of miRNAs molecules toward specific targets. This mechanism is straightforward for physiological and pathological processes (Salmela et al. 2011; Carninci et al. 2005; Guttman et al. 2009; Cabili et al. 2011; Chi et al. 2009; Licatalosi et al. 2008; Kerreth et al. 2011; Tay et al. 2011).

3.2 MicroRNAs and Amyotrophic Lateral Sclerosis

MiRNAs machinery has been found compromised in ALS (Table 1). For instance the absence of processed miRNAs, due to Dicer deletion in spinal motor neurons, resulted in a mouse model with progressive paralysis, astrogliosis, and signs of axonopathy, classical features of ALS (Haramati et al. 2010). Authors identified a single miR-9-binding site on the neurofilament light polypeptide (NFLP) mRNA and observed that miR-9 was also downregulated in Spinal Muscular Atrophy models thereby suggesting direct evidence for miRNAs malfunction in motor neuron diseases (Haramati et al. 2010). In another study, it was shown that the nuclear factor TDP-43, a major component of the inclusions in ALS patients and Frontotemporal Lobar Degenerative Disorder, was found associated with Drosha complex, thereby involving miRNAs biogenesis. In TDP-43^{-/-} mice let-7b was downregulated, and miR-663 upregulated (Buratti et al. 2010). This phenomenon was correlated with the expression of FUS/TLS suggesting that this complex acts as a cofactor involved in the biogenesis of a specific subset of miRNAs (Morlando et al. 2012). Of note, miRNAs dysregulation

differ from the pre-symptomatic and the end-stage of ALS-SOD1 disease (Butowsky et al. 2012; De Felice et al. 2009). Analysis of the altered mitochondrial network genes in skeletal muscle revealed a contribution of miRNAs and that this kind of dysfunction plays a role in the progression of ALS. An accurate miRNAs expression study revealed a miR-23a, miR-29b, miR-206 and miR-455 upregulations in patients of ALS respect to control subjects (Russell et al. 2012). MiR-23a negatively regulates PGC-1 α signaling, determining a significant reduction of PGC-1 α , cytochrome-b and COXIV protein levels in overexpressing miR-23a transgenic mice (Russell et al. 2012). Recently, Morel et al., reported that the reduction of the expression of the glutamate transporter GLT1 in the end-stage SOD1 G93A mice, a mouse model of ALS, was a consequence of miR-124a activity. Interestingly they revealed an exosome-mediated transfer of microRNAs mechanism showing that miR-124a was transferred from neurons to astrocytes through neuronal exosomes (Morel et al. 2013). miR-206 is required for efficient regeneration of neuromuscular synapses after acute nerve injury, which probably accounts for its salutary effects in ALS (Lin et al. 2010). Evidence indicated that, although mice genetically lacking miR-206 were able to engage normal neuromuscular synapses during development,

deficiency of miR-206 in the ALS mouse model accelerates the disease progression, at least in part through the histone deacetylase 4 (HDAC4) and fibroblast growth factor signaling pathways (Williams et al. 2009). Remarkably, the phenotypes of miR-206 and HDAC4 mutant mice indicated that miR-206 and HDAC4 have opposite effects on retrograde signals required for the reinnervation. Additionally, fibroblast growth factor-7 (FGF7), FGF10, and FGF22, known to be regulators of synapse formation (Fox et al. 2007; Umemori et al 2008), were unaltered in miR-206^{-/-} mice compared to wild type animals, whereas the FGFBP1 protein (a factor that interacts with the FGF family members and enhance the FGF7 activity in rat L6 myoblasts by releasing the FGF up-taken by the extracellular matrix (Beer et al. 2005) was downregulated in muscles of miR-206^{-/-} mice and upregulated in muscles of HDAC4^{-/-} mice after denervation. Collectively, these findings suggest that miR-206 and HDAC4 help and block the innervations of neuromuscular junction, respectively, via opposing effects on FGFBP1 (Williams et al 2009).

3.3 Amyotrophic Lateral Sclerosis and Circulating miRNAs

During the past decade there has been a large increase in the number of ALS biomarker studies using CSF as well as blood. Most of these studies have examined changes of individual proteins in the CSF of ALS versus healthy controls or other neurologic disease subjects, typically using a gel-based system or ELISA. However, most are limited by the number of samples used in the analysis, choice of control subjects, and typically the lack of verification in a separate cohort of patients. At present, CSF candidate biomarkers in ALS can be grouped into those that reflect neuronal loss and those indicative of neuroinflammatory (glial) processes. Regarding miRNAs as possible biomarkers in ALS, we have, so far, little knowledge (Table 1). One study was in fact performed on miRNA profiling of ALS subjects, by analyzing 911 human miRNAs using microarray technology in leukocytes (De Felice et al. 2012). The study reported a profile of identified eight miRNAs that were significantly up- or downregulated in sALS patients as compared to healthy controls. In parallel, an analysis on sorted CD14+CD16- monocytes from ALS patients was performed. It is known that inflammatory monocytes were activated and that their progressive recruitment to the spinal cord correlates with neuronal loss. This study had showed a profile constituting an inflammatory signature of 56 miRNAs significantly

affected in CD14+CD16- monocytes that could serve as a biomarker for disease stage or progression (Butowsly et al. 2012). Despite the two analyses were performed with the same technical approach, the populations of dysregulated miRNAs found in leucocytes (De Felice et al. 2012) and monocytes (Butowsly et al. 2012) are not overlapped and comparable. Nevertheless, the study of circulating miRNA in plasma/serum for diagnosis of neurodegenerative disorders needs again more detailed investigations. Overall, there is a lack of overlap little concordance among these miRNA profiles both for the specific disease and when comparing different neurodegenerative disorders, which highlights the difficulties of analyzing different sample types and comparing different methodologies.

4. DNA Damage Response

All living organisms are constantly exposed to genotoxic stress, and DNA thus needs to be repaired to preserve the information that it encodes. DNA Damage Response (DDR) signaling, represented in Figure 3, is specific to the type of DNA damage that occurs, and the pathways that are activated are determined by the activation of the PI3K-like kinases (PIKKs) ataxia-telangiectasiamutated (ATM), ataxia-telangiectasia and Rad3-related (ATR) and DNA-dependent protein kinase catalytic subunit (DNA-PKcs), which consequently phosphorylate and thus activate various proteins that coordinate the arrest of cell cycle progression and DNA repair pathways to preserve genome integrity. Specifically, the DNA damage response (DDR) pathway is composed of two main DNA damage sensors: the MRE11–RAD50–NBS1 (MRN) complex that detects DNA double-strand breaks (DSBs); and replication protein A (RPA) and the RAD9–RAD1–HUS1 (9-1-1) complex that detects exposed regions of single-stranded DNA. These sensors recruit the apical kinases ataxia-telangiectasia mutated (ATM) (through the MRN complex) and ataxia telangiectasia and Rad3-related (ATR) (through RPA and the 9-1-1 complex), which is bound by ATR-interacting protein (ATRIP). These in turn

phosphorylate (P) the histone variant H2AX on Ser139 (known as γ H2AX) in the region proximal to the DNA lesion. Thus, although ATM is predominantly activated by DSBs, ATR responds to the type of genotoxic stress that is caused by DNA replication stress, which is also caused by oncogenes. γ H2AX is required to recruit mediator of DNA damage checkpoint 1 (MDC1) that further sustains and amplifies DDR signalling by enforcing further accumulation of the MRN complex and activation of ATM. BRCA1 is recruited at sites of DNA damage on phosphorylation by ATM and ATR. p53-binding protein 1 (53BP1) is also involved in sustaining DDR signalling by enhancing ATM activation. DDR signalling relies on additional mechanisms that are based on ubiquitylation. Eventually, DDR signalling spreads away from the damaged locus owing to the engagement of diffusible kinases CHK2 (which is mainly phosphorylated by ATM) and CHK1 (which is mainly phosphorylated by ATR) with signalling converging on downstream effectors such as p53 and the cell division cycle 25 (CDC25) phosphatases. DDR-mediated cellular outcomes may be cell death by apoptosis; transient cell cycle arrest followed by repair of DNA damage and resumption of proliferation; or cellular senescence caused by the persistence of unrepaired DNA damage (Ruwied Di Fagagna 2013).

5. FIGURES AND TABLES

Table 1

miRNA	Sample	Experimental approach	Pilot study	Validation study	Reference
8 miRNAs (miR-451, miR-1275, miR-328, miR-638, miR-149, miR-665 and miR-338-3) significantly up- or downregulated	Leukocytes	miRNA profiling	Microarray ALS: 8 CT: 12	TaqMan [®] miRNA qRT-PCR ALS: 14 CT: 14	[64]
Expression of ALS-specific miRNA inflammatory signature	Monocytes	miRNA profiling	Microarray ALS: 8 MS: 8 CT: 8		[65]

ALS: Amyotrophic lateral sclerosis.

(from Grasso et al. 2014, Molecules, Review)

Figure 1

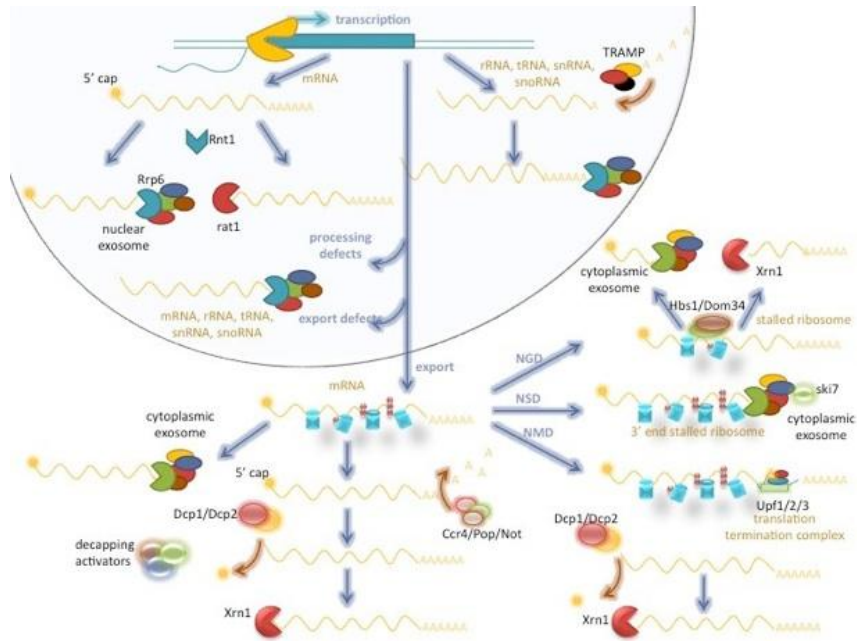


Figure 1: RNA metabolism. The figure (from Lionel Bénard website) describes the main steps of the RNA metabolism.

Figure 2

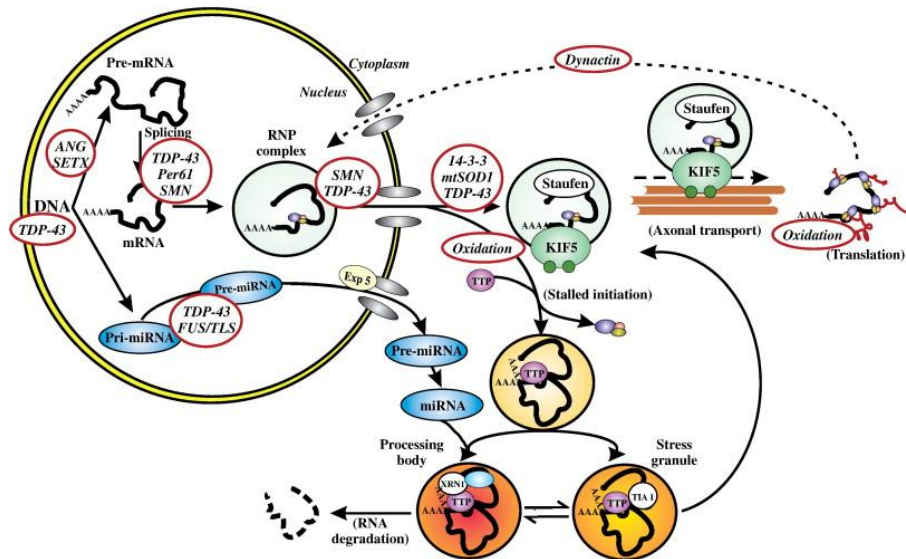


Figure 2: Impairment of RNA metabolism in ALS.

The Figure (from Stong review, Journal of Neurological Science, 2010) represent a schematic illustration of RNA metabolism and potential points of impact for ALS associated mutations or disease processes.

Figure 3

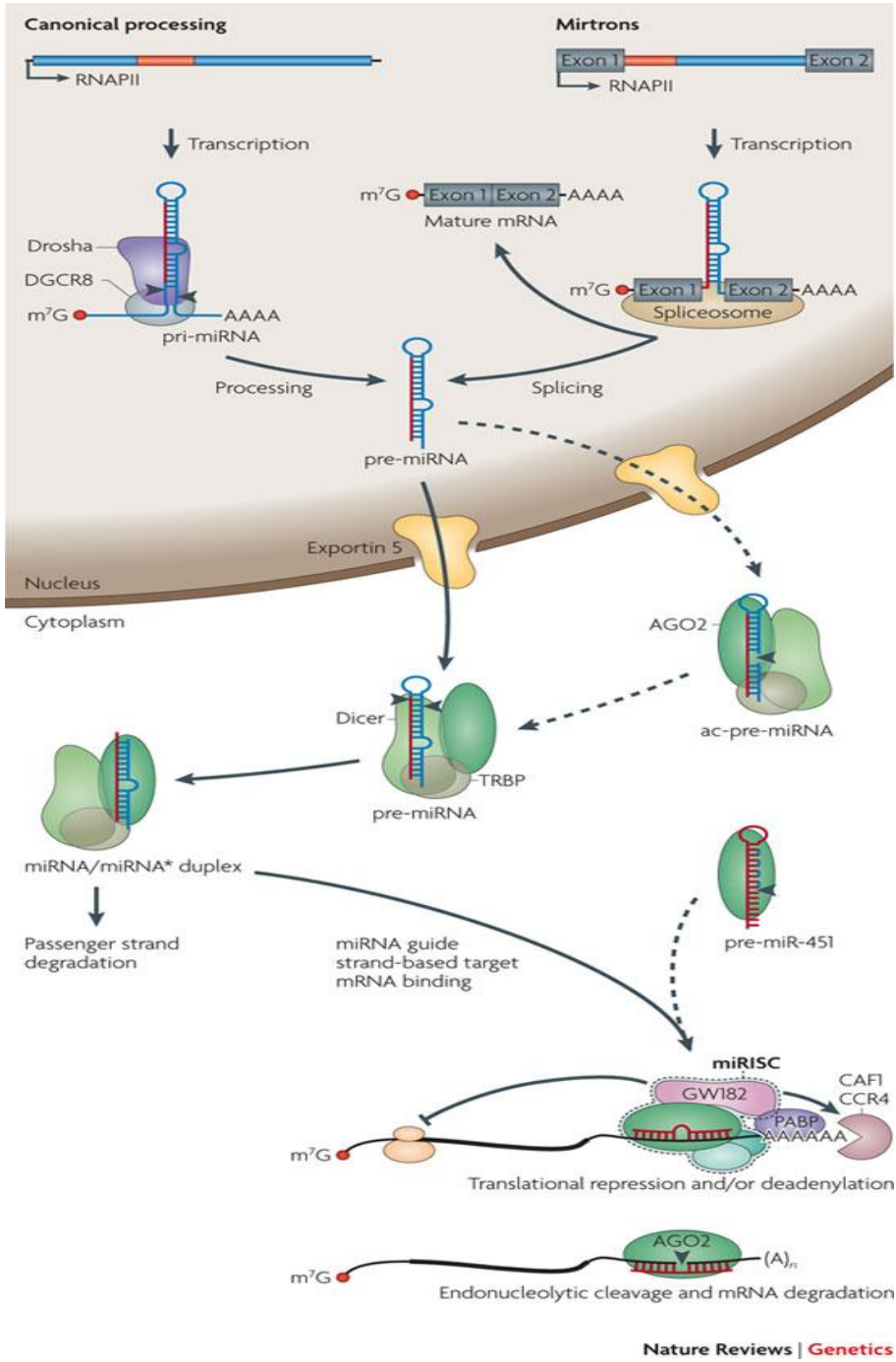


Figure 3: microRNA biogenesis. The figure (from Krol et al. 2010) describes the microRNA synthesis and processing. MicroRNAs (miRNAs) are processed from RNA polymerase II (RNAPII)-specific transcripts of independent genes or from introns of protein-coding genes. In the canonical pathway, primary precursor (pri-miRNA) processing occurs in two steps, catalysed by two members of the RNase III family of enzymes, Drosha and Dicer, operating in complexes with dsRNA-binding proteins (dsRBPs), for example DGCR8 and transactivation-responsive (TAR) RNA-binding protein (TRBP) in mammals.

Figure 4

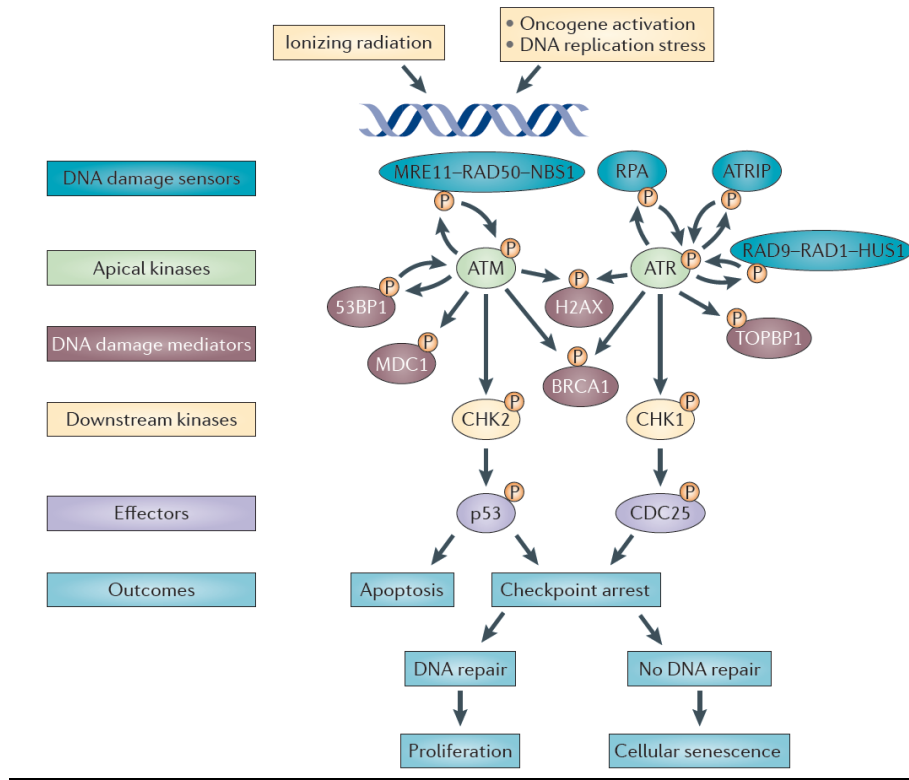


Figure 4: DNA Damage Response. This figure (From F. d’Adda di Fagagna Review 2012) represent the DDR. DNA damage is first detected by sensor proteins which in turn activate transducers in the signal cascade. These transducers then mediate the activation or inhibition of downstream effectors which can arrest the cell cycle or cause apoptosis.

6. Scope of the thesis

The aim of my PhD project was to to obtain new insights into the diverse molecular pathways concerning the impairment of RNA metabolism, involved in ALS pathogenesis.

Chapter 1: General Introduction

This chapter underlines the most recent topic regarding the RNA metabolism and their possible links with Amyotrophic Lateral Sclerosis.

Chapter 2:Unrevealing the impact of microRNA on Amyotrophic Lateral Sclerosis pathogenesis.

In chapter 2, I report the result I have obtained regarding the miRNAs profiles in ALS genetic models and in PBMC of sporadic patients. I characterized the most up-regulated miRNA by studying its targets and I found a potential target that can play a significative role in ALS pathogenesis.

Chapter 3:

In chapter 3, I report the observation obtained from the characterization of loss of function of FUS/TLS, a protein that is causative of ALS. I found that FUS is

implicated with cell proliferation and DNA Damage Response.

Chapter 4: Conclusions and future perspectives

The last chapter summarizes the results obtained and underlines the possible future perspectives, focusing the attention on the putative translational applications of my research.

7. References

Allmang, C., Mitchell, P., Petfalski, E. & Tollervey, D. Degradation of ribosomal RNA precursors by the exosome. *Nucleic Acids Res.* 28, 1684–1691 (2000).

Anderson P, Kedersha N. RNA granules. *J Cell Biol* 2006;172:803–8.

Babiarz, J.E.; Ruby, J.G.; Wang, Y.; Bartel, D.P.; Blelloch, R. Mouse ES cells express endogenous shRNAs, siRNAs, and other microprocesso-independent, Dicer-dependent small RNAs. *Genes Dev.* 2008, 22, 2773–2785, doi:10.1101/gad.1705308.

Bartel, D.P. microRNAs: Genomics, biogenesis, mechanism, and function. *Cell* 2004, 116, 281–297, doi:10.1016/S0092-8674(04)00045-5.

Beer, H.D.; Bittner, M.; Niklaus, G.; Munding, C.; Max, N.; Goppelt, A.; Werner, S. The fibroblast growth factor binding protein is a novel interaction partner of FGF-7, FGF-10 and FGF-22 and regulates FGF activity: Implications for epithelial repair. *Oncogene* 2005, 24, 5269–5277.

Black DL. Mechanisms of alternative pre-messenger RNA splicing. *Annu Rev Biochem.* 2003;72:291–336.

Bognani F, Perrone-Bizzozero NI. RNA–protein interactions and control of mRNA stability in neurons. *J Neurosci Res* 2008;86:481–9.

Bousquet-Antonelli, C., Presutti, C. & Tollervey, D. Identification of a regulated pathway for nuclear pre-mRNA turnover. *Cell* 102, 765–775 (2000).

Buratti, E.; de Conti, L.; Stuani, C.; Romano, M.; Baralle, M.; Baralle, F. Nuclear factor TDP-43 can affect selected microRNA levels. *FEBS J.* 2010, 277, 2268–2281

Burkard, K. T. & Butler, J. S. A nuclear 3'-5' exonuclease involved in mRNA degradation interacts with Poly(A) polymerase and the hnRNA protein Npl3p. *Mol. Cell. Biol.* 20, 604–616 (2000).

Butovsky, O.; Siddiqui, S.; Gabriely, G.; Lanser, A.J.; Dake, B.; Murugaiyan, G.; Doykan, C.E.; Wu, P.M.; Gali, R.R.; Iyer, L.K.; *et al.* Modulating inflammatory monocytes with a unique

Cabili, M.N.; Trapnell, C.; Goff, L.; Koziol, M.; Tazon-Vega, B.; Regev, A.; Rinn, J.L. Integrative annotation of human large intergenic noncoding RNAs reveals global properties and specific subclasses. *Genes Dev.* 2011, 25, 1915–1927.

Carninci, P.; Kasukawa, T.; Katayama, S.; Gough, J.; Frith, M.C.; Maeda, N.; Oyama, R.; Ravasi, T.; Lenhard, B.; Wells, C.; *et al.*; FANTOM Consortium; RIKEN Genome Exploration Research Group and Genome Science Group (Genome Network Project Core Group). The transcriptional landscape of the mammalian genome. *Science* 2005, 309, 1559–1563, doi:10.1126/science.1112014.

Carthew, R.W.; Sontheimer, E.J. Origins and mechanism of miRNAs and siRNAs. *Cell* 2009, 136, 642–655, doi:10.1016/j.cell.2009.01.035.

Chen, X.; Liang, H.; Zhang, C.Y.; Zen, K. miRNA regulates noncoding RNA: A noncanonical function model. *Trends Biochem. Sci.* 2012, 37, 457–459, doi:10.1016/j.tibs.2012.08.005.

Chendrimada, T.P.; Gregory, R.I.; Kumaraswamy, E.; Norman, J.; Cooch, N.; Nishikura, K.; Shiekhattar, R. TRBP recruits the Dicer complex to Ago2 for microRNA processing and gene silencing. *Nature* 2005, 436, 740–744, doi:10.1038/nature03868.

Chi, S.W.; Zang, J.B.; Mele, A.; Darnell, R.B. Argonaute HITS-CLIP decodes microRNA-mRNA interaction maps. *Nature* 2009, 460, 479–486.

Cole, C.; Sobala, A.; Lu, C.; Thatcher, S.R.; Bowman, A.; Brown, J.W.; Green, P.J.; Barton, G.J.; Hutvagner, G. Filtering of deep sequencing data reveals the existence of abundant Dicer-dependent small RNAs derived from tRNAs. *RNA* 2009, 15, 2147–2160, doi:10.1261/rna.1738409.

Cole, C.; Sobala, A.; Lu, C.; Thatcher, S.R.; Bowman, A.; Brown, J.W.; Green, P.J.; Barton, G.J.; Hutvagner, G. Filtering of deep sequencing data reveals the existence of abundant complex. *Cell* **2006**, 125, 887–901.

Czech, B.; Zhou, R.; Erlich, Y.; Brennecke, J.; Binari, R.; Villalta, C.; Gordon, A.; Perrimon, N.; Hannon, G.J. Hierarchical rules for Argonaute loading in *Drosophila*. *Mol. Cell* 2009, 36, 445–456, doi:10.1016/j.molcel.2009.09.028.

Doma, M. K. & Parker, R. Endonucleolytic cleavage of eukaryotic mRNAs with stalls in translation elongation. *Nature* 440, 561–564 (2006).

Ender, C.; Krek, A.; Friedländer, M.R.; Beitzinger, M.; Weinmann, L.; Chen, W.; Pfeffer, S.; Rajewsky, N.; Meister, G. A human snoRNA with microRNA-like functions. *Mol. Cell* 2008, 32, 519–528, doi:10.1016/j.molcel.2008.10.017.

Fox, M.A.; Sanes, J.R.; Borza, D.B.; Eswarakumar, V.P.; Fässler, R.; Hudson, B.G.; John, S.W.; Ninomiya, Y.; Pedchenko, V.; Pfaff, S.L.; *et al.* Distinct target-derived signals organize formation, maturation, and maintenance of motor nerve terminals. *Cell* **2007**, 129, 179–193.

Frischmeyer, P. A. *et al.* An mRNA surveillance mechanism that eliminates transcripts lacking termination codons. *Science* 295, 2258–2261 (2002).

Gherzi, R. *et al.* A KH domain RNA binding protein, KSRP, promotes ARE-directed mRNA turnover by recruiting the degradation machinery. *Mol. Cell* 14, 571–583 (2004).

Grabowski P.J., D.L. Black.. Alternative RNA splicing in the nervous system. *Prog. Neurobiol.*, 65 (2001), pp. 289–308

Gregory, R.I.; Yan, K.P.; Amuthan, G.; Chendrimada, T.; Doratotaj, B.; Cooch, N.; Shiekhattar, R. The Microprocessor complex mediates the genesis of microRNAs. *Nature* 2004, 432, 235–240.

Grosshans, H., Deinert, K., Hurt, E. & Simos, G. Biogenesis of the signal recognition particle (SRP) involves import of SRP proteins into the nucleolus, assembly with the SRP-RNA, and Xpo1p-mediated export. *J. Cell Biol.* 153, 745–762 (2001).

Guttman, M.; Amit, I.; Garber, M.; French, C.; Lin, M.F.; Feldser, D.; Huarte, M.; Zuk, O.; Carey, B.W.; Cassady, J.P.; et al. Chromatin signature reveals over a thousand highly conserved large non-coding RNAs in mammals. *Nature* 2009, 458, 223–227, doi:10.1038/nature07672.

Haase, A.D.; Jaskiewicz, L.; Zhang, H.; Lainé, S.; Sack, R.; Gatignol, A.; Filipowicz, W. TRBP, a regulator of cellular PKR and HIV-1 virus expression, interacts with Dicer and functions in RNA silencing. *EMBO Rep.* 2005, 6, 961–967, doi:10.1038/sj.embor.7400509.

Han, J.; Lee, Y.; Yeom, K.H.; Kim, Y.K.; Jin, H.; Kim, V.N. The Drosha–DGCR8 complex in primary microRNA processing. *Genes Dev.* 2004, 18, 3016–3027, doi:10.1101/gad.1262504.

Haramati, S.; Chapnik, E.; Sztainberg, Y.; Eilam, R.; Zwang, R.; Gershoni, N.; McGlenn, E.; Heiser, P.W.; Wills, A.M.;

Hilleren, P., McCarthy, T., Rosbash, M., Parker, R. & Jensen, T. H. Quality control of mRNA 3'-end processing is linked to the nuclear exosome. *Nature* 413, 538–542 (2001).

Hirokawa N. mRNA transport in dendrites: RNA granules, motors and tracks. *J Neurosci* 2006;26:7139–42.

Houalla, R. et al. Microarray detection of novel nuclear RNA substrates for the exosome. *Yeast* 23, 439–454 (2006).

in leukocytes from sporadic amyotrophic lateral sclerosis. *Gene* **2009**, 508, 35–40.

Kadaba, S. et al. Nuclear surveillance and degradation of hypomodified initiator tRNA^{Met} in *S. cerevisiae*. *Genes Dev.* 18, 1227–1240 (2004). First report that polyadenylation by Trf4 is linked to RNA degradation by the exosome.

Kanai Y, Dohmae N, Hirokawa N. Kinesin transports RNA: isolation and characterization of an RNA-transporting granule. *Neuron* 2004;43:513–25.

Karreth, F.A.; Tay, Y.; Perna, D.; Ala, U.; Tan, S.M.; Rust, A.G.; DeNicola, G.; Webster, K.A.; Weiss, D.; Perez-Keene J, Tenenbaum SA. Eukaryotic mRNPs may represent posttranscriptional operons. *Mol Cell* 2002;9:1161-7

Keene JD. RNA regulons: coordination of post-transcriptional events. *Nat Rev Genet* 2007;8:533–43.

Kent OA, Ritchie DB, Macmillan AM. Characterization of a U2AF-independent commitment complex (E') in the mammalian spliceosome assembly pathway. *Mol Cell Biol.* 2005;25:233–40.

Khvorova, A.; Reynolds, A.; Jayasena, S.D. Functional siRNAs and miRNAs exhibit strand bias. *Cell* 2003, 115, 209–216, doi:10.1016/S0092-8674(03)00801-8.

Kim, D.H.; Saetrom, P.; Snøve, O., Jr.; Rossi, J.J. MicroRNA-directed transcriptional gene silencing in mammalian cells. *Proc. Natl. Acad. Sci. USA* 2008, 105, 16230–16235.

Kim, V.N.; Han, J.; Siomi, M.C. Biogenesis of small RNAs in animals. *Nat. Rev. Mol. Cell Biol.* 2009, 10, 126–139, doi:10.1038/nrm2632.

Kim, Y.K.; Kim, V.N. Processing of intronic microRNAs. *EMBO J.* 2007, 26, 775–783.

Kristjuhan A., J.Q. Svejstrup. Evidence for distinct mechanisms facilitating transcript elongation through chromatin in vivo. *EMBO J.*, 23 (2004), pp. 4243–4252

Kuai, L., Das, B. & Sherman, F. A nuclear degradation pathway controls the abundance of normal mRNAs in *Saccharomyces cerevisiae*. *Proc. Natl Acad. Sci. USA* 102, 13962–13967 (2005).

LaCava, J. et al. RNA degradation by the exosome is promoted by a nuclear polyadenylation complex. *Cell* 21, 713–724 (2005).

Lee, A., Henras, A. K. & Chanfreau, G. Multiple RNA surveillance pathways limit aberrant expression of iron uptake mRNAs and prevent iron toxicity in *S. cerevisiae*. *Mol. Cell* 19, 39–51 (2005). Reports that mRNA-encoding proteins that are involved in iron metabolism are subject to various different nuclear RNA-surveillance pathways.

Lee, Y.; Ahn, C.; Han, J.; Choi, H.; Kim, J.; Yim, J.; Lee, J.; Provost, P.; Rådmark, O.; Kim, S.; Kim, V.N. The nuclear RNase III Drosha initiates microRNA processing. *Nature* 2003, 425, 415–419, doi:10.1038/nature01957.

Lee, Y.; Hur, I.; Park, S.Y.; Kim, Y.K.; Suh, M.R.; Kim, V.N. The role of PACT in the RNA silencing pathway. *EMBO J.* 2006, 25, 522–532, doi:10.1038/sj.emboj.7600942.

Lejeune, F., Li, X. & Maquat, L. E. Nonsense-mediated mRNA decay in mammalian cells involves decapping, deadenylating, and exonucleolytic activities. *Mol. Cell* 12, 675–687 (2003).

Licatalosi, D.D.; Mele, A.; Fak, J.J.; Ule, J.; Kayikci, M.; Chi, S.W.; Clark, T.A.; Schweitzer, A.C.; Blume, J.E.; Wang, X.; et al. HITS-CLIP yields genome-wide insights into brain

alternative RNA processing. *Nature* 2008, 456, 464–469, doi:10.1038/nature07488.

Lin AC, Holt CE. Function and regulation of local axonal translation. *Curr Opin.Neurobiol* 2008;18:60–8.

Lin, N.; Friedlander, R.M. Regeneration of neuromuscular synapses: Action of microRNA-206. *Neurosurgery* **2010**, 66, N19–N20.

Lukong KE, Chang K, Khandjian EW, Richard S. RNA-binding proteins in human genetic disease. *Trends Genet* 2008;24:416-25.

MacRae, I.J.; Ma, E.; Zhou, M.; Robinson, C.V.; Doudna, J.A. In vitro reconstitution of the human RISC-loading complex. *Proc. Natl. Acad. Sci. USA* 2008, 105, 512–517, doi:10.1073/pnas.0710869105.

Mancera, P.A.; et al. In vivo identification of tumor-suppressive PTEN ceRNAs in an oncogenic BRAF-induced mouse model of melanoma. *Cell* 2011, 147, 382–395, doi:10.1016/j.cell.2011.09.032.

Mitchell, P. & Tollervey, D. An NMD pathway in yeast involving accelerated deadenylation and exosome-mediated 3' →5' degradation. *Mol. Cell* 11, 1405–1413 (2003).

Miyoshi, K.; Miyoshi, T.; Hartig, J.V.; Siomi, H.; Siomi, M.C. Molecular mechanism that funnel RNA precursor into endogenous small-interfering RNA and microRNA biogenesis pathways in *Drosophila*. *RNA* 2010, 16, 506–515, doi:10.1261/rna.1952110.

Morlando, M.; Ballarino, M.; Gromak, N.; Pagano, F.; Bozzoni, I.; Proudfoot, N.J. Primary microRNA transcripts are processed co-transcriptionally. *Nat. Struct. Mol. Biol.* 2008, 15, 902–909.

Morlando, M.; Dini Modigliani, S.; Torrelli, G.; Rosa, A.; di Carlo, V.; Caffarelli, E.; Bozzoni, I. FUS stimulates microRNA

biogenesis by facilitating co-transcriptional Drosha recruitment. *EMBO J.* **2012**, *31*, 4502–4510.

Mukherjee, D. et al. The mammalian exosome mediates the efficient degradation of mRNAs that contain AU-rich elements. *EMBO J.* *21*, 165–174 (2002).

Okada, C.; Yamashita, E.; Lee, S.J.; Shibata, S.; Katahira, J.; Nakagawa, A.; Yoneda, Y.; Tsukihara, T. A high-resolution structure of the pre-microRNA nuclear export machinery. *Science* 2009, *326*, 1275–1279, doi:10.1126/science.1178705.

Okamura, K.; Hagen, J.W.; Duan, H.; Tyler, D.M.; Lai, E.C. The mirtron pathway generates microRNA-class regulatory RNAs in *Drosophila*. *Cell* 2007, *130*, 89–100, doi:10.1016/j.cell.2007.06.028.

Polymenidou M, Lagier-Tourenne C, Hutt KR, Bennett CF, Cleveland DW, Yeo GW. Misregulated RNA processing in amyotrophic lateral sclerosis. *Brain Res.* 2012;1462:3–15.

Roth, K. M., Wolf, M. K., Rossi, M. & Butler, J. S. The nuclear exosome contributes to autogenous control of NAB2 mRNA levels. *Mol. Cell. Biol.* *25*, 1577–1585 (2005).

Ruby, J.G.; Jan, C.H.; Bartel, D.P. Intronic microRNA precursor that bypass Drosha processing. *Nature* 2007, *448*, 83–86, doi:10.1038/nature05983.

Salmena, L.; Poliseno, L.; Tay, Y.; Kats, L.; Pandolfi, P.P. A ceRNA hypothesis: The Rosetta Stone of a hidden RNA language? *Cell* **2011**, *146*, 353–368.

Saraiya, A.A.; Wang, C.C. snoRNA, a novel precursor of microRNA in *Giardia lamblia*. *PLoS Pathog.* 2008, *4*, e1000224, doi:10.1371/journal.ppat.1000224.

Schwarz, D.S.; Hutvagner, G.; Du, T.; Xu, Z.; Aronin, N.; Zamore, P.D. Asymmetry in the assembly of the RNAi enzyme complex. *Cell* 2003, *115*, 199–208, doi:10.1016/S0092-8674(03)00759-1.

Schwarz, D.S.; Hutvagner, G.; Du, T.; Xu, Z.; Aronin, N.; Zamore, P.D. Asymmetry in the assembly of the RNAi enzyme complex. *Cell* **2003**, *115*, 199–208.

Seeburg P-H-A-to-I editing: new and old sites, functions and speculations *Neuron*, *35* (2002), pp. 17–20

Siomi, H.; Siomi, M.C. On the road to reading the RNA-interference code. *Nature* 2009, *457*, 396–404, doi:10.1038/nature07754.

Siomi, H.; Siomi, M.C. Posttranscriptional regulation of microRNA biogenesis in animals. *Mol. Cell* 2010, *38*, 323–332, doi:10.1016/j.molcel.2010.03.013.
skin. *Hum. Mol. Genet.* 2013, *22*, 737–748, doi:10.1093/hmg/ddt481.

Takahashi, S., Araki, Y., Sakuno, T. & Katada, T. Interaction between Ski7p and Upf1p is required for nonsense-mediated 3'-to-5' mRNA decay in yeast. *EMBO J.* *22*, 3951–3959 (2003).

Tay, Y.; Kats, L.; Salmena, L.; Weiss, D.; Tan, S.M.; Ala, U.; Karreth, F.; Poliseno, L.; Provero, P.; di Cunto, F.; et al. Coding-independent regulation of the tumor suppressor PTEN by competing endogenous mRNAs. *Cell* 2011, *147*, 344–357, doi:10.1016/j.cell.2011.09.029.

Tollervey, D. RNA lost in translation. *Nature* *440*, 425–426 (2006).

Torchet, C. et al. Processing of 3' extended read-through transcripts by the exosome can generate functional mRNAs. *Mol. Cell* *9*, 1285–1296 (2002).

Tran, H., Schilling, M., Wirbelauer, C., Hess, D. & Nagamine, Y. Facilitation of mRNA deadenylation and decay by the exosome-bound, DExH protein RHAU. *Mol. Cell* *13*, 101–111 (2004).

Umemori, H.; Sanes, J.R. Signal regulatory proteins (SIRPS) are secreted presynaptic organizing molecules. *J. Biol. Chem.* **2008**, *283*, 34053–34061.

van Hoof, A., Frischmeyer, P. A., Dietz, H. C. & Parker, R. Exosome-mediated recognition and degradation of mRNAs lacking a termination codon. *Science* *295*, 2262–2264 (2002).

van Hoof, A., Lennertz, P. & Parker, R. Yeast exosome mutants accumulate 3'-extended polyadenylated forms of U4 small nuclear RNA and small nucleolar RNAs. *Mol. Cell. Biol.* *20*, 441–452 (2000).

Vanacova, S. et al. A new yeast poly(A) polymerase complex involved in RNA quality control. *PLoS Biol.* *3*, e189 (2005). A biochemical analysis of the activity of the TRAMP complex, showing that it can recruit the exosome to degrade an aberrant tRNA in vitro.

Wahl MC, Will CL, Luhrmann R. The spliceosome: design principles of a dynamic RNP machine. *Cell.* 2009;136:701–718.

Wang I-F, Wu L-S, Chang H-Y, Shen C-KJ. TDP-43, the signature protein of FTL-DU, is a neuronal activity responsive factor. *J Neurochem* 2008;105:797–806.

Williams, A.H.; Valdez, G.; Moresi, V.; Qi, X.; McAnally, J.; Elliott, J.L.; Bassel-Duby, R.; Sanes, J.R.; Olson, E.N. microRNA-206 delays ALS progression and promotes regeneration of neuromuscular synapses in mice. *Science* **2009**, *326*, 1549–1554.

Wyers, F. et al. Cryptic Pol II transcripts are degraded by a nuclear quality control pathway involving a new poly(A) polymerase. *Cell* *121*, 725–737 (2005).

Xia, J.; Joyce, C.E.; Bowcock, A.M.; Zhang, W. Noncanonical microRNAs and endogenous siRNAs in normal and psoriatic human

Xia, J.; Joyce, C.E.; Bowcock, A.M.; Zhang, W. Noncanonical microRNAs and endogenous siRNAs in normal and psoriatic human skin. *Hum. Mol. Genet.* **2013**, *22*, 737–748.

Chapter 2

Manuscript in preparation

Unraveling the impact of microRNA on Amyotrophic Lateral Sclerosis pathogenesis

Alessia Loffreda¹, Marc-David Ruepp² and Silvia
M. L. Barabino¹

1: Department of Biotechnology and Biosciences, University of
Milano-Bicocca, Piazza della Scienza 2, Milan, Italy

2: Department of Chemistry and Biochemistry, University of Bern,
Freiestrasse 3, 3012 Bern, Switzerland

Keywords: microRNA, Amyotrophic Lateral Sclerosis, ELAVL4/HuD,
PBMC

2.1 Abstract

Amyotrophic lateral sclerosis (ALS) is a neurodegenerative disease that specifically affects upper and lower motor neurons leading to progressive paralysis and death. There is currently no effective treatment. Thus, identification of the signaling pathways and cellular mediators of ALS remains a major challenge in the search for novel therapeutics.

Recent studies have shown that microRNA have a significant impact on normal CNS development and onset and progression of neurological disorders. Based on this evidence, in this study we test the hypothesis that misregulation of miRNA expression play a role in the pathogenesis of ALS. Hence, we exploited human neuroblastoma cell lines expressing SOD(G93A) mutation as tools to investigate the role of miRNAs in familiar ALS. To this end, we initially checked the key molecules involved in miRNAs biogenesis and processing on these cells and we found a different protein expression pattern. Subsequently, we performed a genome-wide scale miRNA expression, using whole-genome small RNA deep-sequencing followed by quantitative real time validation (qPCR). This strategy allowed us to find a small group of up and down regulated miRNA, which are predicted to play a

role in the motorneurons physiology and pathology. We measured this group of misregulated miRNA by qPCR on cDNA derived from (G93A) mice at different stage of disease and furthermore on cDNA derived from lymphocytes from a group of sporadic ALS patients. We found that mir-129-5p was up-regulated in cells, mice and in patients and we validated that HuD as mir129-5p target. It has been reported that ELAVL4/HuD plays a role in neuronal plasticity, in recovery from axonal injury and multiple neurological diseases. Furthermore, we generated stable cell line overexpressing mir129-5p and we found a reduction in neurite outgrowth and in the expression of differentiation markers in compare to control cells. Taken together these data strongly suggest that microRNAs play a role in ALS pathogenesis and in particular that mir129-5p can affect neuronal plasticity by modulating ELAVL4/HuD level.

2.2 Introduction

ALS is a progressive, fatal neurodegenerative disorder characterised by loss of motoneurons from the spinal cord and motor cortex that leads to death within 2-3 years of onset (Cleveland and Rothstein 2001). It is one of the most common motor neuron diseases occurring 1.7 ~ 2.3 out of 100,000 person per year worldwide (Beghi et al., 2006). The symptoms of ALS usually starts after age 50, but it can occur in younger age group. The disease manifests itself by the onset of degeneration in specific subset of motor neurons. It progressively spreads to neighboring motor neurons and leads to atrophy of associated muscle tissues (Pratt et al., 2012). The genetic and environmental causes of ALS are still under investigation, but 90% of ALS cases are sporadic or caused by unknown genetic factors. So far only about 10% of the cases can be traced to genetic factors (Al-Chalabi et al. 2012). The most well known genetic cause of ALS are mutations in or deletion of Cu/Zn Super Oxide Dismutase 1 (SOD1)(Rosen et al., 1993). Only recently, with advanced genomic screening tools, several other genes associated to ALS have been identified including TAR DNA-binding protein (TDP-43), FUS, ALS 2 (ALS2), neurofilament heavy peptide (NEFH); (Al-Chalabi et al.,

2012) and C9ORF72 (DeJesus-Hernandez et al., 2011; Renton et al., 2011). While C9ORF72 has been identified as the most prevalent mutation among ALS patients, with 40 % of fALS patients carrying the mutation (Majounie et al. 2012), the abundance and variety of identified SOD1 mutations have made this a widespread experimental paradigm (Renton et al.2011). Although the pathological characteristics of ALS are well defined, the cellular and mechanisms causing ALS due to mutation or deletion of these genes are still under investigation.

MicroRNAs (miRNAs) are endogenous non-coding single-stranded RNA molecules that play important roles in eukaryotic gene expression through posttranscriptional regulation (Bartel, 2009). They mainly bind to the 3'-untranslated region (3'-UTR) of messenger RNAs (mRNAs) from target protein-coding genes and lead to gene silencing by mRNA cleavage, translational repression and deadenylation (Huntzinger and Izaurralde, 2011). MiRNAs are involved in a variety of physiological phenomena and diseases (Kim et al., 2009). In the central nervous system diseases, the loss of Dicer, a key regulator of miRNA biogenesis, induces neurodegeneration, suggesting that miRNAs may play important roles in neurological disorders (Cuellar et al., 2008 and Schaefer et al., 2007). In fact, while the role

of individual miRNAs in neurological disorders is not yet fully understood, there are growing evidences that miRNAs play a critical role in neurological disorders, such as miR-206/miR-153 in Alzheimer's disease (Lee et al., 2012; Liang et al., 2012), miR-34b/miR-9/miR-9* in Huntington's disease (Packer et al., 2008; Gaughwin et al., 2011), miR-128a/miR-24/let-7b in mood disorder (Zhou et al., 2009), miR-189 in Tourette's syndrome (Abelson et al., 2005), miR-9 in SMA (Haramati et al., 2010), miR-106/miR-338-3p/miR-451 in ALS (Williams et al., 2009; Butovsky et al., 2012; De Felice et al., 2012), miR-21/miR-431/miR-138 for axonal regeneration for sensory neurons (Strickland et al., 2011; Liu et al., 2013; Wu and Murashov, 2013), and miR-133b/miR-21 for spinal cord injury (Yu et al., 2011; Hu et al., 2013). However, pathological contribution of individual miRNAs to each of these diseases is still under investigation. Especially, our knowledge about the role of miRNAs in motor neuron diseases is very limited. This can be both due to the complexity of the nervous system and the technical difficulties of studying neurological disorders. MicroRNAs have also demonstrated their potential as non-invasive biomarkers from blood and serum for a wide variety of human pathologies as well as neurodegenerative diseases (Keller et al. 2011).

Concerning ALS, miRNA expression in white blood cells from sporadic ALS patients appears to exhibit distinct expression patterns during disease progress. miRNA profiling data from 14 patients and 14 controls showed that expression of miR-338-3p is increased and expression of seven other miRNAs is decreased in leukocyte from ALS patients (De Felice et al., 2012). Moreover, another recent publication reports that miR-206 was found increased in the circulation of symptomatic animals and in a group of 12 definite ALS patients and it suggests that may be an interesting potential candidate as a biomarker. To further characterize the roles of miRNAs in ALS pathogenesis and their potential use as biomarkers and, hopefully, also targets for new therapy in ALS, profiling of miRNA expression in experimental ALS models is necessary. Here, we present a characterization of miRNA expression in a cellular model of SOD(G93A) linked to ALS. Initially, we analysed by Western Blot the expression of crucial factors involved in miRNA biogenesis and processing and we observed an altered pattern between cells carrying the mutation and the control cells. Afterwards, we used the RNA high throughput sequencing to obtain the miRNA profile of SOD1(G93A) cells and we identified a small subset of deregulated miRNAs that we analysed in (G93A)mice,

subsequently. In order to discover a common signature between familial and sporadic ALS, we tested the expression level of the two most up-regulated miRNAs (mir129-5p and mir200c) we found in SOD(G93A) cells as well as mice, in PBMC taken from sporadic ALS patients. We observed that mir-129-5p is upregulated in cells, mice and PBMC and we validated ELAVL4/HuD as mir129-5p new target. Furthermore, we generated stable cell line overexpressing mir129-5p and we found a reduction in neurite outgrowth and in the expression of differentiation markers in compare to control cells. Taken together these data strongly suggest that microRNAs play a role in ALS pathogenesis and in particular that mir129-5p can affect neuronal plasticity by modulating ELAVL4/HuD level.

2.3 Results

Proteins involved in miRNAs biogenesis and processing are differentially expressed in SHSY-5Y SOD1(G93A) cells.

It has been reported that in different neurodegenerative disorders there is an impairment of proteins involved in miRNAs biogenesis and processing (Leea et al 2011; Bicchi et al 2013). Moreover, two ALS associated genes FUS and TDP43 are directly involved in miRNAs biogenesis pathway (Gregory et al. 2004) . In particular TDP-43 is a component of the Dicer and Drosha complexes and more recently, it has been shown that FUS/TLS promotes biogenesis of specific miRNAs via recruiting Drosha to primary miRNA transcripts. In order to unravel the impact of miRNAs in ALS pathogenesis we exploited human neuroblastoma cell lines expressing SOD(G93A) mutation and SOD(WT) as ALS familiar model. As an initial characterization, we analysed, by Western Blot, the protein level of some of the key players in miRNA biogenesis and processing (Figure 1A and 1B). In particular, we analysed Drosha and its cofactor DCRG8, that process pri-miRNA in pre-miRNA and we found an slight decrease of about 0,5-1,5 fold change for both

proteins in G93A cells. EWS and TAF15, the two proteins that together with FUS compose the FET family (known Drosha interactors), were found increased of about 1-2 fold change in cells carrying the mutation in comparison to WT cells, while FUS and TDP43 do not show any change. Intriguingly, we found different proteins level also concerning Dicer, the RNaseIII enzyme that leads pre-miR to mature microRNA, that resulted 2-3 fold change increased. We analysed also the protein level of Exportin 5, but we did not find any changes. These results shows that in our model system there is an impairment of the biogenesis and processing complex that realistically has an impact on miRNAs level, but further analysis are necessary to understand the mechanism underlying the regulation.

The expression of a subset of miRNAs is modified in a genetic cellular model of ALS.

The different protein pattern of miRNAs regulators suggested a misregulation in miRNAs expression. Different approaches can be used to identify expressed miRNAs. As a first screening we used a computational identification inferred from the expression changes in their putative mRNA targets. Previously, in our laboratory, we had performed a whole-genome splicing

sensitive microarray analysis of human neuroblastoma cell line (SHSY-5Y) stably expressing wild-type SOD1 (WT-SOD1) versus cells expressing a pathogenic mutation (G93A-SOD1) (Lenzken et al. 2011). This analysis allowed the definition of both transcription patterns (gene-level analysis) and the alternative pre-mRNA maturation events (exon-level analysis). The results obtained revealed that there are profound changes in the expression of genes involved in relevant pathways for nervous system development and function such as: axon guidance and growth, synaptic vesicles formation and recycling, cytoskeleton structure and movement. Thus, we used the T-REX (Target Reverse Expression) algorithm to identify regulated miRNAs via the modulation of their predicted targets (Volinia et al. 2010). Essentially, this algorithm is based on the assumption that when a miRNA is active in the cell, its target mRNAs are repressed and vice versa if the targets are over-expressed, the controlling miRNA is down-regulated. This computational approach identified 54 (Table 1) putative differentially expressed miRNAs in SH-SY5Y/SOD1(G93A) cells. As a next step, we performed a Next Generation high through-put Sequencing (miRNA-seq) on the same cell lines and we found 9 differentially expressed miRNA (Table 2) between SH-SY5Y cells expressing either SOD1 or the

mutant SOD1(G93A). To validate both the T-REX and the NGS output, we carried out quantitative real time PCRs (qPCR) and we confirmed the differential expression of a group of miRNAs present both in the NGS and T-REX list in line with the qPCR validation (Figure 3A). In particular we observed the up-regulation of mir-129 (six fold change), the mir-200c (three fold change) and the mir-7 (nearly two fold change); and to the down-regulation of mir-124 and mir-455 (about 0.2 fold change for both).

Characterization of miRNAs expression in G93A mice

In order to investigate if the expression of the misregulated miRNAs, validated in a cellular model, could be affected also in a model more related to the pathology, we analysed their level in transgenic mice overexpressing the SOD1-G93A mutation. Fourteen of the differentially expressed miRNAs were analysed on RNA extracted from spinal cord of four transgenic mice carrying the SOD1-G93A. In particular two mice were at preonset stage (<120 days), two at the early stage (135 days) and two were at symptomatic stage (140-170 days) of the disease. As a control we used four normal littermates of the corresponding age group. Our

results at the preonset stage show that the majority of the analysed miRNAs are comparable to the control (Figure 2A). The only exceptions was mir129-5p that was drastically up-regulated, about 4 fold change. As it is shown in Figure 2B, at the early stage of disease progression, we could confirm the up-regulation of mir-129-5p and mir-200c, even with a lower fold change induction and variably also of mir-7 . Instead, the down regulation of mir-124 we had found in SH-SY5Y cells was not comparable in mice. Instead we found an up-regulation of mir-455 that was found to be downregulated in cells. Surprisingly, at the symptomatic stage (Figure 2C) we found a slight global downregulation of each miRNA making most of them again similar to the control mice, with the exception of mir-200c that is drastically reduced. These results may suggest that miRNAs expression may variate in a stage specific manner. In particular mir129-5p shows a strong increase at the pre-onset and its level decreases with the progression of the disease suggesting its potential role in the disease arise.

Mir-129-5p and Mir-200c are up-regulated in PBMC of sporadic ALS patients

Our result suggested a potential role of mir-129-5p and mir-200c in the ALS pathogenesis. The increasing relevance of characterization of miRNAs profiling in biofluids in different neurodegenerative pathologies, has prompted the study of these misregulated miRNA in peripheral blood mononuclear cells (PBMC) of sporadic ALS patients by qPCRs. In particular, we analysed samples of almost thirty patients and twenty-two controls taken from healthy voluntaries (Figure 3). Interestingly, we found a significative up-regulation (2-fold change) of mir129-5p and mir200c in patients samples. While the expression of mir-200c shows an higher standard deviation, mir129-5p has a good reproducibility among patients. Based on these results we decided to further characterize mir129-5p investigating its putative targets and the role they may play in ALS onset and progression.

Mir-129-5p predicted targets

The human genome encodes over 1000 miRNAs that collectively target the majority of mRNAs. Base pairing of the so-called miRNA 'seed' region with mRNAs identifies many thousands of putative targets. The vast majority of predicted targets, often with quite disparate functions, make a real challenge choosing which is

worthy of experimental follow-up. To address this challenge, predictors may use thermodynamic, evolutionary, probabilistic or sequenced-based features. So far the best strategy to pull-out good candidates is to compare which targets have a high score for every one of these features. In order to define the mechanism by which mir-129-5p up-regulation can contribute in ALS pathogenesis we looked at its bioinformatic-predicted targets. Following the criteria mentioned above and wondering which targets could be significantly involved in ALS pathology, we selected four potential targets that are described in the Table 3 with a short description. Starting from the output of the microarray profiling experiment, initially we decide to investigate the genes whose expression was found to be down-regulated in our system: HOXC10 and CACNG2 genes. HOXC10 belongs to the homeobox family of transcription factors. We selected this gene because it has been demonstrated that mutant mice (HoxC10^{-/-}) have a reduction in lumbar motor neurons (Hostikka et al. 2009). CACNG2 (Calcium channel, voltage-dependent, gamma subunit 2) also known as stargazin is involved in the transportation of AMPA receptors to the synaptic membrane, and the regulation of their receptor rate constant (Chen et al., 2000). We decide to investigate this putative target for the well

known implication of AMPA in ALS pathogenesis. Moreover, we decided to further analyze the ELAVL4/HuD transcript which was not present in the output list of the microarray for the well characterized role of HuD in neuronal cell identity, maturation and survival. As a first step we validated the microarray expression data for these genes by qPCR and checked for ELAVL4/HuD transcript level. This validation showed a good correlation with the microarray data and confirmed the down-regulation of the three transcripts (Figure 5).

ELAVL4/HuD is targets of mir-129-5p

In order to validate the putative targets of mir-129-5p by bioinformatic analysis, we performed a luciferase assay. We used a plasmid that express the pre-miR-129 sequence and a plasmid with the UTR of the gene cloned upstream of the luciferase gene (in which we cloned the 3'-UTR of the predicted target). After a transient co-transfection of both plasmids we tested the ability of mir-129 to bind the 3'-UTR of the considered gene by luciferase assay. We first focused on HoxC10. The bioinformatic analysis of this region identified one "conserved sites" for mir-129-5p consisting in a "8mer seed match" that means an exact match to positions 2-

8 of the mature miRNA (the seed + position 8) followed by an 'A'. As it is shown in the Figure 6A the luciferase activity decrease in response to the presence of miR-129-5p with a molar ratio of 1:1 between mir and UTR. Next, we cloned the 3'-UTR of CACNG2. The sequence of UTR has four conserved sites, one of them is "8mer" and three are "7mer-m8" that means an exact match to positions 2-8 of the mature miRNA (the seed + position 8). Finally, we cloned the 3'-UTR of ELAVL4/HuD that shows only one "7mer-m8" conserved seed sequence. As shown in Figure 6B e 6C, for both genes, the luciferase activity decreased in response to the presence of miR129-5p with a molar ratio of 1:1 between mir and UTR of both the UTR sequences. These results show that there is a decrease of luminescence activity for every UTR of almost 40% for ELAVL4/HuD up to the 70%, for CACNG2, suggesting that the three genes examined were targets of mir129-5p.

Since, there are controversial opinions regarding the use of the luciferase assay to test the "miRNA-target interaction" because the transfection is only about the UTR sequence so it is not really possible to measure the available of seed sequence and the thermodynamic features. Thus this method may be considered a way to force the interaction. To escape this controversies and

be more confident about the targets, we generated a stable cell line that over-express pre-mir129-1 and we measured the endogenous protein level of the putative targets we selected. As shown in Figure 8 the Western Blot analysis revealed that only ELAVL4/HuD protein level is really affected by the mir129-5p over-expression (almost 60% of decrease), while stargazin presented only a slight decrease and HOXC10 an up-regulation. These results showed that even if mir129-5p is able to bind the 3'-UTR of the three genes, only ELAVL4/HuD endogenous protein is strongly affected by the miR over-expression.

The Overexpression of pre-mir129-1 inhibits neurite outgrowth and differentiation

Our data strongly suggested that ELAVL4/HuD is target of mir129-5p. The multiple post-transcriptional effects exerted by ELAVL4/HuD on mRNAs whose proteins have key roles in neurons and its expansive spatiotemporal expression within the nervous system strongly suggest that ELAVL4/HuD acts as a "master regulator" of various neuronal processes (Deschenes-Furry et al. 2006; Perrone-Bizzozero and Bird 2013). Although the most established role of HuD is in neurogenesis, studies are surfacing depicting its

importance in neuronal function and survival, as well as plasticity during learning and memory and following neuronal injury. Additionally, there is accumulating support implicating misregulation and mutation of ELAVL4/HuD in neuronal pathologies and neuroendocrine cancers, further stressing the significance of this protein in the nervous system. Moreover a previous publication indicate that ELAVL4/HuD down-regulation is able to inhibit the differentiation of Neurites (Abdelmohsen et al. 2010). Based on these reports and in order to characterize the phenotypical effect of mir129-5p over-expression we checked and measured the neurites outgrowth of SH SY5Y stable transfected with pre-mir129-1 plasmid compared to control cells transfected with empty vector before and after differentiation treatment with retinoic acid. As is shown in Figure 9A the SH SY5Y mir129-1 cell line shows shorter neurites and a bigger and rounded cellular body in compare to control cells. Moreover, the Figure 9A shows the reduced differentiation phenotype following retinoic acid treatment in cells overexpressing mir129-1 relative to empty vector control. To measure the variance in differentiation level between the cells overexpressing the mir129-1 and the cells with the empty vector we performed a qPCR on genes that are marker of

differentiation as ASCL1 and GAD43. As is shown in Figure 9B there is an increase of differentiation markers in SH SY5Y mir129-1 cells but its notably lower in compare to the level in control cells. This results indicate an impairment of neurites formation when mir129-1 is over-expressed.

2.4 Discussion

Post transcriptional regulation of gene expression made by microRNA is increasingly recognized as an important general mechanism by which the function and morphological plasticity of dendrites, axons and synapses are controlled locally in response to various environmental signals. Indeed, there is a consistent number of works that characterize the miRNA expression and their potential role in the mechanism that leads at the majority of the main neurodegenerative diseases. Nevertheless little is known concerning ALS. So far, there are two miRNAs expression study, analysed in skeletal muscle and leukocytes carried out in a small group of ALS patients. Those study revealed a small group of misregulated miRNAs whitout any overlapping between the works. Our study started from the observation that miRNAs machinery was compromised in a chronic mitochondrial

stress and familial ALS cellular model, the SH SY5Y neuroblastoma cells carrying the G93A mutation. In particular, on one hand we found a slight decrease of the two main proteins of microprocessor, Drosha and DGCR8 that could lead to a reduction in the amount of the pre-miRNA cellular pool. The down-regulation of Drosha could be an effect of the observed increase of EWS protein. In fact, it has demonstrated recently, that the FET protein member EWS is able to negative regulates Drosha (Kim et al. 2014). On the other hand, the increase in the level of Dicer may result in the processing of a subset of pre-Mirs compared to other miRNAs that required different cofactors. Indeed, it has been demonstrated that some Dicer partners proteins are able to bind Dicer and promote the processing of particular miRNAs (Krol et al. 2010). However to elucidate the mechanism by which the expression of specific miRNAs can be modified will be needed further investigations. In this study, we carried out the miRNA profiling by RNA high throughput sequencing in cellular line of a familial model of ALS (G93A) that allowed us to identify a small group of misregulated miRNAs. Only one miRNA, mir-124 in this small pool was already characterized in neurodegenerative disorders (Johnson et al. 2008). More recently mir200c was linked to synaptic function and neuronal survival in Huntington

disease (Jin et al 2012). We analysed the dysregulated miRNAs in a small group of ALS mice carrying the same cellular mutation (G93A) at the pronset, at early and symptomatic stage of the disease. We found a correlation between SH-SY5Y (G93A) cells and (G93A) mice concerning the up-regulation of mir129-5p and mir200c. As was reasonably expected miRNAs dysregulation differs from pre-onset to the end-stage of the disease. Intriguingly, we found that the expression of mir129-5p is increased at the pre-onset while its level decreases with the progression of the disease suggesting that this miR could be one of the first player acting in the pathological cascade that leads to ALS. Thereafter, in order to find a common signature between familial and sporadic ALS and in effort to find new biomarker in easily accessible sample such as blood, we checked the two most up-regulated miRNA in PBMC of sporadic ALS patients. This would be not the first case in which a microRNA linked to neurodegenerative disorders is found up-regulated both in neuronally differentiated human cells and in human plasma (Gaughwin et al 2011) candidate it as a biomarker. Subsequently, we studied the predicted targets and we validated ELAVL4/HuD as target of mir129-5p.

Recent en masse analysis of ELAVL4/HuD-associated mRNAs in mouse brain revealed that many ELAVL4/HuD targets encoded proteins with vital roles in neuronal differentiation, cytoskeletal transport, and RNA metabolism (Bolognani 2010). These findings fully support HuD's ability to promote neuronal development, synaptic plasticity, and nerve regeneration (Pascale et al 2008; Perrone-Bizzozzero 2002). Accordingly, ectopic interventions to overexpress or downregulate HuD in cultured neuronal models revealed a role for HuD in the expression of target mRNAs and in controlling neuronal morphology (Deschenes-Furry 2006). HuD-null mice show deficient neurogenesis, nerve development, and motor and sensory functions (Akamatsu 2005). To test the effect of downregulation of HuD due to microRNA regulation, we generated stable cell line overexpressing mir129-5p and we found a reduction in neurite outgrowth and in the expression of differentiation markers in compare to control cells. Taken together these data strongly suggest that microRNAs play a role in ALS pathogenesis and in particular that mir-129-5p can affect neuronal plasticity by modulating HuD level. Additionally, it is important to underline that the correlation among cells, mice and PBMC for mir129-5p, together with the observation that in mice the major

increase of miRNA level is at the preonset stage makes mi129-5p a potential biomarker for ALS. In many patients with ALS in population-based studies, diagnostic certainty currently entails a delay of about 1 year from onset of symptoms to diagnosis (Zoccolella et al 2011); this delay prevents early treatment with a disease-modifying drug. Moreover, at least 30% of anterior horn neurons are thought to have degenerated by the time distal muscle wasting is visible (Swash et al. 1988). Therefore, reliance on symptoms or clinical examination to trigger intervention might not be adequate if degeneration is no longer salvageable at that stage. Thus, an early diagnostic biomarker might prove to be clinically useful only if those at risk of developing ALS can be identified and screened before the onset of symptoms.

ACKNOWLEDGEMENTS

We would like to thank the following people:

Doctor Lucio Tremolizzo and Alessandro Arosio for providing the patients samples;

Raffaele Calogero and Stefano Volvinia for the bioinformatic analysis.

2.5 Figures and Tables

Table 1

MI-RNA	Down-regulated	Up-regulated
miR-30a-5p	0,00079	0,09218
miR-30b	0,00079	0,09218
miR-30c	0,00079	0,09218
miR-30d	0,00079	0,09218
miR-30e-5p	0,00079	0,09218
let-7a	0,00264	0,72438
let-7b	0,00264	0,72438
let-7c	0,00264	0,72438
let-7e	0,00264	0,72438
let-7f	0,00264	0,72438
let-7g	0,00264	0,72438
let-7i	0,00264	0,68389
miR-146a	0,00264	0,25051
miR-146b	0,00264	0,25051
miR-29a	0,00264	0,10903
miR-29b	0,00264	0,10903
miR-29c	0,00264	0,10903
miR-98	0,00264	0,72438
miR-1	0,00455	0,14317

⋮ ⋮ ⋮
(S. Volinia, University of Ferrara)

Table1: Computational identification of miRNAs.

Splicing-sensitive Microarray Analysis of Models of Mitochondrial Stress (SH SY5Y G93A cells) show profound changes in the expression of genes involved in relevant pathways for neuron survival at gene-level and in pre-mRNA splicing. T-REX algorithm identifies regulated miRNAs via the modulation of their predicted

targets.54 putative differentially expressed miRNAs in SH-SY5Y/SOD1(G93A) cells.

Table 2

ENSEMBL ID	miR16 precursor	Log2 FC
ENSG00000199077	hsa-mir-129-2	UP mt
ENSG00000207598	hsa-mir-124-3	DW mt
ENSG00000207705	hsa-mir-129-1	UP mt
ENSG00000207703	hsa-mir-7-2	UP mt
ENSG00000207713	hsa-mir-200c	UP mt
ENSG00000221419	hsa-mir-1287	UP mt
ENSG00000221630	hsa-mir-1179	UP mt
ENSG00000216135	hsa-mir-885	DW mt
ENSG00000207726	hsa-mir-455	DW mt

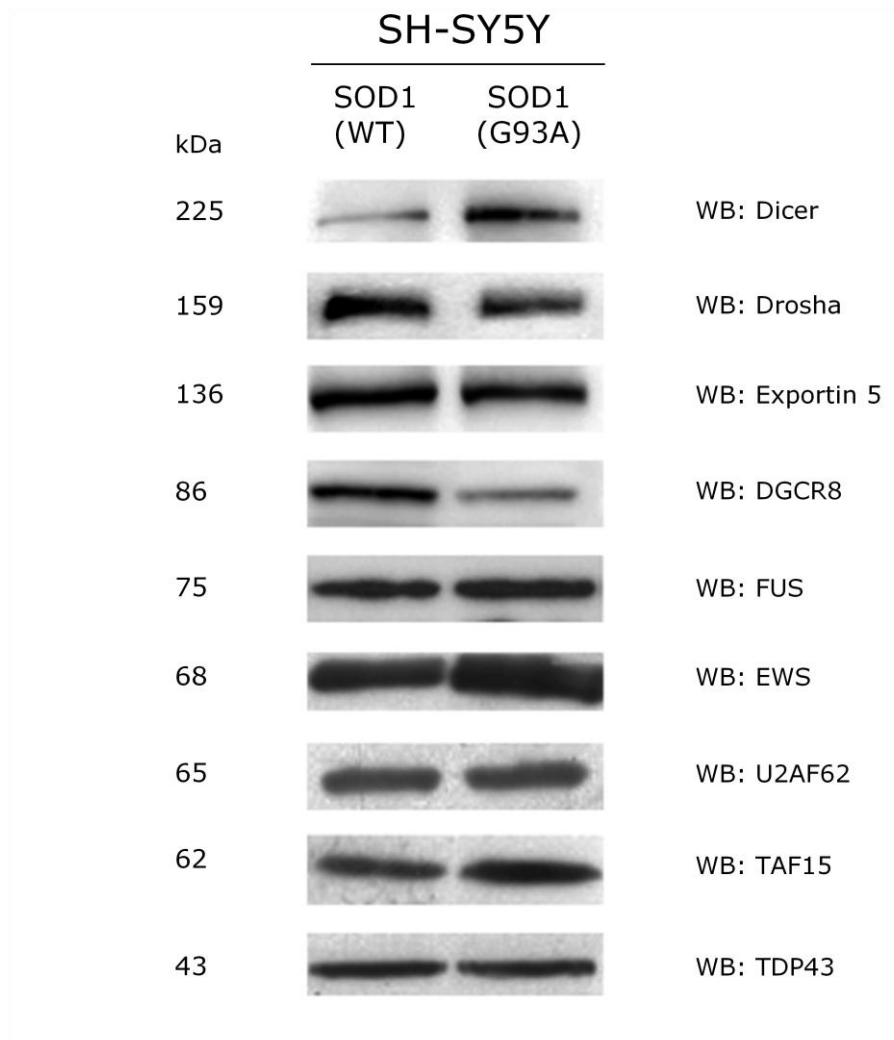
(R. Calogero, University of Turin)

Table2: Next generation High throughput sequencing output. The RNA sequencing shows 9 differentially expressed miRNA between SH-SY5Y cells expressing either SOD1 or the mutant SOD1(G93A).

Table3: List of potential target of mir-129-5p

Homeobox protein Hox-C10	It has been demonstrated that mutant mice have a reduction in lumbar motor neurons
Calcium channel, voltage-dependent, gamma subunit 2 (CACNG2)	CACNG2 also known as stargazin is involved in the transportation of AMPA receptors to the synaptic membrane, and the regulation of their receptor rate constant
ELAVL4	The HuD/ELAVL4 protein is an RNA binding protein. It is expressed only in neurons and it binds to AU rich-element containing mRNAs. As a result of this interaction the half-life of the transcript is increased. HuD is important in neurons during brain development and plasticity.
VCP	The protein encoded by this gene is a member of a family that includes putative ATP-binding proteins involved in vesicle transport and fusion. VCP mutations may account for approximately 1%–2% of familial ALS.

Figure 1



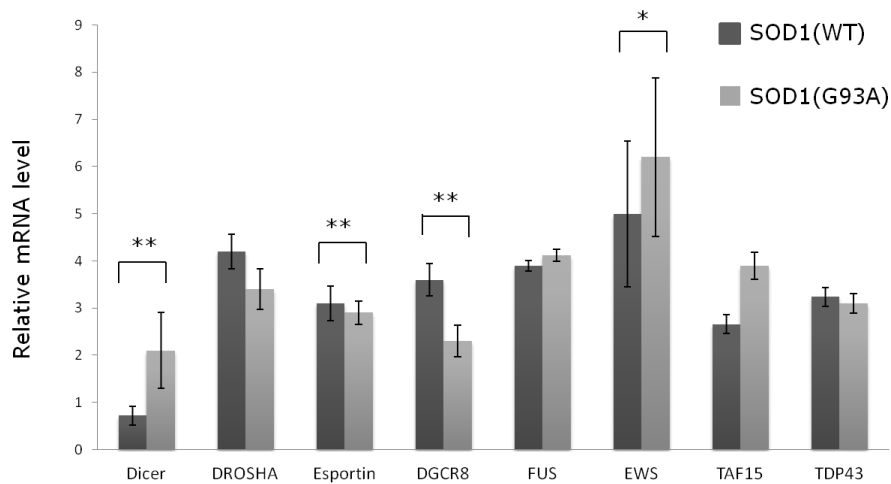


Figure 1: Analysis of proteins involved in microRNA biogenesis by Western Blot. (A) In the first and second lane are shown the proteins from total lysates of cells SOD1(G93A) and SHSY-5Y SOD1(WT) respectively. The proteins were detected using Li-cor Technology. **(B)** Relative quantification of proteins detected. Data were normalized to GAPDH amount for protein with low molecular weight and vinculin for protein with high molecular weight.

Figure 2

microRNA level in SOD1(G93A)
SH-SY5Y cells

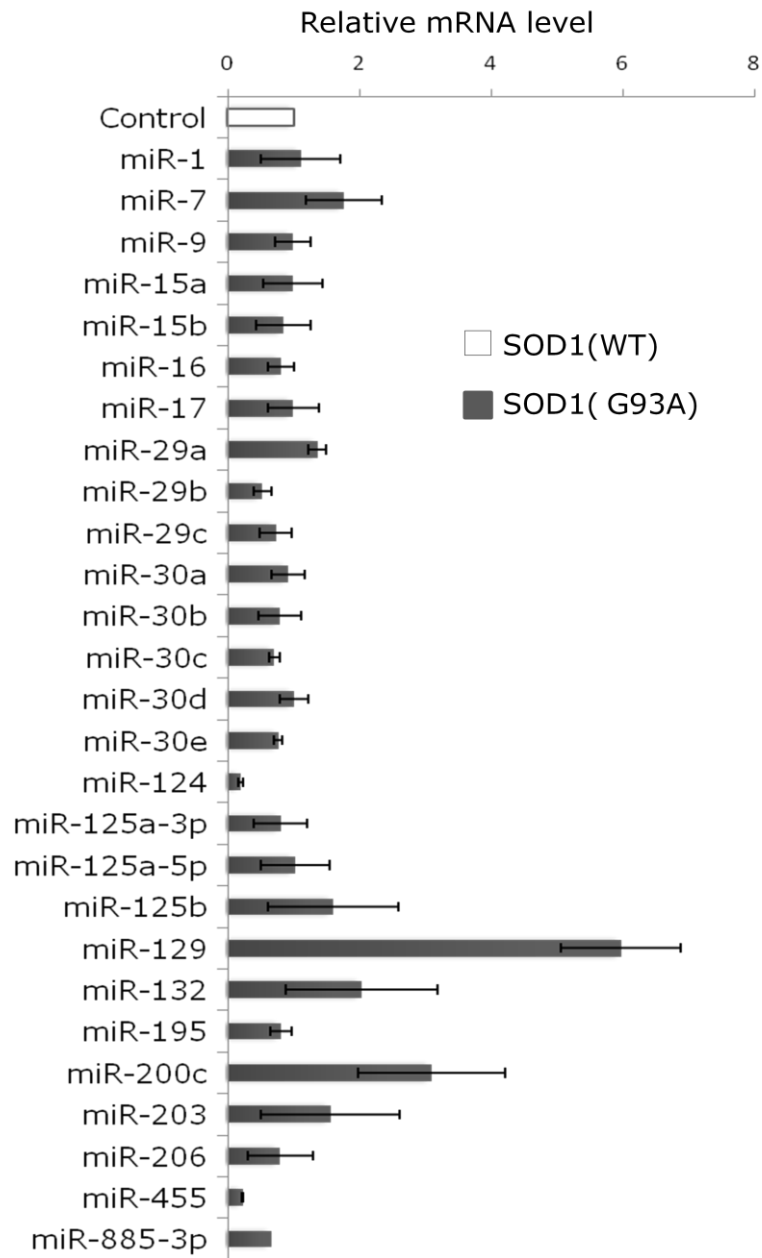
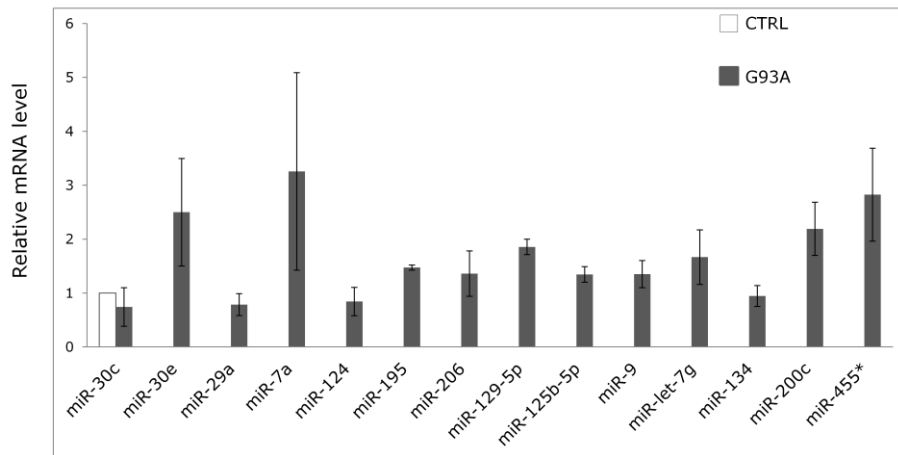


Figure 2: Validation by RT-qPCR of the top ranking up- or down-regulated miRNAs identified by T-REX and those identified by RNAseq. Experimental validation of misregulated miRNA identified by T-REX and by RNA-seq by qPCR (n=3 independent experiments) in SHSY-5Y cells stably expressing SOD1 WT (in blue) and in SHSY-5Y stably expressing SOD1G93A (in violet). Data were normalized to snoRD25.

Figure 3

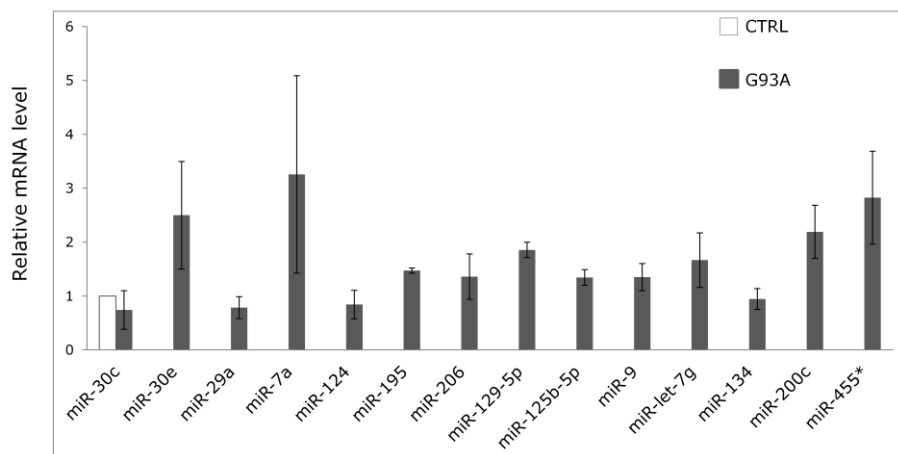
A

microRNA level in G93A mice at early stage of ALS



B

microRNA level in G93A mice at early stage of ALS



C

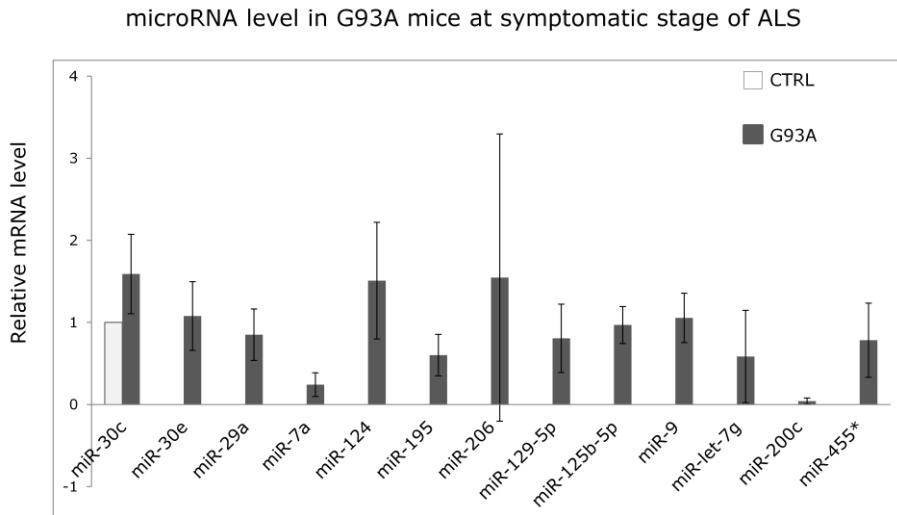


Figure 3: Analysis of misregulated microRNA in ALS mice. Analysis of misregulated microRNA in mice (n=2 biological replicates) carrying the SOD1(G93A) at the preonset (<100 days), Figure 3A; early stage (135 days) of disease, Figure 3 B, and at the symptomatic stage (140-170), Figure 3 C. Data were normalized to RNU1A1 and mir16.

Figure 4

A

	ALS (n=28)	CTRL (n=22)
Age	63,6 ± 12,6	62,9 ± 12,0
Gender (M/F)	15/13	11/11
Form (Spinal/Bulbar)	20/8	n/a
ALSFRS-R	23,3 ± 7,2	n/a
Disease duration (months)	32,5 ± 30,2	n/a

B

microRNA level in PBMC of sporadic ALS patients

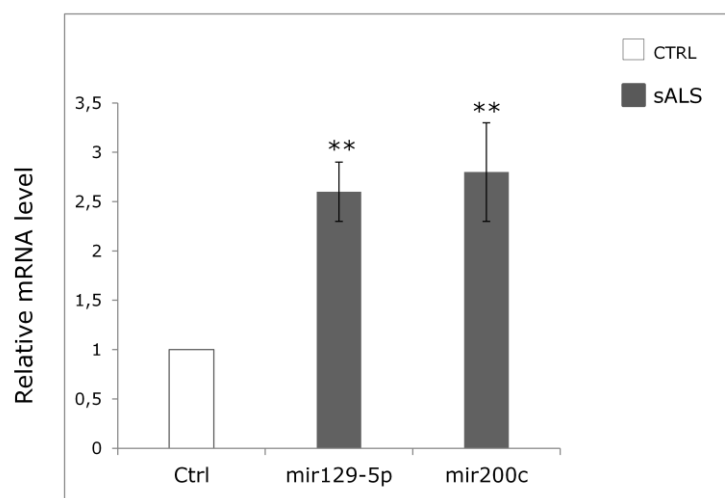


Figure 4: Analysis of the expression of misregulated miRNA in patients. (A): Classification table of the collected samples. **(B):** Analysis of the expression of the top up-regulated miRNAs on RNA extracted from peripheral blood mononuclear cells (PBMC) of sporadic ALS patients. Data were normalized to mir16 expression and Snord25.

Figure 5

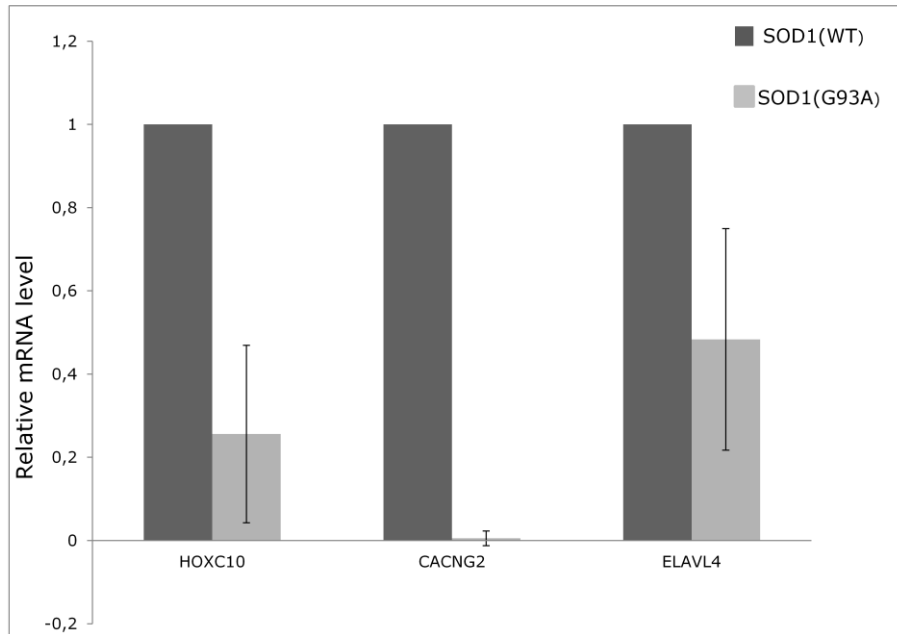
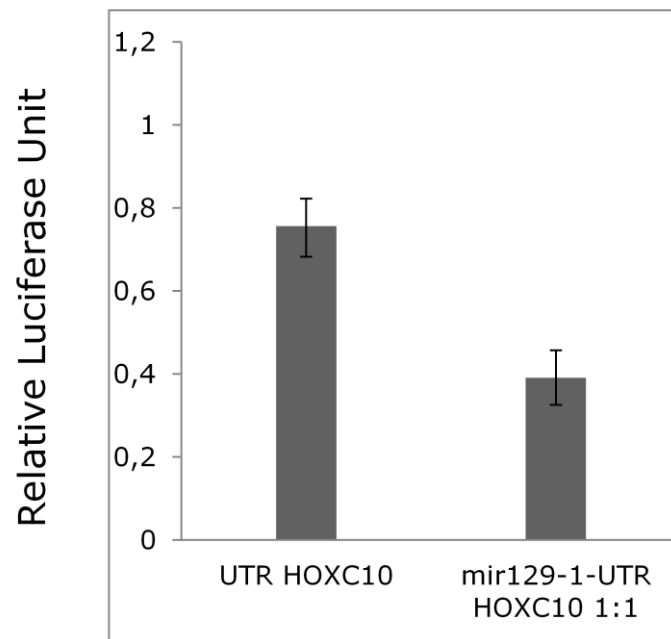


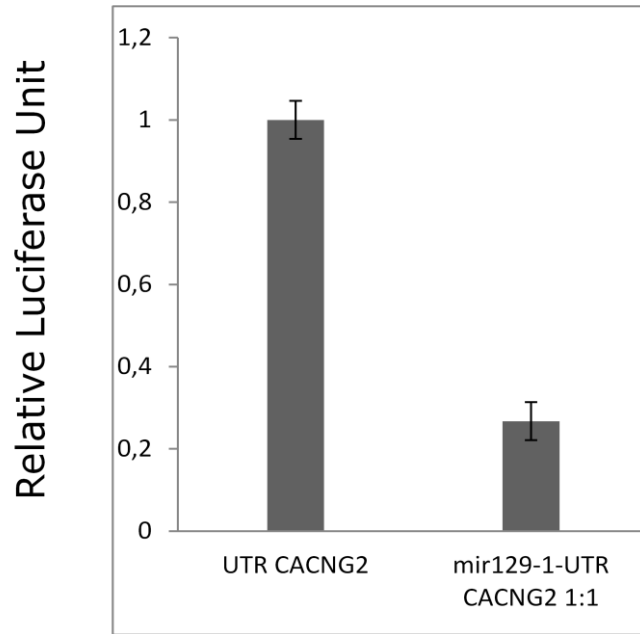
Figure5: Analysis of the expression of miRNA targets. Results of RT-qPCR carried out on SH-SY5Y cells over-expressing the SOD1 wild type (WT) or the mutated SOD1 (G93A) in order to confirm the down-regulation of the putative mir129-5p targets.

Figure 6

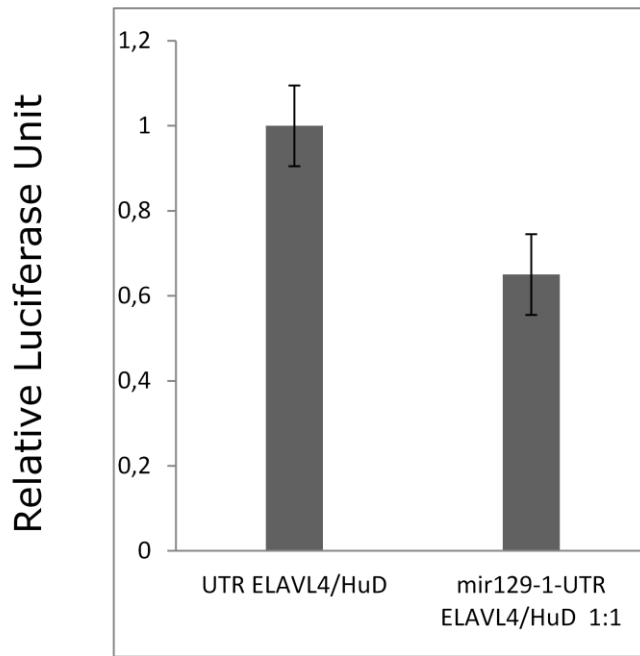
A



B



C



6: Validation of putative targets of mir 129-5p by

luciferase assay. The first histogram shows the luminescence due to the luciferase gene expressed from the the UTR plasmid. The second shows the reduced level of luminescence in presence of mir-129-5p precursor. The amount of microRNA and UTR is 1:1.

A Shows the reduction of luminescence due to the binding of mir129-5p to HOXC10 UTR in SH SY5Y cells.

B Shows the reduction of luminescence due to the binding of mir129-5p to CACNG2 UTR in HEK cells. **C**

Shows the reduction of luminescence due to the binding of mir129-5p to ELAVL4/HUD UTR in HEK cells.

Figure 7

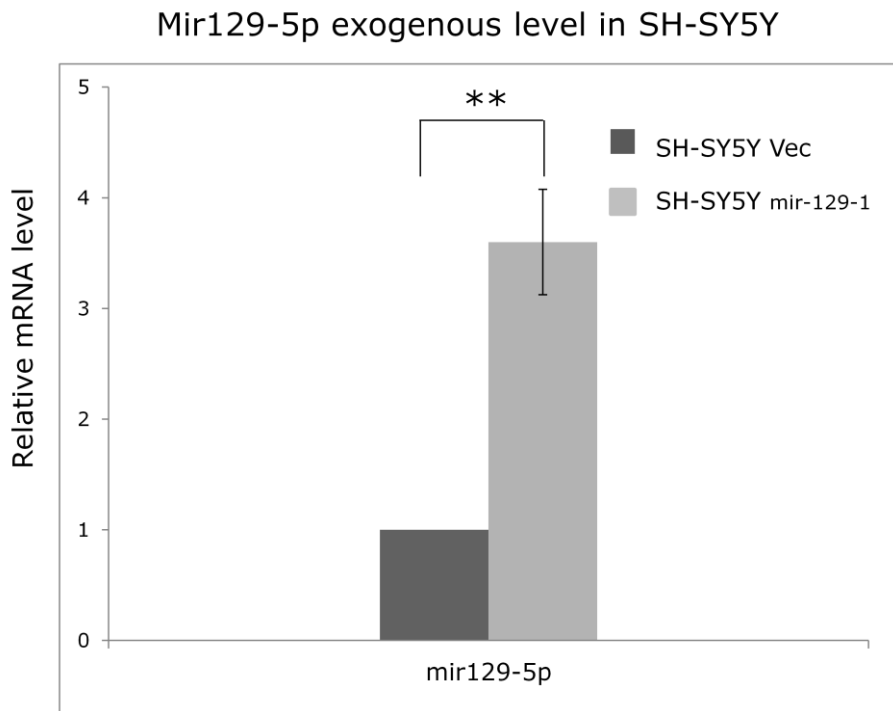
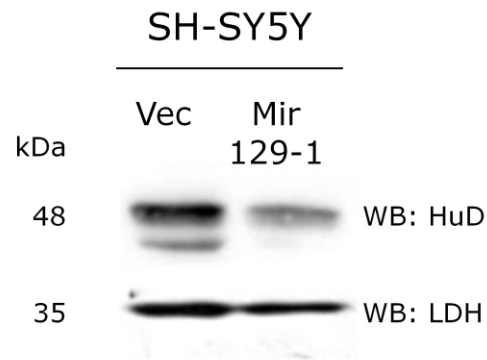
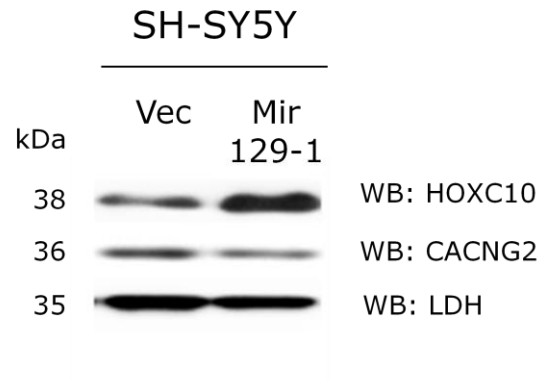


Figure7: Analysis of the expression of exogenous mir129-5p in SH SY5Y. Results of RT-qPCR carried out on SH-SY5Y cells upon transfection of the precursor mir 129-1 in order to confirm the upregulation of the microRNA.

Figure 8

A



B

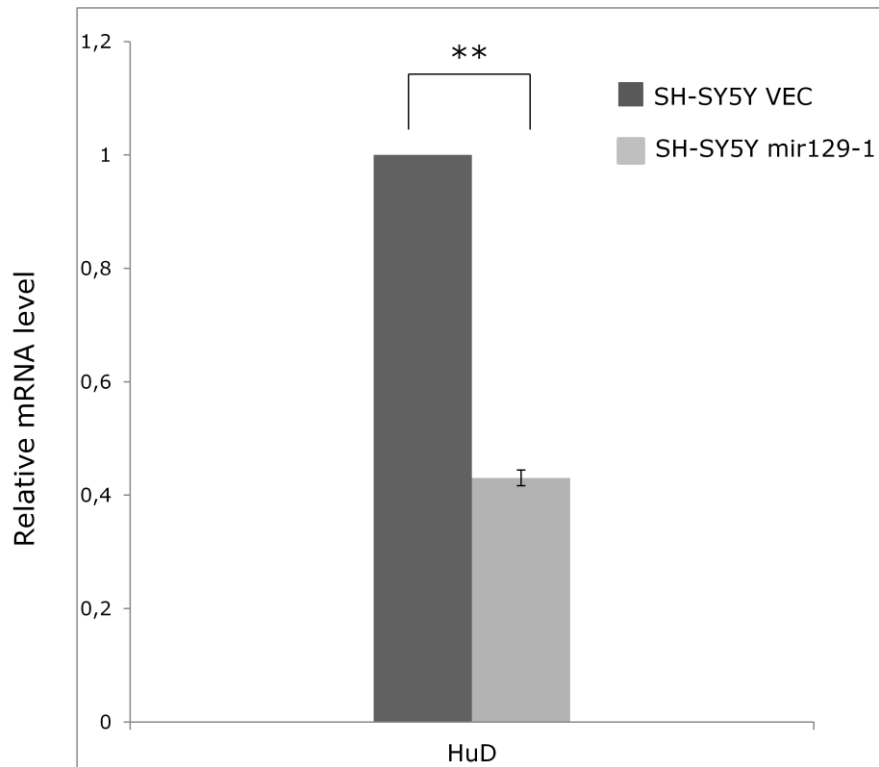
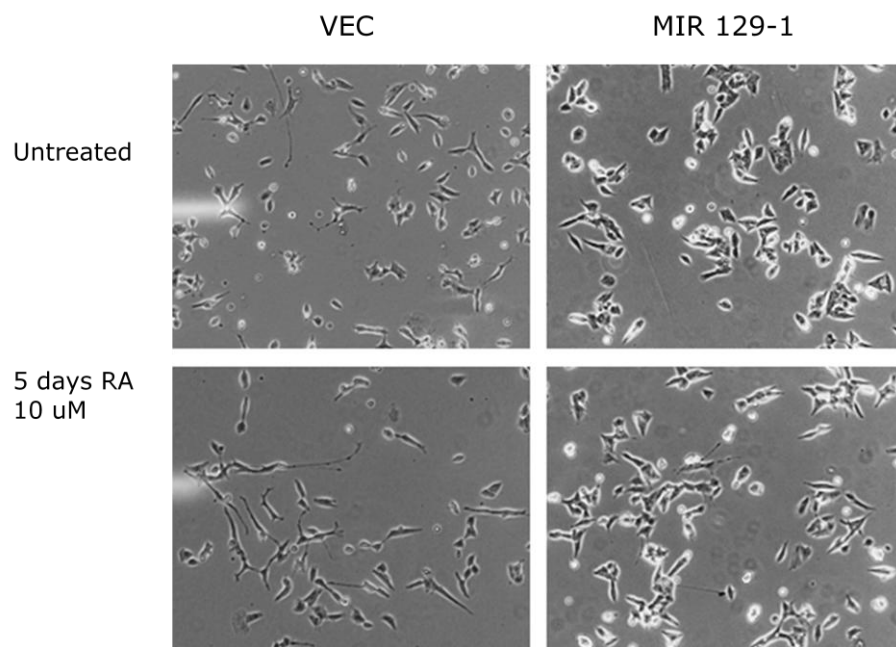


Figure 8: Validation of the putative targets of mir129-5p by western blot. (A) In the first and second lane are shown the proteins from total lysates of cells transfected with the empty vector (Vec) and with pre-mir129-5p (mir129-5p). The protein analysed are the endogenous HOXC10, CACNG2 and HuD. **(B)**

Relative quantification of proteins detected. Data were normalized on LDH amount.

Figure 9

A



B

Differentiation markers in cells overexpressing pre-mir129-1 upon AR treatment

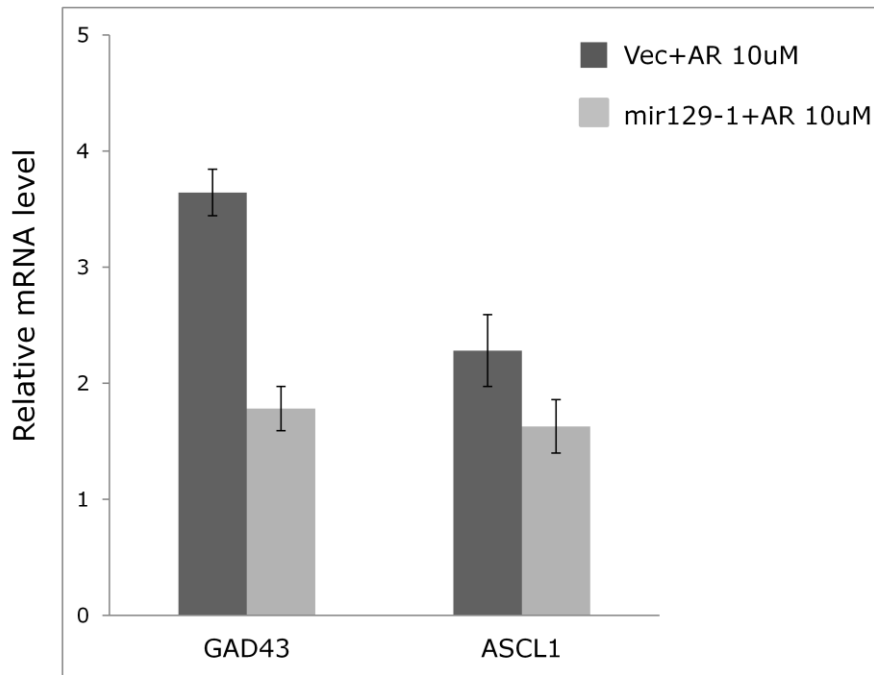


Figure9: Analysis of the overexpression in SH SY5Y cells. A The first lane shows the morphology of the cells transfected with pre-mir129-1 versus cells expressing the empty vector. SH SY5Y mir129-1 cell line shows shorter neurites and a bigger and rounded cellular body in compare to control cells (VEC). Upon Retinoic Acid treatment (10uM for 6 days) the VEC cells show long neurites while only few cells in pre-mir129-1 have an increasing in neurites length. **B** Analysis of differentiation level between the cells overexpressing

the mir129-1 and the cells with the empty vector we performed by qPCR on ASCL1 and GAD43 markers of differentiations. Data were normalized to GAPDH expression.

2.6 Materials and Methods

RNA high throughput sequencing

Human neuroblastoma SHSY-5Y cells untransfected or stably transfected with cDNAs coding for wild type SOD1 or the mutant SOD1(G93A) were sequenced by whole-genome small RNA deep-sequencing (sRNA-seq) using Solexa system. For the statistical analysis (performed by Dr. R. Calogero Bioinformatics and Genomics Unit, University of Turin) were considered only those reads that will be greater than 10 nucleotides.

Cell cultures, transfections and drug

Human neuroblastoma SHSY-5Y cells untransfected or stably transfected with cDNAs coding for wild type SOD1 or the mutant SOD1(G93A) were maintained in Dulbecco's modified Eagle's Medium (Euroclone) supplemented with antibiotics (100 U/mL streptomycin and 100 µg/ml penicillin), 2,5 mM L-Glutamine and 10% Fetal Bovin Serum (all from Euroclone) at 37 °C with 5% CO₂. SOD-1 stably transfected cells were also maintained in the presence of 400 µg/mL Geneticin

(G418 sulphate, Euroclone, prepared as 40 mg/ml stock solution in water). Cells were fed every 2-3 days and passed once a week.

For the luciferase assay experiments, $1,5 \times 10^5$ SHSY-5Y cells were seeded in a 24 multiwell, and the next day plasmids (a total of 1,2 μ g) were co-transfected using Polyethylenimine (PEI, Sigma, 100 mM in H₂O pH 7.00) according to the manufacturer's instruction.

For differentiation treatment cells were incubated with Retinoic Acid treatment at 10 μ M for 6 days before collecting.

PBMC isolation

PBMC were isolated from whole blood by Ficoll-Histopaque (GE Healthcare) density gradient centrifugation. Briefly, blood samples were diluted with the same amount of saline solution, layered on Ficoll-Histopaque and centrifuged (490_g, 30 min, room temperature). PBMC were collected from the interface between plasma and Ficoll-Histopaque, washed with saline solution, aliquoted and stored at -80°C.

RNA extraction reverse-transcription and Quantitative Real-Time PCR assay (qPCRs)

SYSH-5Y cells were seeded on 10 cm plates, and 24 hours after plating the RNAs were extracted using TRIzol Reagent (Invitrogen) and subsequently purified using silica membrane spin columns from RNeasy Mini Kit (Qiagen). RNA quantity and purity were assessed using a NanoDrop instrument (Thermo Fisher Scientific Inc.). 2 µg of total RNA were reverse-transcribed using the random hexamers-based High Capacity cDNA Reverse-Transcription Kit (Applied Biosystem), according to manufacturer's instructions.

In order to validate the microarray data regarding HOXC10, CACNG2, and ELAVL4 genes, level downregulation qPCRs were performed in a final volume of 20 µl with SYBR Green qPCR master mix (Applied Biosystem), 1 µl cDNA diluted (1:50), and 0,5 µM of each primer. The primers used for CACNG2 genes were: forward: 5' CTCTCTACTCCCACCCCTTG 3'; reverse: 5' GCTCTGCTCCGTCTTGATTT 3'; for HOXC10 were: forward: 5'ACTCGAGAAGATGCCGGATAATCGG'; reverse: 5'ATCTAGTCAGCTGTCAAGAGGAAGC3'.

Normalization of cDNA loading was obtained running all samples in parallel using human GAPDH as housekeeping gene. The primers for GAPDH were:

forward: 5'ACGGATTTGGTCGTATTGGG3'; reverse: 5'TGATTTTGGAGGGATCTCGC3'. The amplification protocol was as follow: an initial denaturation and activation step at 95 °C for 10 min, followed by 40 cycles of 95 °C for 15 s, 60 °C for 1 min and 95 °C for 15 s. Normalization of the target amplification over the normalize was performed using Excel software.

miRNA extraction, reverse transcription and qPCR for SHSY-5Y cells and PMBC

The cell pellet from PMBC was lysed by adding 1 ml of Trizol. In order to obtain a microRNA enriched fraction the aqueous phase was processed using the Absolutely RNA miRNA kit (Agilent Technologies) according to the manufacturer's protocol.

The microRNA from SHSY-5Y cells were extracted using the Absolutely RNA miRNA kit (Agilent Technologies) according with the protocol.

2µg of miRNA were used for retro-transcribing reaction that was performed using an home made miRNA detection kit. Essentially in the retrotranscription reaction a poly-A tail is added to the mature microRNA template by E. coli Poly(A) polymerase (New England Biolabs); cDNA is synthesized by the Affinityscript

polymerase (New England Biolabs), using a poly-T primer with a 5' universal tags and a 3' a degenerate anchor. The cDNA template is then amplified using a micro-RNA specific forward primer and a universal reverse primer (that is complementary to the universal tag). SYBR Green (MESA GREEN qPCR MasterMix Plus) is used for detection.

List of specific forward primers:

Hsa-mir30a	Hsa-mir124
ACATCCTCGACTGGAAGAA	CACGCGGTGAATGCCAAA
Hsa-mir30b	Hsa-mir125a-3p
TGTAAACATCCTACACTCAGCTAA	GTSAGGTTCTTGGGAGCCAAA
Hsa-mir30c	Hsa-mir125-5p
TGTAAACATCCTACACTCTCAGCAA	CTGAGACCCTTTAACCTGTGAAA
Hsa-mir30d	Hsa-mir125b
CATCCCCGACTGGAAGAA	CCCTGAGACCCTAACTTGTGAAA
Hsa-mir30e	Hsa-mir-132
AACATCCTTGACTGGAAGAA	CAGTCTACAGCCATGGTCGAAA
Hsa-mir29a	Hsa-mir17
CACCATCTGAAATCGGTTAA	GTGCTTACAGTGCAGGTAGA
Hsa-MIR29b	Hsa-miR7
TAGCACCATTGAAATCAGTGTTAA	TGGAAGACTAGTATTTTGTGTAAA
Hsa-mir1	Hsa-mir200C
TGGAATGTAAAGAAGTATGTATAA	TAATACTGCCGGGTAATGATGGAAAA
Hsa-mir206	Hsa-mir885-3p
TGGAATCTAAGGAAGTGTGTGGAA	AGGCAGCGGGGTGTAGTGGATAAA
Hsa-mir15a	Hsa-mir455-5p
GCAGCACATAATGGTTTGTGAAA	TATGTCCTTTGGACTACATCGAAA
Hsa-Mir15B	Hsa-Mir9
GCAGCACATCATGGTTTACAAA	TCTTTGGTTATCTAGCTGTATGAAA
Hsa-mir16	Hsa-mir455-3p
CAGCACGTAAATATTGGCGAA	GCAGTCCATGGGCATATTCACAA
Hsa-mir195	Hsa-mir1179
TAGCAGCACAGAAATATTGGCAA	AAGCATTCTTTCATTGGTTGGAAA
Hsa-mir203	Hsa-mir1287
GTGAAATGTTTAGGACCACTAGAAA	TGGATCAGTGGTTCGAGTCAAA
Hsa-Mir9	Hsa-mir1179
TCTTTGGTTATCTAGCTGTATGAAA	AAGCATTCTTTCATTGGTTGGAAA
Hsa-mir455-3p	Hsa-mir1287
GCAGTCCATGGGCATATTCACAA	TGGATCAGTGGTTCGAGTCAAA
Snord25	Snord25
GATGAGGACCTTTTCACAGACCTG	GATGAGGACCTTTTCACAGACCTG

SHSY-5Y data were normalized on SnoRD25, mice miRNAs were normalized on RNU1A1 and mir16, instead PMBC miRNA expression were normalized on mir-16 and Snord25 expression level.

Extraction, Reverse transcription and qPCR for RNA extracted from spinal cord of ALS mice.

The RNA isolation was carried out using TRIZOL reagent according to the protocol. 5 nanograms of template RNA samples were retrotranscribed and amplified using the miRCURY LNA™ Universal RT microRNA PCR (Exiqon) according to the manufacturer's protocol. Quantitative PCR was performed on a customized Pick & Mix PCR panels which consist of 96-well PCR plates containing a selection of dried down microRNA LNA™ PCR primer sets.

Plasmids and cloning

The pre-miR 129 expressing plasmid in pMir and the HOXC10 3'UTR Reporter Clone in pMir Target were purchased from Origene. The CACNG2 and ELAVL4/HuD UTR regions were amplified using the Phusion Hot Start High-Fidelity DNA Polymerase (Finnzymes) according to manufacturer's instructions. The human genomic DNA extracted from HeLa cells was used as the template in the PCR reactions. The sequences of the oligos used in this PCR reaction were: CACNG2 UTR forward: 5'TCCACTCCAACACAGCCAAC3'; Reverse: 5'CTTACGCGTTTGTTTTCTTCCCTCGTTTA3'. ELAVL4/HuD

UTR Forward: 5'CCAACAAAGCCCACAAGTCCTGA3';
Reverse: 5'ATTACGCGTATGTCATCAGGTATCCCCCT3'.
The resulting PCR products were purified and cloned into the pGEM T Easy Vector system (Promega). The insert was verified by nucleotide sequencing.

Bioinformatic miRNA target prediction

The target mRNA that have the potential binding sites for individual miRNAs were identified by searching them on public databases endowed with prediction algorithms, such as TargetScan, PicTar, miRBase, Miranda, Diana Lab.

Protein extracts and immunoblotting

Cells on 10 cm plate were washed once in PBS 1X (Euroclone) and then lysed in 100 µl of cold Lysis Buffer (Tris HCl 50 mM pH 7,5, NaCl 150 mM, 1% NP40, 5 mM EGTA) with protease inhibitors (Roche) and phosphatase inhibitor (SIGMA) The samples were put on ice for 20 min and then centrifuged at 15000 rcf for 15 min at 4°C, and the supernatant were collected. An aliquot of the cell lysate was used for protein

analysis with the Comassie protein assay reagent for protein quantification.

Protein were separated in 8% and 10% SDS-polyacrylamide gels (classic Laemli conditions) and transferred to nitrocellulose membranes (Whatman GmbH), in normal Transfer Buffer (25 mM Tris, 192 mM Glicine, 20% Methanol) at 100 Volts for 2h or in High Molecola Weight protein (25 mN Tris, 192 mM Glicine, 10& Methanol and 0,1% SDS) at 15 Volts overnight. Membrane were blocked using 5% non fat dried milk in PBST (0,1% (v/v) Tween 20 in 1X PBS) for 1h at room temperature or overnight at 4 °C. After washing 3 times with PBST, membranes were incubated with peroxidase- conjugated secondary antibody anti-mouse IgG (Cell signaling, 1:3000 dilution) or anti-rabbit IgG (Cell signaling 1:8000 dilution, in PBST with 5% non fat dried milk for 1h at room temperature.

After washing as above, the chemio-luminescent signals developed by ECL reagents (Millipore) were detected using Li-cor technology Biosciences.

Quantificaions of the signals were performed using Li-cor technology software, each band value were normalized on the corresponding housekeeping band intensity, thus obtaining relative intensity values.

Antibodies

The antibodies used for immunoblotting were:

Rabbit polyclonal anti Hoxc10 (AVIVA ARP39274_P050 1:1000 dilution); rabbit polyclonal anti CACNG2 (AVIVA ARP35189_050 1:1000 dilution); mouse monoclonal anti HuD (SC48421, 1:2000 dilution); goat polyclonal anti LDH (Abcam 1222 1:1000 dilution); goat polyclonal anti Drosha (sc31159, 1:500 dilution); mouse monoclonal anti Dicer (sc136980 1:500 dilution); rabbit polyclonal anti TAF15 (bethyl A300-308 1:1000 dilution); rabbit polyclonal anti EWS (bethyl A300-418 1:1000 dilution); mouse monoclonal TDP43 (sc100871 1:1000 dilution); rabbit polyclonal anti FUS (home.made 1:5000 dilution); rabbit polyclonal anti Exportin 5 (sc-66885 1:5000 dilution). All the antibodies were diluted in PBS-Tween 0,01%- MILK 5%.

Luciferase reporter assays

$1,5 \times 10^5$ human neuroblastoma SHSY-5Y cells, stably overexpressing the SOD1 WT or the SOD (G93A) variant, were seeded in 24 multiwells as described above. 24h hours after seeding, cells were co-transfected with a total of 1,2 μg of plasmid DNA composed of a constant amount of Renilla expression

vector pRL-TK (50ng/well, Promega) and a variably amount of pMiR vector containing the pre-miRNA and a variably amount of 3' UTR Reporter Clone in pMir Target containing the Firefly luciferase which expression is driven by SV40 Promoter. The two vector were transfected in different proportion: 1:3, 1:1, 3:1. The experiment were carried out in duplicate. Luciferase expression was manteined for 24 hours, and then cells were lysed in 100 µg/well of the Passive Lysis Buffer 1X according to manufacturer's instructions. To obtain a complete lysis, the cells were subjected to a freeze-thaw cycle. 10 µl of the lysates were subjected to the luciferase assays, which was carried out using the Dual-Luciferase Reporte Assay System (Promega) and a Berthold luminometer (Berthold Inc.) The relative luminescence units (RLUs) were obtained normalizing the Firefly luciferase reading to the corresponding Renilla luciferase readings.

2.7 References

Abdelmohsen K, Hutchison ER, Lee EK, Kuwano Y, Kim MM, et al. (2010) miR-375 inhibits differentiation of neurites by lowering HuD levels. *Mol Cell Biol* 30: 4197–4210.

Abelson, J. F., Kwan, K. Y., O’Roak, B. J., Baek, D. Y., Stillman, A. A., Morgan, T. M., et al. (2005). Sequence variants in SLITRK1 are associated with Tourette’s syndrome. *Science* 310, 317–320. doi: 10.1126/science.1116502

Al-Chalabi, A., Jones, A., Troakes, C., King, A., Al-Sarraj, S., and Van Den Berg, L. H. (2012). The genetics and neuropathology of amyotrophic lateral sclerosis. *Acta Neuropathol.* 124, 339–352. doi: 10.1007/s00401-

Akamatsu W, Fujihara H, Mitsuhashi T, Yano M, Shibata S, et al. (2005) The RNA-binding protein HuD regulates neuronal cell identity and maturation. *Proc Natl Acad Sci U S A* 102: 4625–4630

Bartel, D. P. (2009). MicroRNAs: target recognition and regulatory functions. *Cell* 136, 215–233. doi: 10.1016/j.cell.2009.01.002

Beghi, E., Logroscino, G., Chio, A., Hardiman, O., Mitchell, D., Swingler, R., et al. (2006). The epidemiology of ALS and the role of population-based registries. *Biochim. Biophys. Acta* 1762, 1150–1157. doi: 10.1016/j.bbadis.2006.09.008

Bicchi, I.; Morena, F.; Montesano, S.; Polidoro, M.; Martino, S. MicroRNAs and molecular mechanisms of neurodegeneration. *Genes* 2013, 4, 244–263.

Bolognani F., Contente-Cuomo T., Perrone-Bizzozero N.I. 2010. Novel recognition motifs and biological functions of the RNA-binding protein HuD revealed by genome-wide identification of its targets. *Nucleic Acids Res.* 38:117–130 10.1093/nar/gkp863

Butovsky, O., Siddiqui, S., Gabriely, G., Lanser, A. J., Dake, B., Murugaiyan, G., et al. (2012). Modulating inflammatory monocytes with a unique microRNA gene signature ameliorates murine ALS. *J. Clin. Invest.* 122, 3063–3087. doi: 10.1172/JCI62636

Chen, L., Chetkovich, D. M., Petralia, R. S., Sweeney, N. T., Kawasaki, Y., Wenthold, R. J., et al. (2000). Stargazin regulates synaptic targeting of AMPA receptors by two distinct mechanisms. *Nature* 408, 936–943. doi: 10.1038/35046031

Cleveland, D. W. & Rothstein, J. D. From Charcot to Lou Gehrig: deciphering selective motor neuron death in ALS. *Nature Rev. Neurosci.* 2, 806-819 (2001). (n.d.). doi:10.1038/nrn35097565

Cuellar TL, Davis TH, Nelson PT, Loeb GB, Harfe BD, Ullian E, et al. Dicer loss in striatal neurons produces behavioral and neuroanatomical phenotypes in the absence of neurodegeneration. *Proc Natl Acad Sci U S A.* 2008;105:5614–5619.

De Felice, B., Guida, M., Coppola, C., De Mieri, G., and Cotrufo, R. (2012). A miRNA signature in leukocytes from sporadic amyotrophic lateral sclerosis. *Gene* 508, 35–40. doi: 10.1016/j.gene.2012.07.058

DeJesus-Hernandez, M., Mackenzie, I. R., Boeve, B. F., Boxer, A. L., Baker, M., Rutherford, N. J., et al. (2011). Expanded GGGGCC hexanucleotide repeat in noncoding region of C9ORF72 causes chromosome 9p-linked FTD and ALS. *Neuron* 72, 245–256. doi: 10.1016/j.neuron.2011.09.011

Deschenes-Furry J, Perrone-Bizzozero N, Jasmin BJ. *The RNA-binding protein HuD: a regulator of neuronal differentiation, maintenance and plasticity. Bioessays* 2006;28:822-833.

Gaughwin, P. M., Ciesla, M., Lahiri, N., Tabrizi, S. J., Brundin, P., and Bjorkqvist, M. (2011). Hsa-miR-34b is a plasma-stable microRNA that is elevated in pre-manifest Huntington's disease. *Hum. Mol. Genet.* 20, 2225–2237. doi: 10.1093/hmg/ddr111

Gregory RI, Yan KP, Amuthan G, Chendrimada T, Doratotaj B, et al. (2004) The Microprocessor complex mediates the genesis of microRNAs. *Nature* 432: 235–240. doi: 10.1038/nature03120

Haramati, S., Chapnik, E., Sztainberg, Y., Eilam, R., Zwang, R., Gershoni, N., et al. (2010). miRNA malfunction causes spinal motor neuron disease. *Proc. Natl. Acad. Sci. U.S.A.* 107, 13111–13116. doi: 10.1073/pnas.1006151107

Hostikka SL, Gong J, Carpenter EM (2009) Axial and appendicular skeletal transformations, ligament alterations, and motor neuron loss in Hoxc10 mutants. *Int J Biol Sci* 5: 397-410. PubMed: 19623272.

Hu, J. Z., Huang, J. H., Zeng, L., Wang, G., Cao, M., and Lu, H. B. (2013). Anti-apoptotic effect of microRNA-21 after contusion spinal cord injury in rats. *J. Neurotrauma* 30, 1349–1360. doi: 10.1089/neu.2012.2748

Huntzinger, E., and Izaurralde, E. (2011). Gene silencing by microRNAs: contributions of translational repression and mRNA decay. *Nat. Rev. Genet.* 12, 99–110. doi: 10.1038/nrg2936

Jin J., Cheng Y., Zhang Y., Wood W., Peng Q., Hutchison E., Mattson M.P., Becker K.G., Duan W.

Interrogation of brain miRNA and mRNA expression profiles reveals a molecular regulatory network that is perturbed by mutant huntingtin. *J. Neurochem.* 2012;123:477–490. doi: 10.1111/j.1471-4159.2012.07925.x.

Johnson R, Teh CHL, Jia H, Vanisri RR, Pandey T, Lu ZH, Buckley NJ, Stanton LW, Lipovich L. Regulation of neural macroRNAs by the transcriptional repressor REST. *RNA.* 2009;15:85–96.

Keller, A.; Leidinger, P.; Bauer, A.; Elsharawy, A.; Haas, J.; Backes, C.; Wendschlag, A.; Giese, N.; Tjaden, C.; Ott, K.; et al. Toward the blood-borne miRNome of human diseases. *Nat. Methods* 2011, 8, 841–843, doi:10.1038/nmeth.1682.

K.Y. Kim, Y.J. Hwang, M.-K. Jung, J. Choe, Y. Kim, S. Kim, C.-J. Lee, H. Ahn, J. Lee, N.W. Kowall, Y.K. Kim, J.-I. Kim, S.B. Lee, H. Ryu A multifunctional protein EWS regulates the expression of Drosha and microRNAs. *Cell Death Differ.*, 21 (2014), pp. 136–145

W. -K. Kim, MD, X. Liu, PhD, J. Sandner, BA, M. Pasmantier, BA, J. Andrews, MD, L. P. Rowland, MD and H. Mitsumoto, MD, DSc. Study of 962 patients indicates progressive muscular atrophy is a form of ALS. *Neurology.* 2009 Nov 17;73(20):1686-92. doi: 10.1212/WNL.0b013e3181c1dea3.

Krol J, Loedige I, Filipowicz W (2010) The widespread regulation of microRNA biogenesis, function and decay. *Nat Rev Genet* 11: 597–610

Lee, S. T., Chu, K., Jung, K. H., Kim, J. H., Huh, J. Y., Yoon, H., et al. (2012). miR-206 regulates brain-derived neurotrophic factor in Alzheimer disease model. *Ann. Neurol.* 72, 269–277. doi: 10.1002/ana.23588

Leea S, Paulsona KG, Murchisonc EP (2011) Identification and validation of a novel mature microRNA encoded by the Merkel cell polyomavirus in Homo sapiens Merkel cell carcinomas. *J Clin Virol* 52: 272–275. doi: 10.1016/j.jcv.2011.08.012

Lenzken SC, Romeo V, Zolezzi F, Cordero F, Lamorte G et al. (2011) Mutant SOD1 and mitochondrial damage alter expression and splicing of genes controlling neuritogenesis in models of neurodegeneration. *Hum Mutat* 32: 168-182. doi:10.1002/humu.21394. PubMed: 21120952.

Liang, C., Zhu, H., Xu, Y., Huang, L., Ma, C., Deng, W., et al. (2012). MicroRNA-153 negatively regulates the expression of amyloid precursor protein and amyloid precursor-like protein 2. *Brain Res.* 1455, 103–113. doi: 10.1016/j.brainres.2011.10.051

Liu, C. M., Wang, R. Y., Saijilafu, Jiao, Z. X., Zhang, B. Y., and Zhou, F. Q. (2013). MicroRNA-138 and SIRT1 form a mutual negative feedback loop to regulate mammalian axon regeneration. *Genes Dev.* 27, 1473–1483. doi: 10.1101/gad.209619.112

Elisa Majounie, Alan E Renton, Kin Mok, Elise GP Dopper, Adrian Waite, Sara Rollinson, Adriano Chiò, Gabriella Restagno, Nayia Nicolaou, Javier Simon-Sanchez, John C van Swieten, Yevgeniya Abramzon, Janel O Johnson, Michael Sendtner, Roger Pamphlett, Richard W Orrell, Simon Mead, Katie C Sidle, Henry Houlden, Jonathan D Rohrer, Karen E Morrison, Hardev Pall, Kevin Talbot, Olaf Ansorge, The Chromosome 9-ALS/FTD Consortium, The French research network on FTLD/FTLD/ALS, The ITALSGEN Consortium, Dena G

Hernandez, Sampath Arepalli, Mario Sabatelli, Gabriele Mora, Massimo Corbo, Fabio Giannini, Andrea Calvo, Elisabet Englund, Giuseppe Borghero, Gian Luca Floris, Anne M Remes, Hannu Laaksovirta, Leo McCluskey, John Q Trojanowski, Vivianna M Van Deerlin, Gerard D Schellenberg, Michael A Nalls, Vivian E Drory, Chin-Song Lu, Tu-Hsueh Yeh, Hiroyuki Ishiura, Yuji Takahashi, Shoji Tsuji, Isabelle Le Ber, Alexis Brice, Carsten Drepper, Nigel Williams, Janine Kirby, Pamela Shaw, John Hardy, Pentti J Tienari, Peter Heutink, Huw R Morris, Stuart Pickering-Brown, Bryan J Traynor Frequency of the *C9orf72* hexanucleotide repeat expansion in patients with amyotrophic lateral sclerosis and frontotemporal dementia: a cross-sectional study. *Lancet Neurol.* 2012 April; 11(4): 323–330. doi: 10.1016/S1474-4422(12)70043-1

Packer, A. N., Xing, Y., Harper, S. Q., Jones, L., and Davidson, B. L. (2008). The bifunctional microRNA miR-9/miR-9* regulates REST and CoREST and is downregulated in Huntington's disease. *J. Neurosci.* 28, 14341–14346. doi: 10.1523/JNEUROSCI.2390-08.2008

Pascale A, Amadio M, Quattrone A. Defining a neuron: neuronal ELAV proteins. *Cell. Mol. Life Sci.* 2008;65:128–140.

Perrone-Bizzozero N, Bolognani F (2002) Role of HuD and other RNA-binding proteins in neural development and plasticity. *J Neurosci Res* 68(2): 121–126. doi: 10.1002/jnr.10175

Pratt, A. J., Getzoff, E. D., and Perry, J. J. (2012). Amyotrophic lateral sclerosis: update and new developments. *Degener. Neurol. Neuromuscul. Dis.* 2012, 1–14.

Renton, A. E., Majounie, E., Waite, A., Simon-Sanchez, J., Rollinson, S., Gibbs, J. R., et al. (2011). A hexanucleotide repeat expansion in C9ORF72 is the

cause of chromosome 9p21-linked ALS-FTD. *Neuron* 72, 257–268. doi: 10.1016/j.neuron.2011.09.010

Rosen, D. R., Siddique, T., Patterson, D., Figlewicz, D. A., Sapp, P., Hentati, A., et al. (1993). Mutations in Cu/Zn superoxide dismutase gene are associated with familial amyotrophic lateral sclerosis. *Nature* 362, 59–62. doi: 10.1038/362059a0

A. Schaefer, D. O'Carroll, C.L. Tan, D. Hillman, M. Sugimori, R. Llinas, P. Greengar, Cerebellar neurodegeneration in the absence of microRNAs *J. Exp. Med.*, 204 (2007), pp. 1553–1558

Strickland, I. T., Richards, L., Holmes, F. E., Wynick, D., Uney, J. B., and Wong, L. F. (2011). Axotomy-induced miR-21 promotes axon growth in adult dorsal root ganglion neurons. *PLoS ONE* 6:e23423. doi: 10.1371/journal.pone.0023423

M Swash, D Ingram. Preclinical and subclinical events in motor neuron disease *J Neurol Neurosurg Psychiatry*, 51 (1988), pp. 165–168

S. Volinia, R. Visone, M. Galasso, E. Rossi, and C. M. Croce, "Identification of microRNA activity by targets' reverse eXpression," *Bioinformatics*, vol. 26, no. 1, pp. 91–97, 2010.

Williams, A. H., Valdez, G., Moresi, V., Qi, X., McAnally, J., Elliott, J. L., et al. (2009). MicroRNA-206 delays ALS progression and promotes regeneration of neuromuscular synapses in mice. *Science* 326, 1549–1554. doi: 10.1126/science.1181046

Wu, D., and Murashov, A. K. (2013). MicroRNA-431 regulates axon regeneration in mature sensory neurons by targeting the Wnt antagonist Kremen1. *Front. Mol. Neurosci.* 6:35. doi: 10.3389/fnmol.2013.00035

Yu, Y. M., Gibbs, K. M., Davila, J., Campbell, N., Sung, S., Todorova, T. I., et al. (2011). MicroRNA miR-133b is essential for functional recovery after spinal cord injury in adult zebrafish. *Eur. J. Neurosci.* 33, 1587–1597. doi: 10.1111/j.1460-9568.2011.07643.x

Zhou, R., Yuan, P., Wang, Y., Hunsberger, J. G., Elkahloun, A., Wei, Y., et al. (2009). Evidence for selective microRNAs and their effectors as common long-term targets for the actions of mood stabilizers. *Neuropsychopharmacology* 34, 1395–1405. doi: 10.1038/npp.2008.131

S Zoccolella, E Beghi, G Palagano *et al.* Predictors of delay in the diagnosis and clinical trial entry of amyotrophic lateral sclerosis patients: a population-based study *J Neurol Sci*, 250 (2006), pp. 45–49.

Chapter 3

FUS/TLS depletion leads an impairment of cell proliferation and DNA Damage Response

Alessia Loffreda¹, Silvia Carolina Lenzken¹ ,
Monica Lupi and Silvia M. L. Barabino¹

1: Department of Biotechnology and Biosciences, University of
Milano-Bicocca, Piazza della Scienza 2, Milan, Italy

2: Biophysics Unit, Laboratory of Anticancer Pharmacology,
Department of Oncology, IRCCS - Istituto di Ricerche
Farmacologiche "Mario Negri," Milano, Italy.

3.1 Abstract

FUS/TLS (fused in sarcoma/translocated in liposarcoma) protein, a ubiquitously expressed RNA-binding protein, has been linked to a variety of cellular processes, such as RNA metabolism, microRNA biogenesis and DNA repair. However, the precise role of FUS protein remains unclear. Recently, FUS has been linked to Amyotrophic Lateral Sclerosis (ALS), a neurodegenerative disorder characterized by the dysfunction and death of motor neurons. Based on the observation that some mutations in the FUS gene induce cytoplasmic accumulation of FUS aggregates, we decided to explore a loss-of-function hypothesis (i.e. inhibition of FUS' nuclear function) to unravel the role of this protein. To this purpose, we generated a SH-SY5Y human neuroblastoma cell line which expresses a doxycycline induced shRNA targeting FUS and that specifically depletes the protein. In order to characterize this cell line we performed growth proliferation and survival assays. From these experiments emerged that FUS-depleted cells display alterations in cell proliferation. In order to explain this observation, we tested different hypothesis (e.g. apoptosis, senescence or slow-down growth). We observed that FUS-depleted cells growth slower than

control cells. Based on the notion that FUS interacts with the miRNA processing proteins (Morlando et al. 2012), to explain this phenotype, we looked at miRNAs expression and we found an up-regulation of mir-7. Interestingly, this up-regulation is also observed in cells that express the ALS-linked FUS R521C mutation. Finally, since an increasing number of work correlated FUS with DNA damage and repair we explored the effects of DNA damage in FUS-depleted cells by monitoring important components of DNA Damage Response (DDR). We found that FUS depletion had an effect on the initial level of DNA damage by inducing the phosphorylation of H2AX in basal condition and that it delayed DSB repair when acute DNA damage occurs. Interestingly, genotoxic treatment resulted in changes in the subcellular localization of FUS in normal cells. We are currently exploring on one hand the mechanism by which FUS depletion leads to DNA damage, and on the other the functional significance of FUS relocalization after genotoxic stress. Taken together, these studies may contribute to the knowledge of the role of FUS in these cellular processes and will allow us to draw a clearer picture of mechanisms of neurodegenerative diseases.

3.2 Introduction

Aberrant cell-cycle activity and DNA damage are emerging as important pathological components in various neurodegenerative conditions. In a variety of conditions involving neuronal death such as ischemia and Alzheimer's disease (Hayashi et al., 2000, Rashidian et al., 2007, Vincent et al., 1996 and Yang et al., 2001), neurons engage in aberrant cell-cycle activities, expressing cell-cycle markers such as Ki-67 and proliferating cell nuclear antigen (PCNA) and synthesizing DNA (Yang et al., 2001). This is remarkable considering that neurons are terminally differentiated and remain quiescent for decades prior to the onset of these events. While the underlying mechanisms are poorly understood, these activities may play an early and contributory role in neuronal death (Busser et al., 1998 and Herrup and Busser, 1995). For example, overexpression of cell-cycle activity-inducing proteins such as SV40 large T antigen, c-Myc, c-Myb, or E2F1 can cause neuronal death in vitro and in vivo (al-Ubaidi et al., 1992, Konishi and Bonni, 2003 and Liu and Greene, 2001), while pharmacological inhibitors of cyclin-dependent kinases (CDKs) or other cell-cycle components can exert neuroprotective effects (Padmanabhan et al., 1999).

Mutations in a large number of genes that are important for various DNA repair mechanisms have been linked to neurodegenerative diseases or to complex diseases with neurological components (Rass et al. 2007), suggesting that DNA repair deficiency is involved in the pathogenesis of neurodegeneration. For example, ataxia telangiectasia is caused by mutations in the *ATM* gene, which encodes a protein kinase that is crucial for the cellular response to DNA double-stranded breaks (DSBs). Individuals with mutations in *MRE11* and *NBS1*, which are components of the DNA damage sensor complex MRN (MRE11-RAD50-NBS1), present with severe neurological symptoms, along with manifestations that include hypersensitivity to ionizing radiation and genome instability (Rass et al. 2007; McKinnon et al. 2009). DNA damage and genome instability have also been linked to age-related neurodegenerative diseases such as Alzheimer's and Parkinson's diseases (Bender et al. 2006; Lu et al. 2004; Anderson et al 1996). Furthermore, impairment of the DDR and DNA repair also contribute to motor neuron vulnerability. For example, mice lacking ERCC1, a protein involved in DNA excision repair, show age-related motor neuron degeneration (de Waard et al 2006).

Fused-in-Sarcoma (FUS, also known as TLS) is a multifunctional, multi-domain heterogeneous ribonucleoprotein that belongs to the TET (TAF15, EWS and TLS) family of RNA-binding proteins (Tan et al. 2009). In the brain, FUS is predominantly expressed in the nucleus, but is able to shuttle between the nuclear and cytoplasmic compartments following activity stimulation (Fujii et al 2005;). A number of studies have implicated FUS in the maintenance of genome stability and in DNA repair. For example, inbred *Fus*^{-/-} mice die perinatally and show genome instability, whereas embryonic fibroblasts derived from outbred *Fus*^{-/-} mice display high chromosomal instability and radiation sensitivity (Kuroda et al. 2000; Hicks et al. 2000). FUS promotes the annealing of homologous DNA and the formation of DNA D-loops, an essential step in DNA repair by homologous recombination (Bertrand et al 2000; Baechtold et al. 2000). FUS is also phosphorylated by ATM following the induction of DSBs (Gardiner et al. 2008) and is involved in DNA damage-induced regulation of gene expression (Wang et al. 2008). Recent studies have shown that mutations in FUS are causally linked to familial ALS (fALS-FUS), which is characterized by an aberrant accumulation of FUS in the cytoplasm of motor neurons and glia (Vance et al. 2009; Kwiatkowski et al. 2009). Most ALS-

associated FUS mutations destroy the nuclear localization signal (NLS) of the FUS protein, leading to cytoplasmic accumulation of FUS aggregates in neurons and glial cells of these ALS patients. Besides the proposed toxicity of the cytoplasmic FUS aggregates, there is accumulating evidence indicating that the FUS mutations-associated form of ALS might be caused by the loss of one or several of the nuclear functions of FUS. Here we investigated the loss of function hypothesis. To this end we wanted to elucidate the biological function of FUS in the nucleus, which so far is not well understood. Thus, we generated a cell line using a lentiviral vector-based system for the doxycycline-inducible expression of a FUS-specific short hairpin RNA (shRNA). We found that attenuation of FUS expression leads to an impairment of the cell proliferation and we found that FUS depletion leads to a reduction of the growth rate. Since the observed impairment of cell growth could be either due to cell death or to alterations of the cell cycle, on one hand we assessed apoptosis using the TUNEL assay and senescence by measuring β -galactosidase activity. The results indicate that FUS depletion does not induce a significant increase in apoptotic or senescent cells. On the other hand we determined whether FUS depletion affects DNA replication, by measuring

bromodeoxyuridine (BrdU) incorporation, and/or cell division leading to a growth arrest (by time-lapse microscopy). We found that FUS-depleted cells at day 7 and 10 accumulate in G1 phase. The cells are not arrested since we still observe cells in S phase. However, time-lapse experiments showed that the cells have a longer intermitotic time. From these experiments we conclude that FUS-depletion induces a delay in the G1 phase of the cell cycle. Considering that the G1 cell cycle checkpoint is primarily responsible for preventing damaged DNA from being replicated, we tested the hypothesis that a DNA damage was occurring and we noticed that FUS depletion *per se* leads to H2AX phosphorylation. Thus we analysed the DDR in FUS depleted condition after DSBs formation by IR exposition. We assayed the activation of the ATM- and CHK2- dependent signalling cascade at different time points after irradiation and the intracellular distribution of the FUS protein. Western blot analysis of ATM and CHK2 showed that the activation of DDR was not enhanced in FUS-depleted compared to control cells. However FUS kd cells exhibited a delay in DBS repair in a gamma-H2AX focus assay. Starting from the observation that DDR is delayed in FUS attenuation context we decide to check the FUS behaviour after DBS. The analysis of the intracellular distribution of FUS

in IR-treated SH-SY5Y cells by confocal microscopy showed that FUS relocalizes after irradiation. While in untreated cells FUS is mainly distributed in the nucleoplasm and shortly after irradiation, FUS progressively accumulates in the cytoplasm while in the nucleus it concentrates in few discrete nuclear foci.

3.3 Results

FUS depletion impairs cell proliferation

For deciphering the disease pathway associated with FUS mutations, it is key to understand the physiological functions of FUS. To gain insight into the function of FUS in human cells, we initially characterized the effect of its down-regulation. To this end, we generated SH-SY5Y, human neuroblastoma cells, using a lentiviral vector-based system for the doxycycline-inducible expression of a FUS-specific short hairpin RNA (shRNA). Upon 5 days of induction the level of FUS protein was reduced by almost 60% (Figure 1). To investigate whether FUS depletion affects viability and cell cycle kinetics *in vivo*, we performed proliferation curves at different time points after induction. As is shown in Figure 2A, from the fifth day of induction, the proliferation significantly slow down in FUS depleted cells in comparison to control cells. Moreover, to further study the cell proliferation-inhibitory effects of FUS knockdown, we performed a clonogenicity assay and we confirmed the previous results (Figure 2B). In fact, FUS depleted plate shown a reduced number of colonies (almost seven times less) and most of them shown a smaller size. To check if the reduced cell growth was

linked to FUS depletion we performed recovery experiments. As is shown in Figure 3A, when the doxycycline-containing medium was replaced by Tet-free medium cell recovered the normal growth rate which belongs. The recovery of cell growth was concomitant with the increase of FUS protein expression (Figure 3B). We checked FUS protein level across the experiment, as is indicated in the Figure 3B, the levels of FUS in FUS-depleted cells showed a clear increase of FUS after doxycycline removal that correlates with the growth rescue, while mock cells don't display significant changes. Thus, our findings together suggest a novel role for the wild-type FUS protein in the maintenance of cell proliferation.

FUS-depleted cells do not show increased apoptosis and are not entering senescence

Since we found that FUS depletion leads to an impairment in cell proliferation, we tested if there was an induction of cell death. To this end, we collected cells at different time after doxycycline induction and we performed a TUNEL assay (Figure 4). However we detected only a slight increase in apoptotic cells level:

the dUTP positive cells increased at a maximum of 7% in FUS depleted cells compared to control cells.

An alternative explanation for the reduction of cell proliferation could be the induction of senescence. A classic characteristic of the senescent phenotype is the induction of senescence-associated β -galactosidase (SA- β -gal) activity. SA- β -gal is present only in senescent cells, not in pre-senescent, quiescent, or proliferating cells. Moreover, as is shown in Figure 4, cells growing in doxycycline containing medium do not display significant levels of senescence. Although, FUS depleted cells entering senescence were about twice the control cells, this effect could not explain the reduction in cell growth that we observed. These observations suggest that the impairment of proliferation is not due to activation of apoptosis or to senescence.

FUS-depleted cells accumulate in G0/G1 phase

To further clarify the growth phenotype of FUS-depleted cells, we performed flow cytometry analysis to study the cell cycle at different time of induction. We used BrdU staining to identify only replicating cells, and propidium iodide staining to detect DNA quantity. As is shown in Figure 5A, while the pattern of control cells

did not change, the cloud of cells in S phase of FUS-depleted cells was slowly depleted. In FUS-depleted cells, especially at day 7 and 10, we observed an increase in the proportion of cells in G1/G0, from 50% to 70%. However, we observed a residual population of cells of about 10% that could still enter S phase, indicating that replication was not completely blocked. In addition we performed time lapse microscopy over a period of 5 days (Figure 5B). This approach allows the analysis of two parameters: first: the time at which occurs the first mitosis, and second the time required between two mitosis that is the intermitotic time. As is shown in Figure 5B, the time of the first mitosis did not differ between FUS-depleted and control cells. However, we observed that in FUS attenuating condition, cells take more time to divide (Figure 5B). Taken together these findings demonstrate that FUS depleted cells accumulate at G1 phase.

The G1 delay could be linked to DNA damage

Several recent reports have implicated FUS in DDR (Paronetto et al. 2011; Wang et al. 2013; Hicks et al. 2010; Mastrocola et al. 2013; Haley et al. 2009). Specifically, FUS is recruited at sites of DNA damage

very rapidly (Mastrocola et al 2013; Wang et al 2013). Moreover, when levels of FUS protein are decreased, the damage response is dampened and the amount of accumulated DNA damage increased (Wang et al. 2013). Based on these reports, we wanted to verify the hypothesis that the G1 delay was due to a DNA damage condition and an activation of DDR. Phosphorylation of H2AX serine 139 creates the γ -isoform, producing foci that can be visualized by immunostaining using anti- γ -H2AX antibody. These foci correspond 1:1 with unrepaired DSBs. We found an activation of DDR when FUS is depleted, as indicated by H2AX phosphorylation both in Western blot analysis and for the appearing of γ H2AX foci in Immunofluorescence experiment (Figure 10A,B). From these results we concluded that FUS depleted cells stay longer in G1 phase and that they shown an activation of DDR in basal condition.

Attenuation in FUS expression delays DBS repair

The phosphorylation of H2AX in basal condition suggested an accumulation of DNA damage which could be due to an impairment of signal transduction and repair of DNA damaged in FUS-depleted cells. Thus, we wondered if FUS-depleted cells may be more sensitive

to genotoxic stress. Considering the proliferation impairment of FUS-depleted cells, we decided to use IR as source of genotoxic damage. In fact, IR induces DNA double strand breaks at short time after exposition (few seconds), and activate a response called DNA Damage Response (DDR), in order to stop cell cycle and repair the damage. We started analyzing apical and downstream kinases in the DDR cascade, at different time points after the damage, by Western Blot analysis and by immunofluorescence to check the localization and the recruitment of the proteins.

ATM is called "apical kinase" because is the first kinase activated in DDR and triggers diverse cellular responses to DSBs. Activation of ATM is facilitated by autophosphorylation. The inactive ATM exists as dimer. In response to DNA damage, the kinase domain of one monomer phosphorylates Ser-1981 of the other interacting ATM, resulting in subunit dissociation and ATM activation. We analysed ATM activation by Western Blot using an antibody that recognize the phosphorylation of ATM on Ser-1981, but we did not find significant changes in the ATM activation between FUS-depleted and control cells (Figure 7A). Instead, by immunofluorescence, we observed that after 1 hours of IR, phosphor-ATM displays a more cytoplasmatic localization in FUS cells (Figure 7A). Phospho-ATM

exerts its effect by phosphorylating and hence activating target proteins such as CHK2, a downstream kinase, that transduce DNA damage signals from lesions and stalls the replication forks. Thus we analysed the phosphorylation state of CHK2, and both Western blotting and immunofluorescence failed to detect a significant change between control and FUS-depleted cells (Figure 7B). These results suggested that there was not an enhanced activation of DDR.

However, considering that we observed the formation of the gamma-H2AX foci in basal condition upon FUS depletion, we tested for efficiency of DNA repair at different time points after IR exposition, using a histone g-H2AX focus assay. As is shown in Figure 8, FUS-depleted cells presented a delay in DDR activation. At 0,5h point, there was a weak increase of gamma-H2AX foci in compare to control cells. At later time points (2h and 4h), control cells showed significant recovery, while FUS depleted cells still presented a discrete number of foci. At the 8 h time point, only a few repair resistant foci remained in control as well as FUS-depleted cells. This results suggested that although attenuation of FUS has an effect on the initial level of DNA damage, it delays DSB repair.

FUS accumulates in the cytoplasm after DNA damage

Starting from our observation that FUS depletion induced a delay in DDR and considering the increasing number of reports that link FUS to the DDR we decided to investigate the behavior of endogenous FUS after DNA damage. To this end we exposed SH SY5Y cells to IR and we checked FUS expression and localization at different time point. Western Blot analysis showed that there were no changes in FUS expression. Intriguingly, the analysis of the intracellular distribution of FUS in IR-treated SH-SY5Y cells by confocal microscopy showed that FUS relocates after irradiation. While in untreated cells FUS is mainly distributed in the nucleoplasm with the exclusion of the nucleoli, shortly after irradiation, FUS concentrates in few discrete nuclear foci. Then, starting from 3 h after irradiation, FUS progressively accumulates in the cytoplasm (Figure 9). We further investigate FUS localization after other genotoxic treatments, such as camptothecin or hydroxyurea but failed to observe any changes in FUS localization (data not shown). To define if this phenotype was restricted only to neuroblastoma cells we performed IR treatment in other cell lines as HeLa,

T98G and U2OS cells and we confirmed the cytosolic localization of FUS after IR exposition (Figure10).

Activation of DDR results in a cascade of phosphorylation events. To test if FUS itself undergoes post-translational modifications that induce its translocation to the cytoplasm, we treated cells with specific inhibitors prior to IR. Since it is known that FUS could be both phosphorylated, we started with Roscovitine (a cyclin-dependent kinase (CDK) inhibitor) and Caffeine (an inhibitor of the catalytic activity of both ATM and the related kinase, ATM and Rad3-related (ATR)) that affect the phosphorylation cascade of the DDR but we did not find any effect on FUS translocation, so far (data not shown). Currently we are going to test other specific phosphorylation inhibitor and to test other post translational modification that can lead at the translocation of FUS such as metylation.

FUS down-regulation leads to the up-regulation of mir-7

The interaction of FUS with miRNA processing factors encouraged us to test if the ablation of FUS influences the expression of one or more miRNA that may influence cell proliferation. Among the differentially expressed miRNA we found that mir-7 is up-regulated

in FUS depleted cells (Figure 11). Fang et al. recently show that miR-7-overexpressing subclones showed significant cell growth inhibition by G(0) /G(1) -phase cell-cycle arrest (Fang et al. 2014). Moreover it has been demonstrated that up-regulation of mir-7 increases the radiosensitivity of cells (Lee et al. 2011). Furthermore, we measured and confirmed the up-regulation of mir-7 level even in SH SY5Y cells stable expressing the FUS-R521C mutant, which is causative of ALS (Figure11B). Interestingly, the mutation FUS-R521C (in transgenic mice) has been found to exhibit evidence of DNA damage in cortical neurons and spinal motor neurons (Qiu et al. 2014). This result suggested that FUS ablation may leads to an accumulation in G0/G1 phase through mir-7 and that there could be present a DNA damage condition. Anyway further investigation to demonstrate this hypothesis are necessary.

3.4 Discussion

Research on the causes of ALS made a leap forward in 2006 with the identification of the 43 kDa transactive response (TAR) DNA-binding protein (TDP-43), followed three years later by the identification of another DNA/RNA binding protein, *Fused in sarcoma* (FUS). Since their identification there have been a consistent and increasing number of works that associate mutations of these proteins with ALS and other neurodegenerative disease, and that correlates them with crucial cellular pathways such as transcription, pre-mRNA splicing, RNA localization, miRNAs processing, DDR etc. Despite the efforts in FUS and TDP-43 characterization the pathogenic mechanism leading to neurodegenerative disorders are still not well understood. Therefore, It is now crucial to determine the normal functions of TDP-43 and FUS in order to identify the disease pathway associated with their mutations.

In this study, we focused in understanding the FUS physiological function. Since most ALS-associated FUS mutations destroy the nuclear localization signal (NLS) of the FUS protein, leading to cytoplasmic accumulation of FUS and the resulting lost of several nuclear functions of FUS, we decided to characterize the cellular

effect of FUS down-regulation. We found that FUS depletion leads to a reduction of the growth rate without induction of a significant increase in apoptotic or senescent cells. A further characterization by measuring bromodeoxyuridine (BrdU) incorporation revealed that FUS-depleted cells accumulate in G1 phase. The cells are not arrested since we still observe cells in S phase. However, time-lapse experiments showed that the cells have a longer intermitotic time. Thus, we conclude that FUS-depletion induces a delay in the G1 phase of the cell cycle. We hypothesized different explanations for this phenotype. It has been demonstrated that TAF15 (that belongs to FUS protein family) is able to impair cell proliferation and cell cycle through modulation of miRNAs. Considering that FUS is involved in microRNA biogenesis and processing we profiled by RNAseq the miRNAs expression and we found the up-regulation of mir-7, not only in FUS-depleted cells but also in cells that express the ALS-linked FUS mutant R521C. Interestingly Fang et al. demonstrated that miR-7-overexpressing subclones showed significant cell growth inhibition due to G(0)/G(1) -phase cell-cycle arrest. Thus we can speculate that FUS depletion may lead to a reduction in proliferation through the regulation of mir-7. An alternative explanation could be related with FUS

capability to interact with cyclins. It has been demonstrated that after DNA damage, FUS protein together with ncRNAs inhibit CyclinD promoter, causing cell cycle arrest (Wang et al 2008). However, we measured CyclinD mRNA level and we did not find any change (data not shown).

The G1 cell cycle checkpoint is primarily responsible for preventing damaged DNA from being replicated, thus cells use to arrest in G1 phase in DNA damage condition. Therefore, we decided to test the hypothesis that the G1 delay was due to a DNA damage condition and an activation of DDR. Immunoreactivity for γ H2AX, a modification that is a prerequisite for DSB repair, is one of the earliest markers of DNA damage (Pilch et al. 2003). Following DNA damage, H2AX is rapidly phosphorylated to γ H2AX by ATM, which facilitates the retention of a number of proteins, including NBS1, MDC1 and 53BP1, to the vicinity of the DNA breaks (Fillingham et al. 2006). We found that FUS-depletion leads to the formation of γ -H2AX foci, that correspond 1:1 with unrepaired DSBs, in the absence of genotoxic treatment. The phosphorylation of H2AX in basal condition suggested us an accumulation of endogenous DNA damage. However, we performed a characterization by WB e IF of phosphor-ATM and phosphor-CHK2 an apical and a downstream activated

kinase of DDR respectively, and we did not find any enhancement in the DDR cascade. Consistent with this resulted we observed that FUS depletion led to a dampening of the DDR reflected at first by the delay in in H2AX phosphorylation shortly after IR induction; and then by the observation that while at latter time points (2h and 4h), the control cells showed significant recovery, FUS-depleted cells kept on to show a discrete number of foci. This finding can suggest that FUS is important to appropriately activate repair pathways. In fact, the γ -H2AX foci we found in FUS depleted cells could represent the physiological foci that normally form during the DNA replication and that an impairment in DDR can make slow to be repaired. This is consistent with the delay in repairing after IR exposition and that the DSBs did not enhance the phosphorylation of ATM or CHK2 in FUS depleted condition.

Recent studies have found direct evidence that FUS is involved in DNA damage repair. FUS facilitates DNA damage repair in neurons through interaction with histone deacetylase 1 (HDAC1) and recruitment to sites of double-strand DNA damage (Wang et al., 2013). FUS is also recruited to sites of oxidative DNA damage through the activity of poly (ADP-ribose) polymerase (Mastrocola et al., 2013; Rulten et al., 2014). Although these studies globally support our result that FUS,

respond to DNA damage, they all report a rapid recruitment (seconds to minutes) of FUS to sites of DNA damage. This is in contrast to our study, in which we found cytoplasmic relocalization of FUS after DNA damage from 3 h after inducing DNA damage. There are a number of potential explanations for the different effects we observe. First, all three groups used laser-induced DNA damage, which can induce many types of DNA lesions, although single-strand DNA breaks are thought to predominate (Reynolds et al., 2013). Therefore, it seems probable that FUS responds or is regulated differently depending on the DNA lesion. In support of this idea, Mastrocola et al. (2013) reported that FUS did not accumulate at foci induced by ionizing radiation or defined DSBs produced in a cell line using an inducible restriction endonuclease system. Second, FUS may be initially recruited to sites of DNA damage, where it could be modified (for instance by phosphorylation), leading to release from the DNA lesion and export to the cytoplasm. This is supported by the observation that GFP-FUS is rapidly recruited within seconds to DNA damage and slowly decreases over the course of 30 min (Mastrocola et al., 2013). The precise role of FUS in DNA damage repair is presently unclear, and this is an important area of future research. Notably, FUS mutations are associated

with earlier disease onset compared with SOD1, TARDBP or C9ORF72 mutations in patients (Millecamps et al.2012; Huang et al. 2010). Thus, impaired DNA repair may render motor neurons more vulnerable to intrinsic and/or extrinsic genotoxicity. This idea implies that DNA damage may represent the initial pathogenic trigger that causes phosphorylation and cytoplasmic accumulation of FUS in the cytosol. Thus, DNA damage could be the upstream trigger of the pathological changes in ALS- and FTLD-FUS cases suggest that strategies to reduce DNA damage, or activate DNA repair pathways, may be a viable therapeutic route to prevent or treat these kind of neurodegenerations.

3.5 Figures and Tables

Figure 1

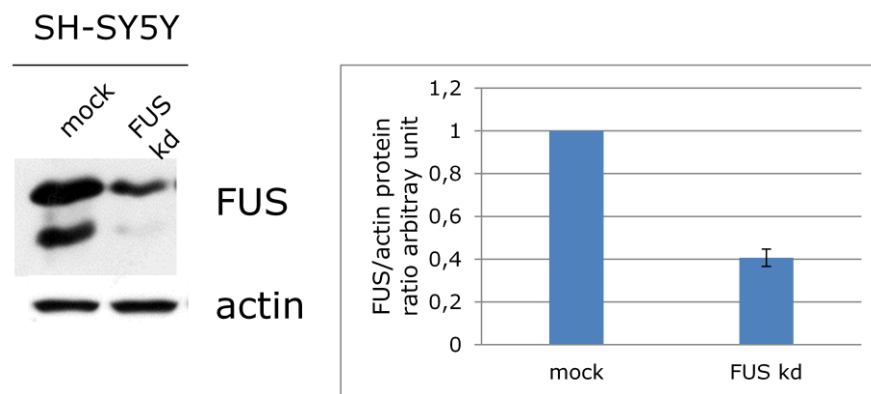


Figure1: Representative western blot from SH-SY5Y mock and FUS-depleted neuroblastoma cell lines is shown. Cells were exposed to doxycycline (5 μ g/ml) for 5 days and then whole extracts prepared. Membrane was immunoblotted with FUS and actin antibody. The quantification show that FUS level results reduced of about 60%. Mock represent the control cells, while FUS kd the FUS-depleted cells.

Figure 2

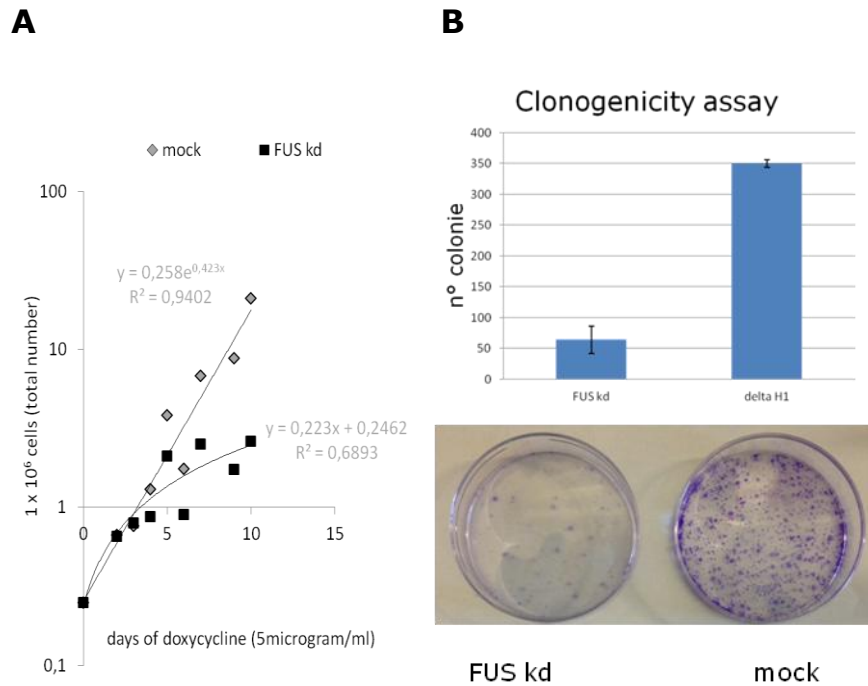
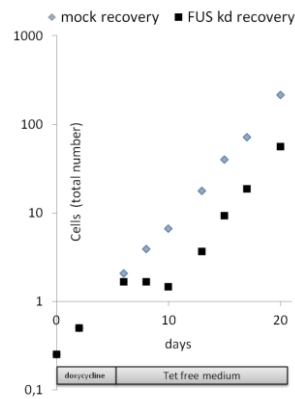


Figure 2: (A) Growth proliferation curves display a slow down rate proliferation in FUS depleted cells. The plot represents the number of cells vs. days of doxycyclin treatment. **(B)** Clonogenicity assay performed in FUS depleted condition. Cells were plated on the 5th day of doxycyclin induction, colonies formed by mock and FUS-depleted cells were counted after 21-days of doxycyclin treatment.

Figure 3

A



B

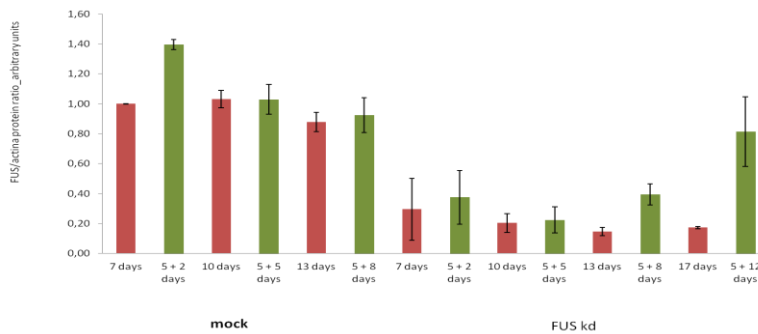
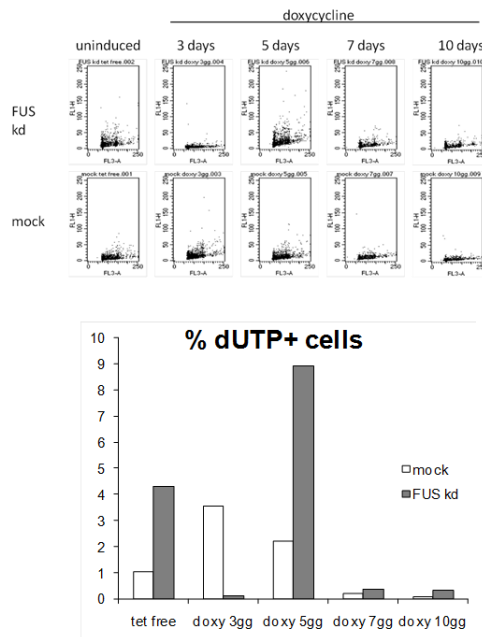


Figure3: (A) Growth proliferation curves in FUS kd recovery condition. Cells were grown in doxycycline containing medium until day 5 cells then doxy was removed and replaced by tet free medium. **(B)** FUS protein level was measured across the experiment and normalized on actin level.

Figure 4

A



B

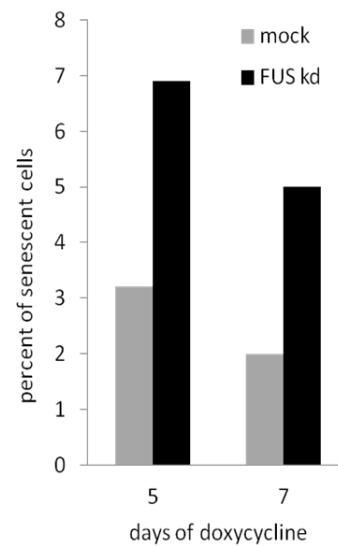
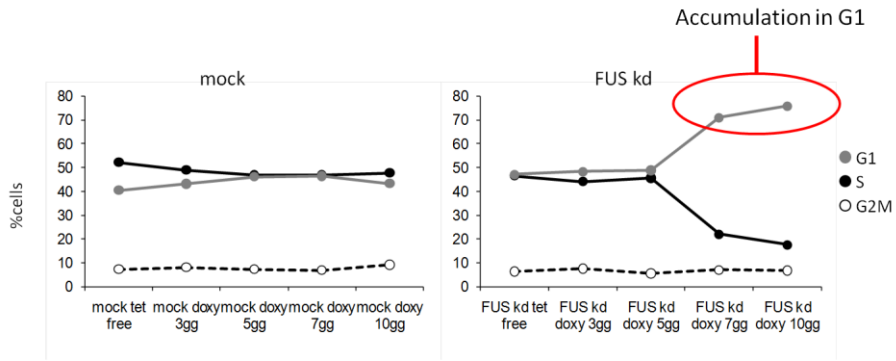


Figure 4: (A) upper panel: TUNEL assay performed at different time point after induction. Lower panel: the graph shows mock and FUS kd cells positive for dUTP incorporation. **(B)** The graph represents the senescence-associated β -galactosidase (SA- β -gal) activity in mock and FUS kd cells.

Figure 5

A



B

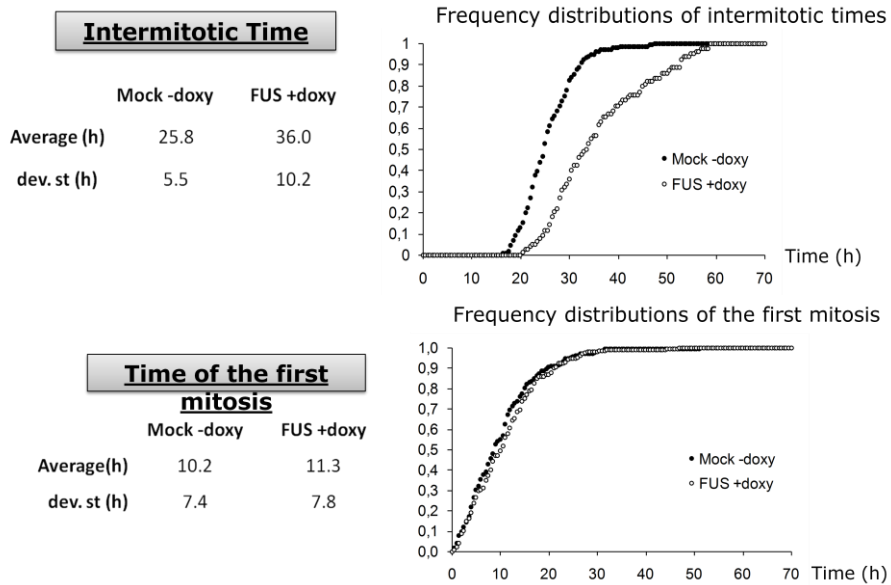
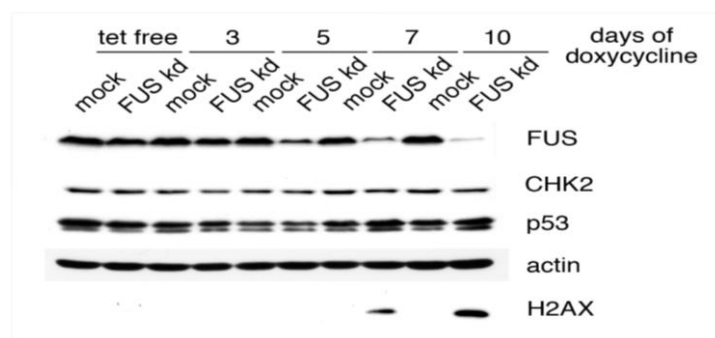


Figure 5: (A) Assessment of the effect of FUS depletion on the cell cycle. Cell proliferation was measured by BrdU incorporation. Quantification was performed by FACS analysis. Represented is the percentage of cells in the different cell cycle phases. **(B)** Assessment of cell cycle duration by time-lapse microscopy. Upper panel: the first plot show the time of first mitosis in mock and FUS kd cells. Lower panel: the second plot shows the intermitotic time.

Figure 6

A



B

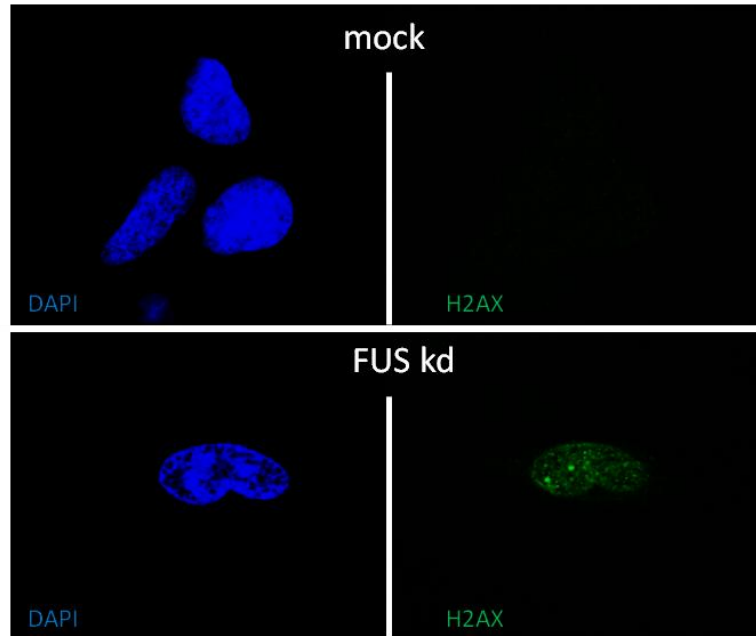
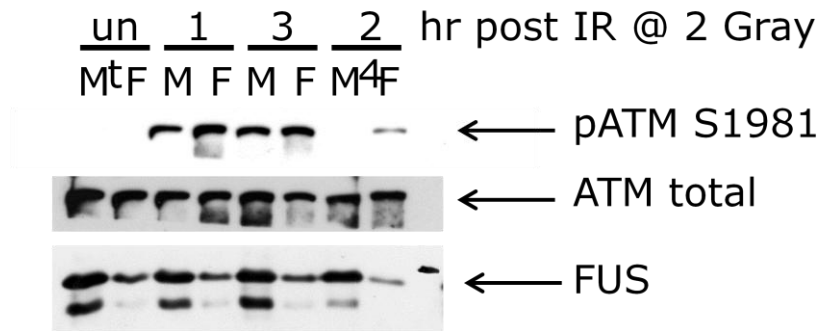


Figure 6: (A) Representative western blot from mock and FUS depleted neuroblastoma cell lines is shown. Cells were exposed to doxycycline (5 μ g/ml) by the times indicated and then whole extracts prepared. Strong H2AX phosphorylation is observed at days 7 and 10 in FUS depleted cell. **(B):** Representative immunofluorescence of mock and FUS depleted cells (day 6 of doxycycline treatment), evident H2AX phosphorylation is observed in FUS depleted cells.

Figure 7

A



B

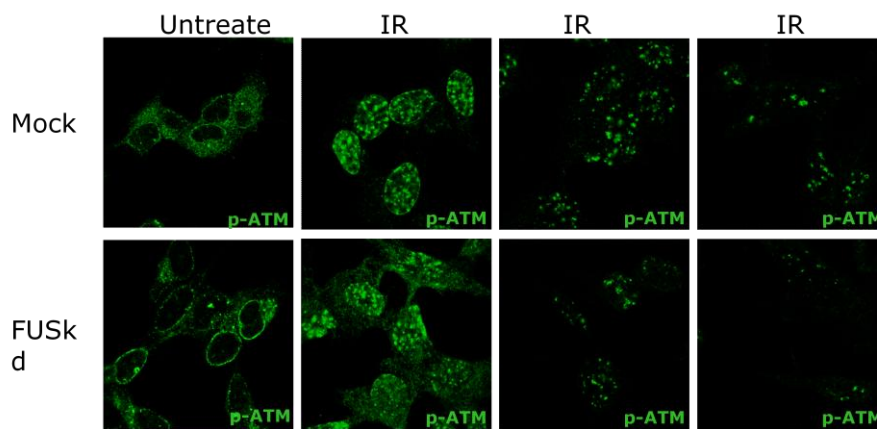
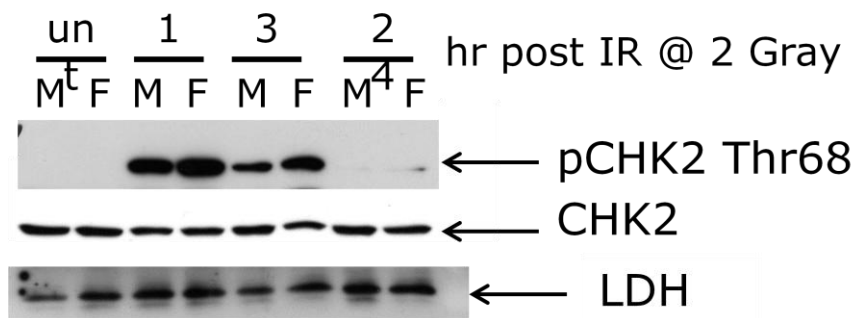


Figure 7: (A) Representative western blots from mock and FUS depleted neuroblastoma cell lines exposed to Ionizing Radiation (2 Gray) are shown. Mock and FUS depleted cells at day 5 of doxycycline treatment, were

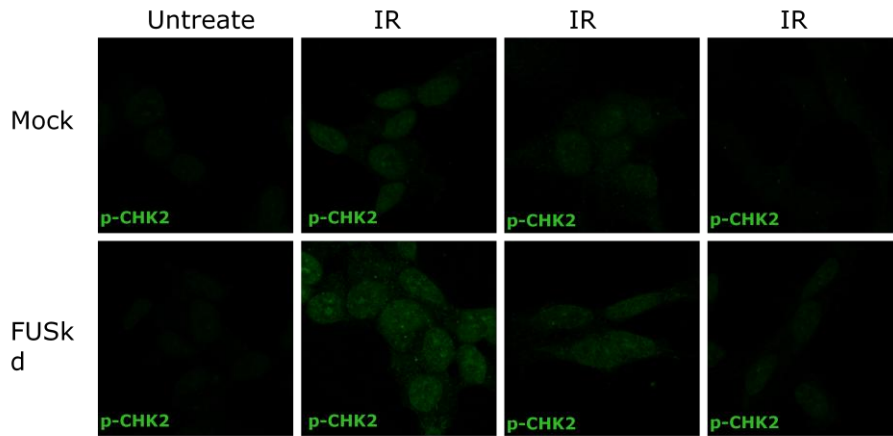
irradiated and whole extracts prepared at the indicated times post irradiation. Membranes were immunoblotted with anti-phospho-ATM serine-1981, anti total-ATM or anti FUS antibodies. **(B)** Representative immunofluorescence images of mock and FUS depleted cells exposed to IR (2 Grays) are shown. Cells were fixed at the times post irradiation indicated and stained with an anti-phospho-ATM serine-1981 antibody.

Figure 8

A



B



3th meeting
Sinergia_Bern_December 14th

Figure 8:(A) Representative western blots from mock and FUS depleted neuroblastoma cell lines exposed to Ionizing Radiation (2 Gray) are shown. Mock and FUS depleted cells at day 5 of doxycycline treatment, were irradiated and whole extracts prepared at the indicated times post irradiation. Membranes were immunoblotted with anti-phospho-CHK2 threonine-68, anti total CHK2 or anti-LDH antibodies. **(B)** Representative immunofluorescence images of mock and FUS depleted cells exposed to IR (2 Grays) are shown. Cells were fixed at the times post irradiation indicated and stained with anti-phospho-CHK2 threonine-68.

Figure 9

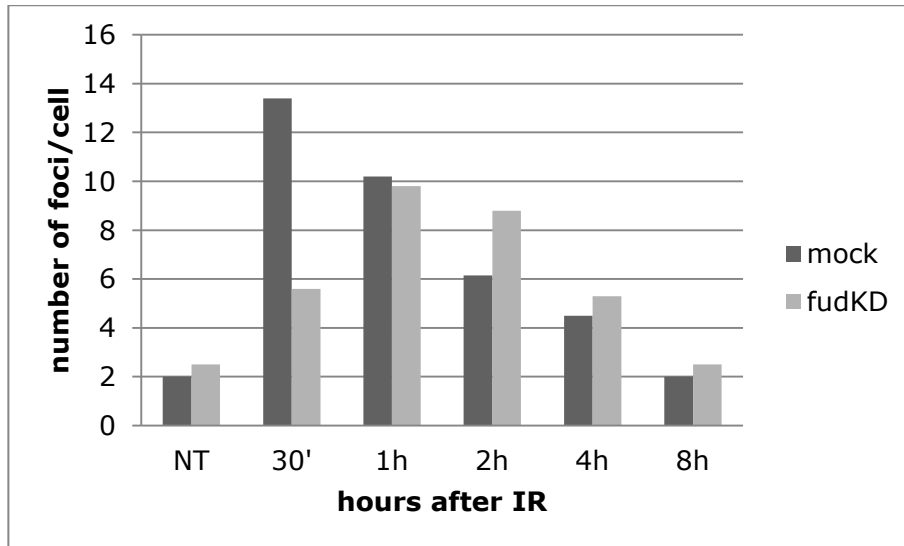


Figure 9: Histograms showing number of g-H2AX foci in FUS kd and mock cells that were exposed to 2 Gy of ionizing radiation and allowed to recover for the indicated times.

Figure 10

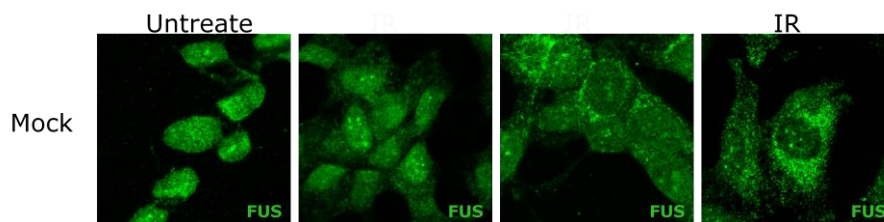
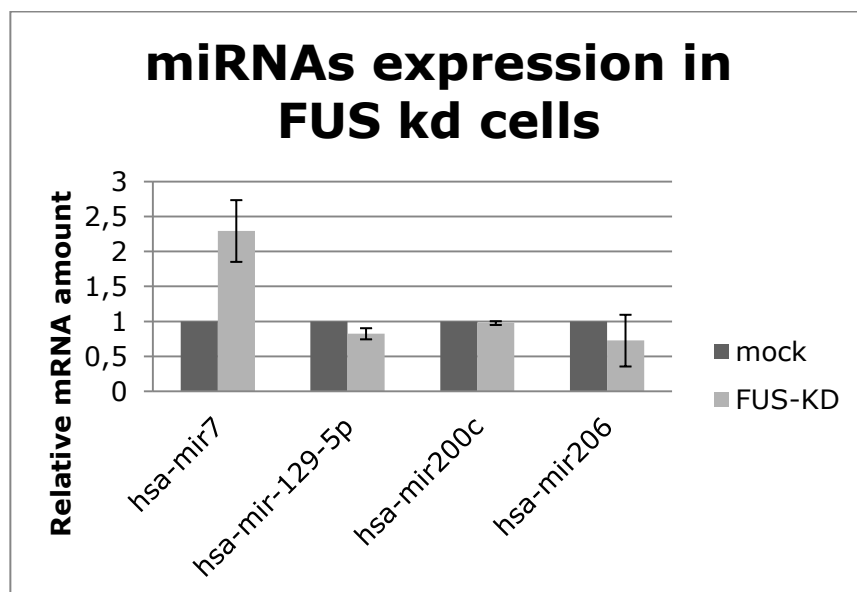


Figure 10: Representative immunofluorescence images of mock cells exposed to IR (2 Grays) are

shown. Cells were fixed at 24h post irradiation indicated and stained with an anti-FUS antibody. While in untreated cells FUS is mainly distributed in the nucleoplasm with the exclusion of the nucleoli and shortly after irradiation, FUS concentrates in few discrete nuclear foci. Then, starting from 3 h after irradiation, FUS progressively accumulates in the cytoplasm.

Figure 11

A



B

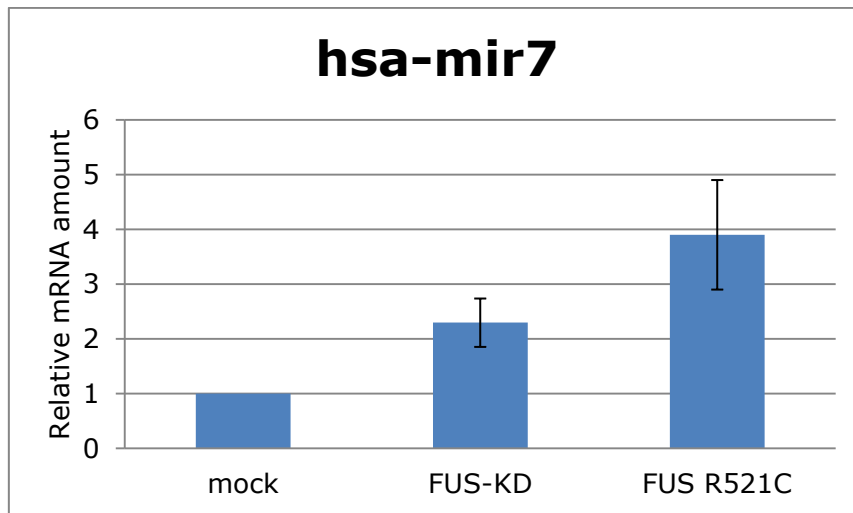


Figure 11: (A) Analysis of a small group of microRNA in FUS kd cells (n=3 biological replicates) Data were normalized to Snord25 and mir16. **(B)** Analysis of mir-7 expression in FUS kd and in FUS-R521C mutant.

3.6 Materials and Methods

Cell cultures and treatment

Human neuroblastoma SHSY-5Y transduced with cDNAs coding for FUS R521C were maintained in Dulbecco's modified Eagle's Medium (Euroclone) supplemented with antibiotics (100 U/mL streptomycin and 100 µg/ml penicillin), 2,5 mM L-Glutamine and 10% Fetal Bovin Serum (all from Euroclone) at 37 °C with 5% CO₂. The SH-SY5Y cells stably transduced with the sequencing of the short hairpin that induce specific FUS silencing were maintained in Dulbecco's modified Eagle's Medium (Euroclone) supplemented with antibiotics (100 U/mL streptomycin and 100 µg/ml penicillin), 2,5 mM L-Glutamine and 10% TET Free Fetal Bovin Serum (all from Euroclone) at 37 °C with 5% CO₂. Cells were fed every 2-3 days and passed once a week. For the short hairpin expression induction, Doxycyclin was added at final concentration of 5µM/mL for the days required in the experiment. Ionizing radiation was induced by a high-voltage X-ray generator tube (Faxitron X-Ray Corporation). In general, mock and FUS-depleted cells were exposed to 2Gy for the DDR foci formation studies and FUS translocation experiments. To measure clonogenicity,

SH-SY5Y mock and FUS-kd cells were induced for 5 days with doxycyclin and plated in 10 cm² dishes in triplicate at 3000 cells/dish density. Cells were grown for 10–15 days and colonies were stained using crystal violet.

Proliferation curve, TUNEL and BrdU analysis

To perform proliferation curve $2,5 \times 10^5$ cells were plated in 6MW and counted and re-plated in alternating days. For the flow cytometry analysis 4×10^6 cells were plated in 10cm² dish and BrdU was added in complete medium to a final concentration of 30uM. Cells were incubated for 30 minutes then the trypsin was used to harvest the cells. The cells were collected in complete medium and pelleted by centrifugation, washed with cold PBS and finally resuspended with 70% EtOH and PBS. The samples can be stored at 4° until the FACS analysis. The day of the analysis cells were centrifuged and washed to remove ethanol. Then the cell pellet was resuspended 100 µl of FITC- (or Alexa Fluor 488)- conjugated anti-Br-dU mAb solution and incubated at room temperature for 1h. Finally an ml of PI staining solution was added and cells were incubate for 30 min at room temperature in the dark. Cells were analyzed by flow cytometry. For the TUNEL assay we

followed the same protocol without the BrdU staining and antibody.

miRNA extraction, reverse transcription and qPCR for SHSY-5Y cells

The microRNA from SHSY-5Y cells (mock, FUS kd and FUS R521C), were extracted using the Absolutely RNA miRNA kit (Agilent Technologies) according with the protocol.

2 μ g of miRNA were used for retro-transcribing reaction that was performed using an home made miRNA detection kit. Essentially in the retrotranscription reaction a poly-A tail is added to the mature microRNA template by E. coli Poly(A) polymerase (New England Biolabs); cDNA is synthesized by the Affinityscript polymerase (New England Biolabs), using a poly-T primer with a 5' universal tags and a 3' a degenerate anchor. The cDNA template is then amplified using a micro-RNA specific forward primer and a universal reverse primer (that is complementary to the universal tag). SYBR Green (MESA GREEN qPCR MasterMix Plus) is used for detection. List of specific forward primers:

Data were normalized on SnoRD25 and mir16 expression level.

Protein extracts and immunoblotting

Cells on 10 cm plate were washed once in PBS 1X (Euroclone) and then lysed in 100 μ l of cold Lysis Buffer (Tris HCl 50 mM pH 7,5, NaCl 150 mM, 1% NP40, 5 mM EGTA) with protease inhibitors (Roche) and phosphatase inhibitor (SIGMA) The samples were put on ice for 20 min and then centrifuged at 15000 rcf for 15 min at 4°C, and the supernatant were collected. An aliquot of the cell lysate was used for protein analysis with the Comassie protein assay reagent for protein quantification.

Protein were separated in 6% and 10% SDS-polyacrylamide gels (classic Laemli conditions) and transferred to nitrocellulose membranes (Whatman GmbH), in normal Transfer Buffer (25 mM Tris, 192 mM Glicine, 20% Methanol) at 100 Volts for 2h or in High Molecola Weight protein (25 mM Tris, 192 mM Glicine, 10% Methanol and 0,1% SDS) at 15 Volts overnight. Membrane were blocked using 5% non fat dried milk in PBST (0,1% (v/v) Tween 20 in 1X PBS) for 1h at room temperature or overnight at 4 °C. After washing 3 times with PBST, membranes were incubated with peroxidase- conjugated secondary antibody anti-mouse

IgG (Cell signaling, 1:3000 dilution) or anti-rabbit IgG (Cell signaling 1:8000 dilution, in PBST with 5% non fat dried milk for 1h at room temperature.

After washing as above, the chemio-luminescent signals developed by ECL reagents (Millipore) were detected using Li-cor technology Biosciences.

Quantifications of the signals were performed using Li-cor technology software, each band value were normalized on the corresponding housekeeping band intensity, thus obtaining relative intensity values.

The antibodies used for immunoblotting were: rabbit polyclonal anti FUS (home.made 1:5000 dilution); rabbit monoclonal anti phosphor histone h2ax ser139 (cell signaling 20E3 1:1000 dilution); monoclonal mouse anti ATM (sigma A1106 1:1000 dilution) monoclonal anti actin (sigma A3853 1:2000 dilution); mouse monoclonal p53 (cell signaling 2524 1:1000 dilution); mouse monoclonal anti gapdh (sigma g8795 1:1000 dilution); mouse monoclonal anti Phospho-ATM Ser1981 (cell signaling 4526 1:1000 dilution)

All the antibodies were diluted in PBS-Tween 0,01%-MILK 5%.

Immunofluorescence

Cells grown on the glass coverslips were fixed with Carnoy Buffer (3:1 Methanol and Acetic Acid) for 10 min and permeabilized with CKS solution (Hepes 20 mM, sucrose 300 mM, NaCl 50 mM, MgCl₂ 3 mM, Triton 0,2%) cold for 5 min. After blocking with FBS 10% in PBS with 0,05% Tween for 30 min, coverslips were incubated for 1 h in a humid chamber with the following primary antibodies in PBS containing 0,2% BSA: rabbit polyclonal anti-FUS (Home made), mouse monoclonal phosphor-ATM ([\[1\]](#)), mouse monoclonal anti-phosphor-CHK2A ([\[2\]](#)), rabbit polyclonal anti-phosphor-H2AX ([\[3\]](#)).

After washing three times with PBS plus 0.2% BSA, the coverslips were stained with the respective fluor-conjugated secondary antibody in PBS and 0.2% BSA. The secondary antibodies were: Alexa 488-conjugated donkey anti-goat (A11055, Molecular Probes), Alexa 488-conjugated goat anti-mouse (A11001, Molecular Probes), Alexa 488-conjugated goat anti-rabbit IgG (A-11070, Molecular Probes), and Alexa 546-conjugated donkey anti-mouse (A10036, Molecular Probes). After dark incubation for 1 h, coverslips were washed three times with PBS plus 0.2% BSA, incubated in a solution containing 4,6-diamidino-2-phenylindole (DAPI, D9542, Sigma) 1 µg/mL in PBS for 10 min at RT, and mounted

with FluorSave Reagent (345789, 20 mL, Calbiochem). The fluorescence 12-bit images were collected with a Leica TCS SP2 AOBS confocal microscope with the 63× oil immersion objective.

3.7 References

Anderson, A.J., Su, J.H. & Cotman, C.W. DNA damage and apoptosis in Alzheimer's disease: colocalization with c-Jun immunoreactivity, relationship to brain area, and effect of postmortem delay. *J. Neurosci.* 16, 1710–1719 (1996).

Baechtold, H. *et al.* Human 75-kDa DNA-pairing protein is identical to the pro-oncoprotein TLS/FUS and is able to promote D-loop formation. *J. Biol. Chem.* 274, 34337–34342 (1999).

Bender, A. *et al.* High levels of mitochondrial DNA deletions in substantia nigra neurons in aging and Parkinson disease. *Nat. Genet.* 38, 515–517 (2006).

Bertrand, P., Akhmedov, A.T., Delacote, F., Durrbach, A. & Lopez, B.S. Human POMp75 is identified as the pro-oncoprotein TLS/FUS: both POMp75 and POMp100 DNA homologous pairing activities are associated to cell proliferation. *Oncogene* 18, 4515–4521 (1999).

J. Busser, D.S. Geldmacher, K. Herrup. Ectopic cell cycle proteins predict the sites of neuronal cell death in Alzheimer's disease brain. *J. Neurosci.*, 18 (1998), pp. 2801–2807

de Waard, M.C. *et al.* Age-related motor neuron degeneration in DNA repair-deficient Ercc1 mice. *Acta Neuropathol.* 120, 461–475 (2010).

Fang Y, Xue JL, Shen Q, et al. MicroRNA-7 inhibits tumor growth and metastasis by targeting the phosphoinositide 3-kinase/Akt pathway in hepatocellular carcinoma. *Hepatology.* 2012;55:1852–62.

Fillingham, J., Keogh, M.C. & Krogan, N.J. GammaH2AX and its role in DNA double-strand break repair. *Biochem. Cell Biol.* 84, 568–577 (2006).

Fujii, R. *et al.* The RNA-binding protein TLS is translocated to dendritic spines by mGluR5 activation and regulates spine morphology. *Curr. Biol.* 15, 587–593 (2005).

Fujii, R. & Takumi, T. TLS facilitates transport of mRNA encoding an actin-stabilizing protein to dendritic spines. *J. Cell Sci.* 118, 5755–5765 (2005).

Gardiner, M.T.R., Vandermoere, F., Morrice, N.A. & Rouse, J. Identification and characterization of FUS/TLS as a new target of ATM. *Biochem. J.* 415, 297–307 (2008).

T. Hayashi, K. Sakai, C. Sasaki, W.R. Zhang, K. Abe. Phosphorylation of retinoblastoma protein in rat brain after transient middle cerebral artery occlusion. *Neuropathol. Appl. Neurobiol.*, 26 (2000), pp. 390–397

K. Herrup, J.C. Busser. The induction of multiple cell cycle events precedes target-related neuronal death. *Development*, 121 (1995), pp. 2385–2395

Hicks, G.G. *et al.* Fus deficiency in mice results in defective B-lymphocyte development and activation, high levels of chromosomal instability and perinatal death. *Nat. Genet.* 24, 175–179 (2000).

Huang, E.J. *et al.* Extensive FUS-immunoreactive pathology in juvenile amyotrophic lateral sclerosis with basophilic inclusions. *Brain Pathol.* 20, 1069–1076 (2010).

Kwiatkowski, T.J. Jr. *et al.* Mutations in the FUS/TLS gene on chromosome 16 cause familial amyotrophic lateral sclerosis. *Science* 323, 1205–1208 (2009).

Kuroda, M. *et al.* Male sterility and enhanced radiation sensitivity in TLS(-/-) mice. *EMBO J.* 19, 453–462 (2000).

Lee KM, Choi EJ, Kim IA. microRNA-7 increases radiosensitivity of human cancer cells with activated EGFR-associated signaling. *Radiother Oncol.* 2011;101:171–6.

Lu, T. *et al.* Gene regulation and DNA damage in the ageing human brain. *Nature* 429, 883–891 (2004).
McKinnon, P.J. DNA repair deficiency and neurological disease. *Nat. Rev. Neurosci.* 10, 100–112 (2009)

Mastrocola AS, Kim SH, Trinh AT, Rodenkirch LA, Tibbetts RS (2013) The RNA-binding protein fused in sarcoma (FUS) functions downstream of poly(ADP-ribose) polymerase (PARP) in response to DNA damage. *J Biol Chem* 288:24731–24741.

Millecamps, S. *et al.* Phenotype difference between ALS patients with expanded repeats in C9ORF72 and patients with mutations in other ALS-related genes. *J. Med. Genet.* 49, 258–263 (2012).

Padmanabhan J, Park DS, Greene LA, Shelanski ML. Role of cell cycle regulatory proteins in cerebellar granule neuron apoptosis. *J Neurosci.* 1999;19:8747–8756

Paronetto MP, Miñana B, Valcárcel J (2011) *The Ewing sarcoma protein regulates DNA damage-induced alternative splicing.* *Mol Cell* 43:353–368.

Pilch, D.R. *et al.* Characteristics of gamma-H2AX foci at DNA double-strand breaks sites. *Biochem. Cell Biol.* 81, 123–129 (2003).

Qiu, H., Lee, S., Shang, Y., Wang, W.Y., Au, K.F., Kamiya, S., Barmada, S.J., Finkbeiner, S., Lui, H., Carlton, C.E. *et al.* (2014) ALS - Associated mutation FUS - R521C Causes DNA Damage and RNA Splicing defects *J.Clin.Invest.*,124,981-999.

J. Rashidian, G.O. Iyirhiaro, D.S. Park. Cell cycle machinery and stroke. *Biochim. Biophys. Acta*, 1772 (2007), pp. 484–493

Rass, U., Ahel, I. & West, S.C. Defective DNA repair and neurodegenerative disease. *Cell* 130, 991–1004 (2007)

Reynolds P, Botchway SW, Parker AW, O'Neill P (2013) *Spatiotemporal dynamics of DNA repair proteins following laser microbeam induced DNA damage—when is a DSB not a DSB? Mutat Res 756:14–20.*

Rulten SL, Rotheray A, Green RL, Grundy GJ, Moore DA, Gómez-Herreros F, Hafezparast M, Caldecott KW (2014) *PARP-1 dependent recruitment of the amyotrophic lateral sclerosis-associated protein FUS/TLS to sites of oxidative DNA damage. Nucleic Acids Res 42:307–314.*

Tan, A.Y. & Manley, J.L. The TET family of proteins: functions and roles in disease. *J. Mol. Cell Biol.* 1, 82–92 (2009).

Vance, C. *et al.* Mutations in FUS, an RNA processing protein, cause familial amyotrophic lateral sclerosis type 6. *Science* 323, 1208–1211 (2009).

Vincent, M. Rosado, P. Davies. Mitotic mechanisms in Alzheimer's disease?. *J. Cell Biol.*, 132 (1996), pp. 413–425

Wang I-F, Wu L-S, Chang H-Y, Shen C-K. TDP-43, the signature protein of FTLD-U, is a neuronal activity responsive factor. *J Neurochem* 2008;105:797–806.

Wang WY, Pan L, Su SC, Quinn EJ, Sasaki M, Jimenez JC, Mackenzie IR, Huang EJ, Tsai LH (2013) *Interaction of FUS and HDAC1 regulates DNA damage response and repair in neurons. Nat Neurosci* 16:1383–1391

Y. Yang, D.S. Geldmacher, K. Herrup. DNA replication precedes neuronal cell death in Alzheimer's disease. *J. Neurosci.*, 21 (2001), pp. 2661–2668

Wang, X. *et al.* Induced ncRNAs allosterically modify RNA-binding proteins in cis to inhibit transcription. *Nature* 454, 126–130 (2008).

Chapter 4

Conclusions

4.1 Summary

In the present thesis, I report the results obtained from my research activity carried out during the PhD program. My efforts in these three years were devoted to obtain new insights into the diverse molecular pathways concerning the impairment of RNA metabolism, involved in ALS pathogenesis. RNA processing is a tightly regulated, highly complex pathway which includes RNA transcription, pre-mRNA splicing, editing, transport, translation, and degradation of RNA. In particular my main project was focused on translation and/or degradation, studying the impact of miRNAs in ALS. To this end, I performed a characterization of miRNA expression in a cellular model of SOD(G93A) linked to ALS. Initially, I analysed by Western Blot analysis the expression of crucial factors involved in miRNA biogenesis and processing

and I found an altered expression pattern in G93A cells in compare to the control. Next, I used small RNA high throughput sequencing to obtain the miRNA profile. This analysis identified a small subset of deregulated miRNAs that I subsequently analysed in G93A mice. In order to discover a common signature between familial and sporadic ALS I tested the expression level of the two up-regulated miRNAs, mir-200c and mir129-5p both in human SOD(G93A) cells, in the spinal cord of (G93A)mice and in PBMC taken from sporadic ALS patients in effort to identify new biomarkers in an easily accessible sample such as blood. I observed that mir-129-5p is up-regulated in all three models. In addition, I validated HuD as mir129-5p new target. Considering that a consistent number of reports show that HuD plays a role in neuronal plasticity, in recovery from axonal injury and multiple neurological diseases, I generated stable cell line overexpressing mir129-5p to validate ELAVL4/HuD down-regulation and to study its effect. I found a reduction in neurite outgrowth and in the expression of differentiation markers in compare to control cells. Taken together these data strongly suggest that microRNAs play a role in ALS pathogenesis and in particular that mir129-5p can affect neuronal plasticity by modulating ELAVL4/HuD level.

In parallel with the main project, I further investigate another aspect of RNA metabolism and ALS. Over the past few years, several RNA processing genes have been shown to be mutated or genetically associated with amyotrophic lateral sclerosis (ALS), including the RNA-binding proteins TDP-43 and FUS/TLS. FUS is a member of the TET (TLS/EWS/TAF15) protein family of DNA/RNA-binding proteins. It is characterized by a N-terminal domain enriched in serine, tyrosine, glutamine and glycine residues (SYQG region), a glycine-rich region, an RNA recognition motif (RRM), multiple RGG repeats implicated in RNA binding, a C-terminal zinc finger motif and a highly conserved extreme C-terminal region. The vast majority of the ALS-linked mutations clustered in the extreme C-terminus. Most of these mutations destroy the nuclear localization signal (NLS) of the normally predominantly nuclear FUS protein, leading to cytoplasmic accumulation of FUS aggregates in neurons and glial cells of these ALS patients. Moreover, FUS-positive inclusions are also the characteristic hallmark lesions in a subset of patients with frontotemporal lobar degeneration. It is currently unclear if the FUS mutations-associated form of ALS develops due to a gain-of-function of the mutated protein (i.e. toxicity of the cytoplasmic FUS aggregates), due to a loss-of-function (i.e. inhibition of

FUS' nuclear function), or due to a combination of both. I studied the loss-of-function hypothesis. To this end, the aim of the project was to elucidate the biological function of FUS in the nucleus, which so far is not well understood. Thus, I characterized a cell line in which FUS is individually silenced by addition of doxycycline which induces the expression of a FUS-specific short hairpin RNA (shRNA). I found that attenuation of FUS expression leads to an impairment of the cell proliferation and a reduction of the growth rate by performing proliferation curve and clonogenicity assay. These effects could be due either to cell death or to alterations of the cell cycle. Thus, I assessed apoptosis using the TUNEL assay and senescence by measuring β -galactosidase activity. The results indicate that FUS depletion does not induce a significant increase in either apoptosis or senescence. I also tested whether FUS depletion affects DNA replication, by measuring bromodeoxyuridine (BrdU) incorporation, and/or cell division leading to a growth arrest (by time-lapse microscopy). I found that FUS-depleted cells at day 7 and 10 accumulate in G1 phase. The cells were not completely arrested since a small fraction of cells in S phase could still be observed. However, time-lapse experiments showed that the cells have a longer intermitotic time. From these experiments I conclude

that FUS-depletion induces a delay in the G1 phase of the cell cycle.

I analysed different hypothesis to explain this phenotype. Considering that the G1 cell cycle checkpoint is primarily responsible for preventing damaged DNA from being replicated, I first tested the possibility that a DNA damage was occurring. I noticed that FUS depletion *per se* leads to H2AX phosphorylation. At this point I decided to analyze the DDR in FUS depleted condition after DSBs formation by IR exposition. Considering that most cells accumulate in G0/G1 phase after 7 days depletion induction I selected IR a source of DNA damage because it leads DSBs immediately after irradiation. To investigate the DDR, I performed a characterization of phospho-ATM and phospho-CHK2, an apical and a downstream activated kinase of DDR, respectively, at different time points after irradiation. Western blot analysis of phosphor-ATM and phosphor-CHK2 shown that the activation of DDR was not enhanced in FUS-depleted compared to control cells. Furthermore, I tested for efficiency of DNA repair at different time points after IR exposition, using a histone γ -H2AX focus assay. Consistent with this resulted I observed that FUS depletion led to a dampening of the DDR reflected at first by the delay in in H2AX phosphorylation shortly

after IR induction and then by the observation that while at latter time points, the control cells showed significant recovery, FUS-depleted cells kept on to show a discrete number of foci. This findings can suggest that FUS is important to appropriately activate repair pathways.

Afterwards, considering that FUS is involved in microRNA biogenesis and processing I checked the miRNAs expression in FUS-depleted condition, and I found the up-regulation of mir-7, not only in FUS-depleted cells but also in FUS R521C cells which express a ALS-linked FUS mutant. Interestingly Fang et al. demonstrated that miR-7-overexpressing subclones showed significant cell growth inhibition by G(0) /G(1) - phase cell-cycle arrest, and Qui et al. demonstrated that FUS R521C mutant exhibited evidence of DNA damage as well as profound dendritic and synaptic phenotypes in brain and spinal cord.

Finally, starting from the observation that the DDR is delayed when FUS is down-regulated, I decided to check the behaviour of endogenous FUS after DBS. The analysis of the intracellular distribution of FUS in IR-treated SH-SY5Y cells by confocal microscopy showed that FUS relocalizes after irradiation. While in untreated cells FUS is mainly distributed in the nucleoplasm, after irradiation, FUS progressively accumulates in the

cytoplasm while in the nucleus it concentrates in few discrete nuclear foci.

4.2 Future perspective

From the present thesis new insight in the RNA metabolism impairment in ALS emerges. In particular, my results brings to light a new miRNAs characterization in ALS familial models and sporadic patients and suggest that a miRNAs may represent potential downstream actor in the neurodegeneration. I observed that mir-129-5p and mir200c were upregulated in cells, mice and PBMC and I followed this observation with the characterization of target of mir129-5p. However also mir200c is worth further investigation. Chegini's group have identified that VEGFA as a target of mir200c (Panda et al.2012; Chuang et al.2012). The role of VEGFA in ALS is widely documented. It has been reported that individuals homozygous for a variety of mutations in the VEGFA promotor region, resulting in lower VEGF protein expression, are at almost two times greater risk for developing ALS (Lambrechts, et al. 2003). Baseline VEGF levels in human cerebral spinal fluid are reduced

in ALS patients compared to controls (Devos, *et al.* 2004). Further, SOD1G93A/VEGF double mutant mice, in which both the Cu/Zn superoxide dismutase associated with human familial ALS and VEGF are dysfunctional or dysregulated, display more severe symptoms and decreased life expectancy (Lambrechts, *et al.* 2003). My result may suggest that the depletion of VEGFA in ALS patients could be due to mir-200c regulation. In the future, it will be interesting to check the VEGFA level in our models and validate the regulation on VEGFA by mir200c in order to find a potential correlation with this miRNA and the disease. From the analysis and subsequent validation of mir129-5p targets, I found that ELAVL4/HuD and (even with a slight downregulation) CACNG2 known as stargazin are targets of mir129-5p. Stargazin is an AMPA auxiliary subunit involved in the transportation of the receptors to the synaptic membrane, and the regulation of their receptor rate constants. ALS is a complex and multifactorial process. In addition to VEGFA also AMPA is well known to be linked to the pathology, since motor neurons are particularly vulnerable to AMPA receptor stimulation. Thus, could be potentially interesting to start a collaboration with neurophysiologists to further investigate AMPA stimulation and trafficking in mir129-5p over-expressing condition.

Finally, I found that mir129-5p negatively regulates ELAVL4/HuD and I suggested that ELAVL4/HuD depletion may affect neurite outgrowth and plasticity. However, further investigation concerning the regulation of ELAVL4/HuD are necessary. In fact, ELAVL4/HuD is an RNA binding protein which in turn is able to regulate a wide range of mRNAs. In the future, it will be of major interest to better characterize this model, for instance, by measuring mRNAs reported to be affected by ELAVL4/HuD regulation as Kv 1.1 mRNA (Sosanya et al. 2013).

From my parallel project a novel role for FUS in the regulation of cell proliferation emerges. FUS is a member of the FET (FUS, EWS, TAF15) family of RNA- and DNA-binding proteins whose genes are frequently translocated in sarcomas. Recently another member of FET family, TAF15 was implicated with cell cycle. In fact It has been demonstrated that TAF15 depletion had a growth-inhibitory effect (Ballarino et al. 2013). The results of my FUS-depletion characterization showed that as well as TAF 15, FUS attenuation leads to an impairment of cell proliferation and a reduction of the growth rate. In particular FUS knock-down cells shown an accumulation in G0/G1 phase. My results concerning the DDR efficiency activation shown that DDR is

delayed and that there is an increase of DNA damage in FUS-depleted condition, suggesting that the slowing of proliferation is due to an occurring DNA damage. In the future, it will be of major interest to find out the main players that act downstream FUS-depletion and bring to G1 accumulation.

In the last year different groups published reports concerning FUS and DDR and they started the characterization of the role and the recruitment of this DNA/RNA binding protein to the DNA damage sites. They demonstrated that FUS is recruited to sites of oxidative DNA damage through the activity of poly (ADP-ribose) polymerase (Mastrocola et al., 2013; Rulten et al., 2014). Moreover, Wang et al. showed that FUS facilitates DNA damage repair in neurons through interaction with histone deacetylase 1 (HDAC1) and recruitment to sites of double-strand DNA damage. This work showed that FUS depletion leads to a dampening of the DDR, reflected by decreased H2AX phosphorylation and an increase in the amount of DNA damage which is consistent with what I found in my model. However it is important to underline that FALS FUS mutations (causative of ALS) may not cause a complete loss of function of FUS protein. This is supported by the findings that FUS mutant proteins are still recruited to

sites of DNA damage, but are impaired in the later steps of assembly or stabilization of the repair complex. This observation indicates that the role of FUS in the human brain is multi-faceted and warrants a great deal of further study.

Only one work together with us, instead, shown the translocation of FUS after DSBs. They demonstrated that FUS cytosolic accumulation was due to the phosphorylation by DNA-PK kinase, or at least it act in concert with another kinase. An opened, interesting question remains: why FUS after an immediately recruitment on DNA damage sites then move to the cytosol at latter time point? Which is its role in the cytoplasm?

Moreover, I observed that after IR FUS relocalized in the nucleus, redistributing to few nuclear foci. Recent reports revealed that FUS together with TDP43 binds NEAT1_2 lncRNA (Tollervey et al. 2011; Wang et al. 2008), Accordingly, TDP-43 and FUS/TLS have been found enriched in nuclear paraspeckles in cultured cells (Nishimoto et al. 2013). Furthermore, using a proteomic approach, in collaboration with Bachi group from IFOM, we found that FUS coimmunoprecipitates with p54/NONO and SFPQ/SFPQ in a RNA-independent manner. Taking together these observation suggest a potential recruitment of FUS in paraspeckles (PSPs).

PSPs are foci enriched in RNA-binding proteins. For long time since PSPs were identified, the only characterized role was in controlling expression of hyperedited mRNAs. More recently PSPs have been reported to participate in a number of other processes relating to mRNA biogenesis (splicing, pre-mRNA 3'-end formation, cyclic AMP signaling etc.) and interestingly, it was found a correlation between PSPs proteins and DDR. Characterize the potential recruitment of FUS in PSPs after DNA damage and reveal its role in these nuclear foci could be particularly significant.

Finally, starting from my result of mir-7 up-regulation in two FUS-related cellular model of ALS, it will be very interesting to verify this up-regulation in cell lines expressing other FUS mutant and analyze its effect by target study. Moreover, since FUS is involved in miRNAs biogenesis and processing, I can speculate a possible direct role of FUS on mir-7 metabolism and this represent another interesting hypothesis to investigate.

4.3 References

Ballarino M, Jobert L, Dembele D, de la Grange P, Auboeuf D, Tora L: TAF15 is important for cellular proliferation and regulates the expression of a subset of cell cycle genes through miRNAs. *Oncogene* 2012, 32(39):4646-4655.

Chuang TD, Panda H, Luo X, Chegini N (2012) miR-200c is aberrantly expressed in leiomyomas in an ethnic-dependent manner and targets ZEBs, VEGFA, TIMP2, and FBLN5. *Endocr Relat Cancer* 19: 541–556

Devos, D., Moreau, C., Lassalle, P., Perez, T., De Seze, J., Brunaud-Danel, V., et al. (2004). Low levels of the vascular endothelial growth factor in CSF from early ALS patients. *Neurology* 62, 2127–2129. doi: 10.1212/01.wnl.0000129913.44351.a3

Lambrechts D, Storkebaum E, Morimoto M, Del-Favero J, Desmet F, et al. (2003) VEGF is a modifier of amyotrophic lateral sclerosis in mice and humans and protects motoneurons against ischemic death. *Nat Genet* 34: 383–394. doi: 10.1038/ng1211

Mastrocola AS, Kim SH, Trinh AT, Rodenkirch LA, Tibbetts RS. The RNA Binding Protein Fused In Sarcoma

(FUS) Functions Downstream of PARP in response to DNA damage. *J. Biol. Chem.* 2013;288:24731-24741.

Panda H, Pelakh L, Chuang TD, Luo X, Bukulmez O, Chegini N. Endometrial miR-200c is altered during transformation into cancerous states and targets the expression of ZEBs, VEGFA, FLT1, IKKbeta, KLF9, and FBLN5. *Reproductive Sciences.* 2012 doi:10.1177/1933719112438448

Rulten SL, Rotheray A, Green RL, Grundy GJ, Moore DA, Gómez-Herreros F, Hafezparast M, Caldecott K (2014) PARP-1 dependent recruitment of the amyotrophic lateral sclerosis-associated protein FUS/TLS to sites of oxidative DNA damage. *Nucleic Acids Res* 42:307–314.

Sosanya, N. M., Huang, P. P., Cacheaux, L. P., Chen, C. J., Nguyen, K., Perrone-Bizzozero, N. I., et al. (2013). Degradation of high affinity ELAVL4/HuD targets releases Kv1.1 mRNA from miR-129 repression by mTORC1. *J. Cell Biol.* 202, 53–69. doi: 10.1083/jcb.201212089

Tollervey JR, Curk T, Rogelj B, Briese M, Cereda M, Kayikci M, Konig J, Hortobagyi T, Nishimura AL, Zupunski V, Patani R, Chandran S, Rot G, Zupan B, Shaw CE, Ule J: Characterizing the RNA targets and

position-dependent splicing regulation by TDP-43. *Nat Neurosci* 2011, 14:452-458.

Wang X, Arai S, Song X, Reichart D, Du K, Pascual G, Tempst P, Rosenfeld MG, Glass CK, Kurokawa R: Induced ncRNAs allosterically modify RNA-binding proteins in cis to inhibit transcription. *Nature* 2008, 454:126-130.

Yoshinori Nishimoto, Shinichi Nakagawa, Tetsuro Hirose, Hirotaka James Okano, Masaki Takao, Shinsuke Shibata, Satoshi Suyama, Ken-ichiro Kuwako, Takao Imai, Shigeo Murayama, Norihiro Suzuki and Hideyuki Okano. The long non-coding RNA nuclear-enriched abundant transcript 1_2 induces paraspeckle formation in the motor neuron during the early phase of amyotrophic lateral sclerosis. *Mol Brain*. 2013 Jul 8;6:31. doi: 10.1186/1756-6606-6-31.

RINGRAZIAMENTI

Il mio primo ringraziamento va sempre alla mia famiglia. A papà e mamma che mi hanno lasciata seguire i miei sogni, sono ormai dieci anni che sono andata via di casa e voglio ringraziarvi per il supporto non invadente che mi avete sempre assicurato, per la tristezza malcelata che ho visto nei vostri occhi ogni singola volta che dopo un we o una vacanza sono dovuta ripartire. E alla mia famiglia qui a Milano: a mia sorella, mio cognato e al piccolo gioiello che hanno messo al mondo. Grazie a tutti voi per credere sempre in me e per tutto l'amore immenso che mi date.

Un dottorato non consiste solo di 3 anni di lavoro, dati e risultati, sono 3 anni di vita nei quali conosci persone, intrecci relazioni, impari cose e cresci dentro e fuori dal laboratorio, quindi mi sembra buono e giusto spendere qualche parola per ringraziare chi con me ha condiviso questi anni.

Grazie alla Prof. Barabino, per avermi accettata come membro del suo gruppo, per il suo tempo e per gli insegnamenti. Un grazie speciale va a tutti i membri del laboratorio Barabino che per brevi o lunghi periodi hanno percorso parte di questo dottorato con me. Quindi grazie a Gabriele, Natalia, Gui, Maria Giovanna, Cristina, Gionatan, Miren, Roberta. Grazie allo Zini ai suoi consigli da guru e alle nostre birrette terapeutiche, a Mafio e ai suoi film raccontati in modo stra-buffo, grazie alla Vale per l'amicizia impagabile i suoi sguardi profondi e eloquenti, grazie a Sudhi, alla Caro e a Rei per il supporto, la complicità, le risate e le belle

giornate assieme. Soprattutto grazie ad Aurora, una collega e amica migliore di te non potevo trovarla, grazie per avermi dimostrato che "mi odi" ogni giorno di questi anni, il risultato più bello, riproducibile e importante di questo dottorato è di sicuro la nostra amicizia.

Grazie a Claudia e Flavia, le splendide amiche con le quali ho condiviso gioie e scleri di questi lunghi anni, a voi che mi avete fatto fare pace con questa città, che avete rasserenato i momenti neri, appianato le salite più irte, che avete il dono di far nascere una risata praticamente in ogni situazione va tutta la mia gratitudine e il mio affetto.

Grazie agli amici di sempre, quelli che senti vicini anche da lontano: grazie a Nadia, Tutina e Zittino, grazie a Angela il mio punto fermo da una vita, per le innumerevoli volte che mi hai rimesso in sesto con due parole e un abbraccio. Grazie a Giusy e Max per avermi riportato un po' di "casa" qui al NordE.

Grazie al mio gruppo di IWTB per le belle amicizie nate, la complicità, la condivisione dell'ossessione patologica per la musica, le risate quotidiane e le feste meravigliose e qui ringrazio anche Vasco e Manuel, dire perché è assolutamente superfluo.

Grazie a tu, che mi hai insegnato che serenità e felicità non si escludono a vicenda, grazie per avermele portate entrambe e per tutte le cose impossibili che sai fare e che grazie a te riesco a fare anche io.

Infine grazie a tutte le persone che mi hanno donato anche solo un sorriso in questi tre anni, qui a Milano

(grazie a Gloria, Gio, Jessica, Alexandra, Checca, Reby, Sara, Alessandro, Lucio e Antonella Ronchi e tutto il 3 piano dell'U3) e i miei colleghi svizzeri, in particolare un grazie enorme va a Marc.